Geotechnical Behaviour of Two Novel Polymer Treatments of Oil Sands Fine Tailings

by

Kwaku Akrofi Amoako

A thesis submitted in partial fulfillment of the requirements for the degree of

Master of Science

in

GEOENVIRONMENTAL ENGINEERING

Department of Civil and Environmental Engineering
University of Alberta

Abstract

Reclamation of oil sands fluid fine tailings (FFT) is a challenge for mine operators in Alberta because of their high water content and slow self-weight dewatering. Chemical additives, including polymer flocculants, are used by operators as a treatment technology to reduce volumes and increase the density and strength of FFT deposits through dewatering. This research investigates the geotechnical behaviour of two novel polymer treatments on FFT with a focus on the immediate and long-term dewatering performance compared to that of an existing commercially available anionic polyacrylamide. A suite of basic and advanced laboratory characterization tests was conducted to evaluate the compressibility, hydraulic conductivity and undrained shear strength of tailings resulting from each polymer treatment and untreated FFT. Thixotropic effects on the strength and dewatering properties of polymer amended FFT were also examined.

This study shows that the addition of each of the new polymers to FFT produces a distinct floc structure with physical and chemical properties that affect the dewatering and strength characteristics of the tailings. The neutral polymer produces rapid initial dewatering after treatment, while the cationic polymer treatment exhibits better initial dewaterability, but poor immediate dewatering efficiency. The neutral polymer achieves high early deposit strength and small long-term settlement, owing to its strong floc bonds. However, the sensitivity of these flocs to shear can affect the near-term dewatering performance of the neutral polymer treatment. In contrast, the cationic polymer treatment promotes long-term dewatering, leading to large long-term settlement and continual gain in deposit density and strength. This research also indicates the benefit of thixotropy in the strength development of polymer amended FFT after deposition. It is concluded that the new polymer treatments provide superior initial dewaterability and shear

strength compared to the anionic polymer treatment. Both new polymer treatments provide improved dewatering, either in the immediate or long term, that can be potentially leveraged with further polymer modification and additional engineering to reclaim FFT deposits into acceptable landscapes with reduced risk.

Preface

This thesis is an original work by Kwaku A. Amoako under the supervision of Dr. Nicholas Beier. Technical guidance and critical feedback on this research work were provided by Dr. Beier. Technical advice and input were also provided by Dr. Ahlam Abdulnabi.

The author completed the experimental work for this research. Tailings samples tested in external laboratories were prepared and supplied by the author. Dean stark analysis of untreated FFT and Atterberg limits test on both untreated and polymer amended FFT were completed by AGAT laboratories Ltd. Methylene blue adsorption analysis to determine the clay content of untreated and polymer amended FFT was performed by Dr. Heather Kaminsky at NAIT on samples provided by the author. The University of Alberta nanoFAB laboratory completed the scanning electron microscopy imaging of tailings samples provided to the lab by the author. The author analyzed and interpreted the imaging data.

The literature review in chapter 2, data analysis and interpretation in chapter 4, discussion in chapter 5, as well as the conclusions and recommendations for future work in chapter 6 are the author's original work. This thesis manuscript was written by the author.

Parts of Chapter 3 and Chapter 4 of this thesis have been published in the 2020 GeoVirtual conference as Amoako, K., Abdulnabi, A., Beier, N., Soares, J., and Simms, P., "Long-term consolidation of two new polymer treatments of oil sands fine tailings". These results will also be published in a forthcoming Canadian Geotechnical Journal paper that discusses the geotechnical performance of these treatments in a broader scope.

Acknowledgements

I would like to thank my supervisor, Dr. Nicholas Beier, for his guidance, encouragement and financial support throughout this project. It has been an honour working with the geotechnical group. I am also grateful to NSERC and COSIA for sponsoring this research as part of the Collaborative Research Development program.

Special thanks to Dr. Ahlam Abdulnabi for the immense support and encouragement from the outset of this research to my defense. I would like to also thank Dr. Paul Simms for his technical contributions and the opportunity to work with his research group at Carleton University. Also, thank you to Christine Hereygers, Dr. Louis Kabwe and Dr. Heather Kaminsky for the support in my laboratory work.

Finally, I would like to express my deepest gratitude to my wife, son and entire family in Ghana for their love, understanding and prayers throughout my studies in Canada.

Table of Contents

List of Tables

List of Figures

Chapter 1: Introduction

1.1 Statement of Problem

Surface mining of oil sands in Northern Alberta has been in operation for over five decades. The bitumen extraction process produces tailings, consisting of sand, silt, dispersed clay, residual bitumen and process water. Deposition and containment of the tailings material in a surface storage facility allows fluid fine tailings (FFT) at less than 10% solids content to form and accumulate. Within a few years, FFT settles to a solids content of 30 to 35 % with little to no effective stress and are expected to remain unconsolidated for decades to centuries due to dispersed clay (Chalaturnyk et al. 2002, Jeeravipoolvarn et al. 2009). Therefore, FFT are unable to develop enough density and trafficable strength to be reclaimable. The total volume of legacy and new FFT now exceeds 1.2 billion m^3 (AER, 2019) and occupies a storage footprint of over 250 km^2. The growing inventory of FFT and their slow rate of dewatering pose a challenge to both reclamation efforts and the physical stability of tailings impoundments and present huge environmental impacts and liability.

The need to manage these impacts and risks has spurred the industry to develop new technologies to speed up the dewatering of FFT and reduce their rate of accumulation. Driven by a regulatory policy, which sought to achieve a specific trafficable strength in deposited tailings in the short term, these technologies aimed to densify fine tailings by maximizing dewatering before and immediately after deposition. Some of these technologies have been successfully implemented at both pilot and commercial scales, including in-line flocculation, centrifugation and thickened tailings. These technologies utilize polymer flocculants (sometimes with coagulants) to enhance the dewatering performance of FFT. However, the costs associated with the efforts to achieve the short-term regulatory target were high, and the dewatering performance of the tailings produced from the use of these new technologies was not consistent. Therefore, research and development of tailings treatment technologies over the last five years are focusing more on the long-term dewatering and reclamation methods.

Polymer-based treatment has become increasingly essential to the long-term dewatering of fine tailings as a cost-effective solution. Oil sands operators often use anionic polyacrylamides with a high molecular weight to increase the settling rates of FFT. However, tailings amended using these polymers are unable to meet the long-term dewatering performance required by the industry (Vedoy and Soares 2015). Efforts to overcome this challenge are driving the development of new flocculants and enhancement of existing ones by the industry to continue improving environmental performance.

1.2 Objectives and Scope of Thesis

This research forms part of an on-going Natural Sciences and Engineering Research Council of Canada (NSERC) Collaborative Research Development (CRD) program being undertaken by Carleton University, in partnership with the University of Alberta. The CRD program aims to develop new and rapid ways of evaluating the long-term dewatering properties of prospective oil sands tailings technologies. In addition, the project is exploring methods to assist and monitor the production and quality of tailings that meet the desired performance criteria.

One of the specific objectives of the CRD program is to test, modify and develop methods to rapidly predict the consolidation properties of candidate amended oil sands fine tailings. The program also seeks to investigate how specific polymer modifications can enhance the long-term dewatering of fine tailings. To this end, two novel polymers (cationic and neutral) have been developed at the University of Alberta with specific features aimed at improving the dewatering performance of FFT. The polymer design recipes, including their optimum flocculation conditions, have been published by Bazoubandi and Soares (2020) and Vajihinejad and Soares (2018).

The objective of this research is to determine if the addition of these novel polymers to FFT will enhance the immediate and long-term dewatering properties of FFT to meet reclamation goals. This study investigates the effects of the polymer treatments (PT) on the geotechnical properties of FFT, and the findings of this work will be used in other CRD studies to evaluate proposed correlations to rapidly predict the consolidation properties. The scope of this research consists of the following:

1. Characterize fine tailings amended using the new polymers at specific dosages and mixing protocols provided by the polymer designer.
2. Conduct bench-scale hindered sedimentation and large strain consolidation tests with vane shear tests on the amended FFT to determine the consolidation properties and shear strength of the tailings.

3. Evaluate and compare the effects of the new polymer treatments to an existing polymer treatment used in the industry.
4. Assess the effects of thixotropy on the trafficability and large strain consolidation properties of polymer amended FFT.

The goal of this work was not to determine the optimal polymer dosage and mixing condition for the polymer treatments, but instead to test the tailings properties for a specific polymer dose and mixing specifications provided by the polymer designer.

1.3 Organization of the Thesis

This thesis comprises five chapters. This chapter, Chapter 1, introduces the research topic and describes the objectives and scope of this thesis. A brief overview of the following chapters is presented as follows.

Chapter 2 provides a brief overview of oil sands and the bitumen extraction process, followed by a review of fluid fine tailings properties from available literature. Regulatory policies, reclamation targets and treatment technologies for fluid fine tailings management are reviewed and presented. A review of sedimentation and consolidation processes and experimental studies on the effects of existing polymer-based treatments on the long-term consolidation behaviour of fine tailings is also presented.

Chapter 3 describes the materials, equipment, and methods used in this body of work. Standard test methods and accepted test procedures employed in the experimental testing program are referenced and/or described.

Chapter 4 presents the results of experiments conducted in this study, including tailings characterization, hindered sedimentation, large strain consolidation, and thixotropic strength of polymer amended fine tailings. One-dimensional finite strain consolidation modelling using the large strain consolidation datasets to predict the long-term consolidation behaviour of the tailings is presented as well.

Chapter 5 provides a discussion of the results, observations and findings from the experimental study, supported with the results of the finite strain consolidation modelling.

Chapter 6 presents the conclusions from this research and the contribution of these findings to improving current tailings treatment are presented. Recommendations for future work are also provided.

Chapter 2: Literature Review

2.1 Oil Sands Tailings

Oil sands reserves in Northern Alberta contain about 1.7 trillion barrels of bitumen, half of which extends beneath about 140,000 km^2 of land (Mercier et al. 2018). Out of the volume beneath this land area, about 170 billion barrels of bitumen are mineable (Beier et al. 2013) and are generally found within the unconsolidated sedimentary deposits of the McMurray and Wabiskaw geological formations that underlie the Athabasca region (Jeeravipoolvarn 2010). The Athabasca oil sands deposit is approximately 50m to 80m thick (Mercier et al. 2018), and typically consists of sand, silts and clays, bitumen, and water. The fines exist as interbedded layers of clay-shale within the sand. The depth of mineable oil sands allows the use of shovel and truck technology for surface mining of the ore. Currently, active oil sands surface mining areas in Alberta account for about 3% of total oil sands surface area and 20% of total reserves (Government of Alberta 2020).

Bitumen is extracted from crushed oil sands ore using the Clark Hot Water Extraction Process developed in 1932 (Chalaturnyk et al. 2002). The extraction process utilizes hot water and process aids such as sodium hydroxide (NaOH) and calcium citrate to separate bitumen from the mineral solids. The ore is first conditioned with hot water during pipeline transport from the mine pit to the extraction plant to break down the fine particles, and then bitumen is separated by froth flotation in separation vessels. Following froth treatment, the middlings are further processed to recover the remaining bitumen droplets. The addition of NaOH or bicarbonate to the ore processing disperses the clay minerals in oil sands in order to maximize bitumen recovery to more than 90 % (Mercier et al. 2018). The recovered bitumen is further upgraded into light synthetic crude oil, and the waste products from the extraction process are removed as whole tailings.

Oil sands tailings consist of sand, silts, dispersed clays, and process water (FTFC, 1995). The bitumen recovery process leaves residual bitumen in the tailings stream, which varies depending on the extraction process. Produced at solids content ranging from 40% to 60% (Jeeravipoolvarn 2010), whole tailings are conventionally transported through pipelines and discharged into tailings containment facilities. Tailings are typically stored in large surface ponds enclosed by dykes due to the lack of in-pit space several years after mining operation begins. The pond configuration allows tailings to gently flow away from the dykes after discharge. Due to their particle size and weight, the sand fraction settles near the discharge point to form the beach, while fine tailings suspension at a solids content of 6% to 10% by mass accumulates farther away. When a more controlled segregation of tailings is desired, the coarse fractions are separated from the fines using cyclones, and the resulting tailings stream, which consists of fines and fines/sand mixtures, are discharged into the tailings pond in a similar fashion. The fine tailings suspension can settle to a solids content of 30% to 35% by total mass within a few years (Beier et al. 2013). However, generically, fine tailings suspensions with a fines content greater than 50% are called FFT (Kaminsky and Omotoso 2016). Extraction of a barrel of crude oil generates 1 m^3 of sand and 0.25 m^3 of FFT on average (Norwest 2018, Beier and Sego 2008).

2.2 Fluid Fine Tailings Characteristics

2.2.1 Basic Properties

Oil sands deposits are heterogeneous but typically consist of ~85 % mineral content (sand, silts and clays),~12 % bitumen, and 3% connate water by weight (wt.%) (Mikula 2018). Typical basic tailings properties from the oil sands extraction process are provided in Table 2-1 (Sobkowicz and Morgenstern, 2009; Beier et al. 2013). On average, the solid fraction of the extraction tailings comprises~85 wt.% coarser than 44 microns, 14 wt.% fines and 1 wt.% bitumen (Hockley 2018a).

Table 2-1: Typical oil sands tailings properties.

Parameter	Whole tailings	Fluid fine tailings
Solids content (%)	55	30–35 (mature)
Sand content (% by dry mass)	82	<5
Fines content (% by total dry mass including bitumen)	17	>95
Clay content (% by dry mass of fines)	-	30–50

Studies have shown that the properties of FFT can vary widely at a mine site, within the same pond, and even with time (Kaminsky and Omotoso, 2016). These authors compiled survey data from Suncor's ponds from 1972 to 2015 shown in Figure 2-1, which suggest a large variability in bitumen and solids contents of FFT that can be found in impoundment areas. The average solids content (by total mass) and bitumen content (by solids mass) of FFT were 38% and 3%, with a standard deviation of 14% and 2%, respectively. Furthermore, the bitumen to mineral solids distribution in FFT can vary considerably with an average bitumen to solids ratio of 0.09±0.14.

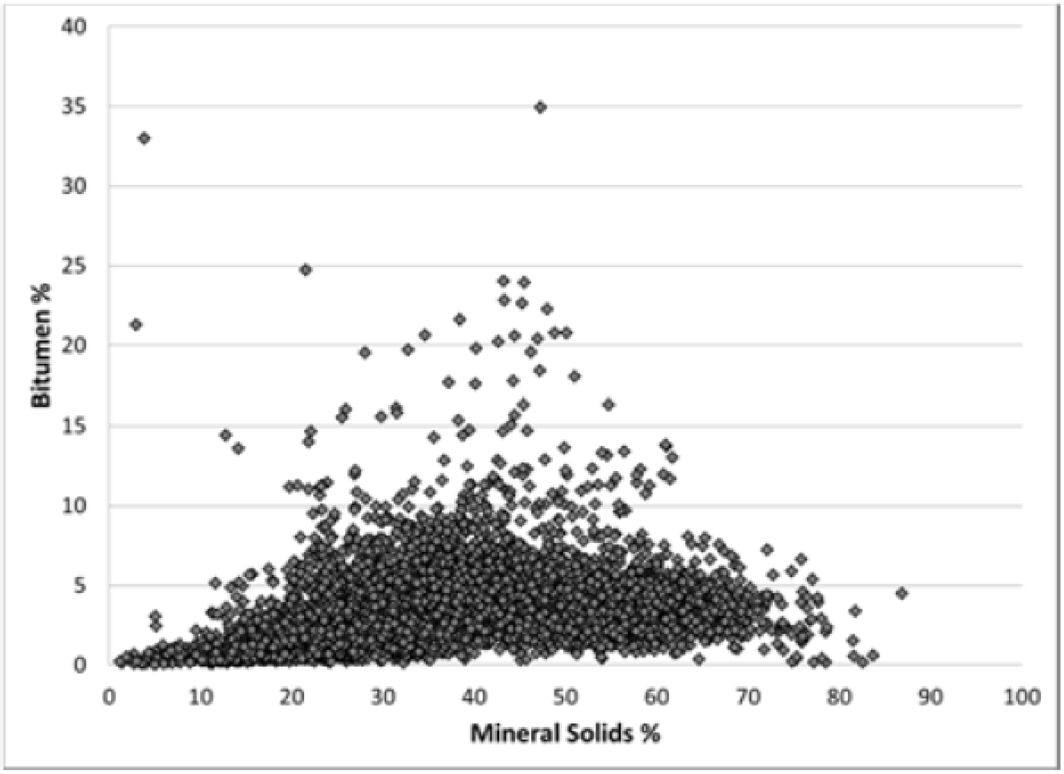

Figure 2-1: Distribution of bitumen and solids within the data set of FFT material sampled from ponds from 1972-2015 (Kaminsky and Omotoso, 2016)

The grain size composition of the mineral solids directly affects the mechanical properties of FFT. While the Dean-Stark extraction method is conventionally used to quantify the gravimetric contents of solids, bitumen and water in oil sands tailings, researchers and mine operators rely on the hydrometer (Jeeravipoolvarn, 2010; Wilson et al., 2018), sedigraph (Elias, 2019) and laser diffraction (Kaminsky and Omotoso 2018) techniques to classify the size fractions of FFT solids. Figure 2-2 shows that the particle size distribution of the mineral solids of FFT obtained by the hydrometer and sedigraph methods are consistent with typical ranges of sand, fines, and clay contents reported by Beier (2013). Kaminsky and Omotoso (2018) pointed out that although the clay size (2 μm) measured by the hydrometer and laser diffraction techniques are similar, the hydrometer method is more useful for FFT as it mimics the settling process in a pond.

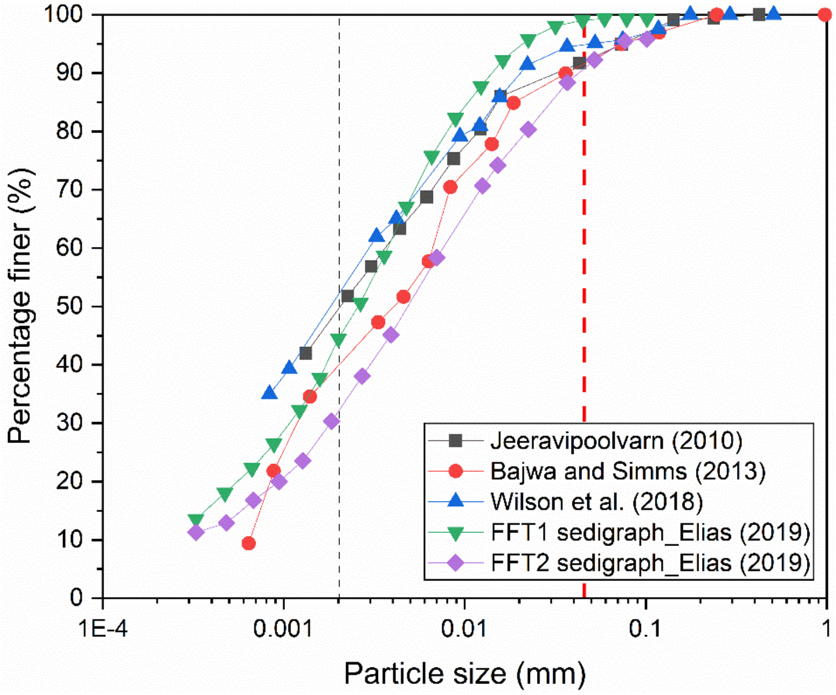

Figure 2-2: Particle size distribution of oil sands fluid fine tailings

Atterberg limits account for the effect of clay content and mineralogy and indicate the critical water contents at which fine-grained materials exhibit liquid, plastic and non-plastic behaviour. The liquid limit and plastic limit are commonly measured in geotechnical index testing, and the difference in water content between the two limits is referred to as the plasticity index, which is the range of water contents over which the material is plastic. Figure 2-3 shows the liquid limit and plasticity index of MFT and polymer amended MFT produced by Syncrude and Shell that show that MFT contains clay ranging from low to high plasticity (Beier et al. 2013). The liquid limit of MFT ranges from 40% to 65%, with a plasticity index ranging from 20% to 30%. The addition of chemical flocculants can increase the liquid limit of FFT up to 100% and plasticity index up to 73% (Beier et al. 2013, Bajwa and Simms 2013).

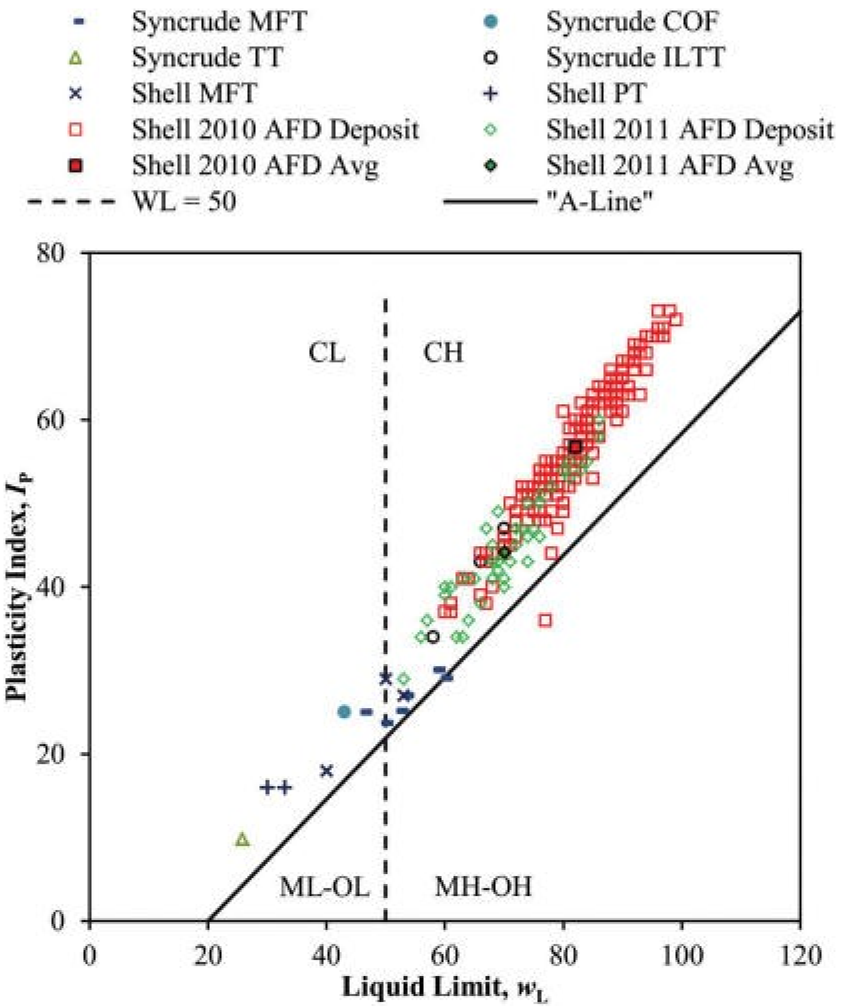

Figure 2-3: Plasticity chart of oil sands fine tailings (Beier et al. 2013)

2.2.2 Clay Mineralogy and Water Chemistry

Clay mineralogy and water chemistry largely control the settling and consolidation behaviour of FFT (Mikula and Omotoso, 2006). Sedimentation methods provide indirect measurements of clay-sized particles; however, the assumptions of Stoke's Law present several limitations to measuring the equivalent size of clay minerals (Kaminsky and Omotoso 2018). The Methylene Blue absorption technique is commonly used in the oil sands industry to determine the clay content of the ore and FFT by directly measuring clay activity using the halo method. While bench-scale studies often suggest FFT clay contents between 30% and 50% (Beier et al. 2013), a wider variability can be found in tailings ponds due to settling processes (Kaminsky and Omotoso, 2016). In addition, the majority of clay to water ratio (CWR) measurements from Suncor's ponds in 2009 and 2015 ranged between 0.15 and 0.52 (Kaminsky and Omotoso, 2016), but a typical upper limit of 0.25 is often used (Mikula 2018).

Kaolinite and illite with minor amounts of chlorite are known to be the main clay mineral constituents present in oil sands FFT. X-ray diffraction is widely used to identify and quantify these minerals in slurries. Studies show that kaolinite is the dominant clay mineral in FFT and typically varies between 18% and 45% by total weight, while illitic constituents can make up between 7% and 15% (Omotoso and Melanson 2014).

The process water quality is essential to oil sands extraction as more than 80% of this water is recycled during operation (Vietti 2018). Major ions, such as Na, Ca, Mg, K, Cl, SO_4 and HCO_3, commonly characterize the FFT pore water chemistry, and the high concentrations of Na and HCO_3 are due to the use of NaOH as process enhancing aids (Kaminsky and Omotoso, 2016). Also, the pH of process-affected water controls the degree of clay dispersion in FFT. MacKinnon and Zubot (2013) reported a pH range of 8 to 8.4 for typical oil sands process-affected water, although lower pH values of about 7.4 have been measured in tailings ponds (Kaminsky and Omotoso, 2016). Vietti (2018) pointed out that clay suspensions are highly dispersed and will settle very slowly at pH close to 8.

2.3 Fine Tailings Management

2.3.1 Tailings Management Regulations

Accumulation of large volumes of FFT behind fluid retaining dykes due to tailings management practices in the early decades of oil sands mining poses huge environmental risks and reclamation challenges for oil sands mine operators. These concerns spurred the need for the Alberta Government to introduce measures to regulate and manage FFT. Thus, the Alberta Energy Regulator (AER) issued Directive 074, which sought to reduce FFT accrual through 50% fines capture in the dedicated disposal area (DDA) and trafficability performance criteria for progressive reclamation (ERCB 2009). The directive required FFT to have a minimum undrained shear strength of 5 kPa one year after deposition, and a minimum surface shear strength of 10 kPa must be achieved within five years after active deposition ends for the deposit to be trafficable and reclaimable. Following the release of this policy, efforts by mine operators to develop and implement new tailings dewatering technologies to achieve these reclamation targets were not successful (ERCB 2013). Nonetheless, the directive has been the driver of major research and development in oil sands tailings treatment technologies, particularly the development of chemical treatments to improve FFT strength gain.

For a more holistic management of FFT, the Alberta government introduced the Tailings Management Framework (TMF) policy to enable the progressive reclamation of FFT in the Athabasca region (Alberta Government 2015). In line with the TMF policy direction, the AER issued Directive 085 to replace Directive 074. This new directive aims to manage new and legacy fluid tailings, reduce liability and environmental risk, and promote the development of cost-effective technologies in the industry to increase the rate of reclamation (AER, 2017). Per the policy, fluid tailings deposits must be ready to reclaim within ten years of the life of mine. The regulator sets volume thresholds and triggers to limit the volume of FFT that mine operators can deposit, but allows operators to develop project-specific solutions for managing fine tailings to meet regulatory commitments.

Management of process-affected water is a major component of the tailings management system in mining operations. Presently, there is no water discharge criteria for the oil sands mining industry. However, mine operators recycle process-affected water from the tailings settling pond to maintain a zero-effluent discharge into the environment, a policy that has been implemented in the oil sands industry since commercial-scale mining began in Alberta (Hyndman et al., 2018).

2.3.2 Reclamation Targets

Tailings management technologies aim to transform existing and new tailings deposits into reclaimed landforms and sustainable mine closure landscapes. COSIA (2014) outlines six fluid fine tailings management objectives for achieving a sustainable mine closure and progressive reclamation. These closure landscapes include terrestrial upland landforms and aquatic features, which must be safe, stable and self-sustaining (Hyndman et al. 2018).

Trafficability and physical stability are two key criteria that govern reclamation efforts and the long-term geotechnical performance of above-ground tailings deposits. Reclaimable deposits for terrestrial landscape must be trafficable by heavy equipment for the construction of a soil cap and have sufficient strength throughout its depth to support upland relief without excessive settlement (McKenna et al. 2016). Applicable capping technologies for various types of oil sands tailings based on their undrained shear strength and solids content are provided in Figure 2-4

(McKenna et al. 2016). The chart indicates that tailings with firm to stiff consistencies have sufficient bearing capacity for soil capping with a moderate to low risk of failure. Thus, terrestrial landforms require the underlying fine tailings to have undrained shear strength greater than 25 kPa with water contents approaching the plastic limit and post-closure settlement less than 2 m in order to function as intended (Hyndman et al. 2018). This implies that fine tailings dewatered or mixed with sand with more than 70% solids and adequate trafficable strength can be readily reclaimed into a terrestrial landscape compatible with the local boreal forest (Hyndman et al. 2018). If fine tailings deposits would achieve these densities and shear strength within the reclamation timelines, the hydraulic conductivities of treated tailings should be about two orders of magnitude higher compared to the untreated FFT as shown in Figure 2-5 (Hyndman et al. 2018).

Fine tailings of low density (< 60% solids) and low post-treatment strength (< 5kPa) having a fluid or semi-fluid consistency present several geotechnical risks to above-ground containment. Capping of these tailings with soil is not feasible, and post-deposition settlements are large and extend over long timeframes. Therefore, such fluid fine tailings or treated fine tailings are more securely stored as deep deposits in mined-out pits, where large volumes of tailings can be contained, and volume reduction occurs through self-weight consolidation and creep (Hyndman et al. 2018). These settling processes are time-dependent and influence the reclamation requirements of deep deposits. To reduce long-term monitoring and maintenance efforts, it is recommended to reclaim deep fines-dominated deposits by placing a water cap over the deposit to create an End Pit Lake (EPL) (COSIA 2012, CEMA 2012). This aquatic landscape feature requires minimum geotechnical tailings properties to limit tailings resuspension into the overlying water body (McKenna et al. 2016). Nonetheless, the material properties, depth of the deposit, and the rate of deposition control the rate of volume reduction and the consolidation time of deep deposits (Hyndman et al. 2018). The consolidation rate of these deep deposits is enhanced by in-line thickening of FFT using polymers before deposition.

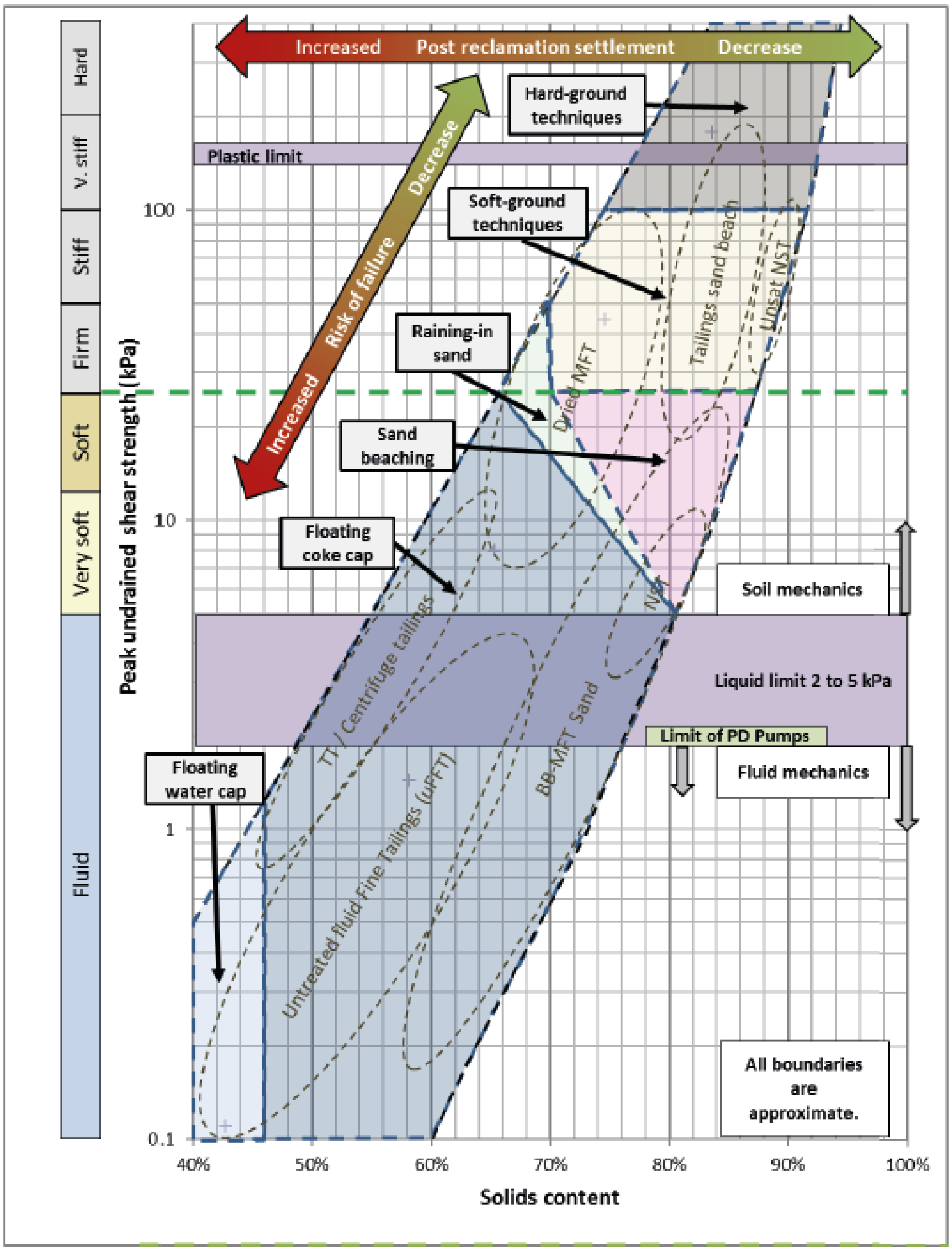

Figure 2-4: Applicability of capping technologies for approximate ranges of oil sands fine tailings shear strength and solids contents (McKenna et al., 2016)

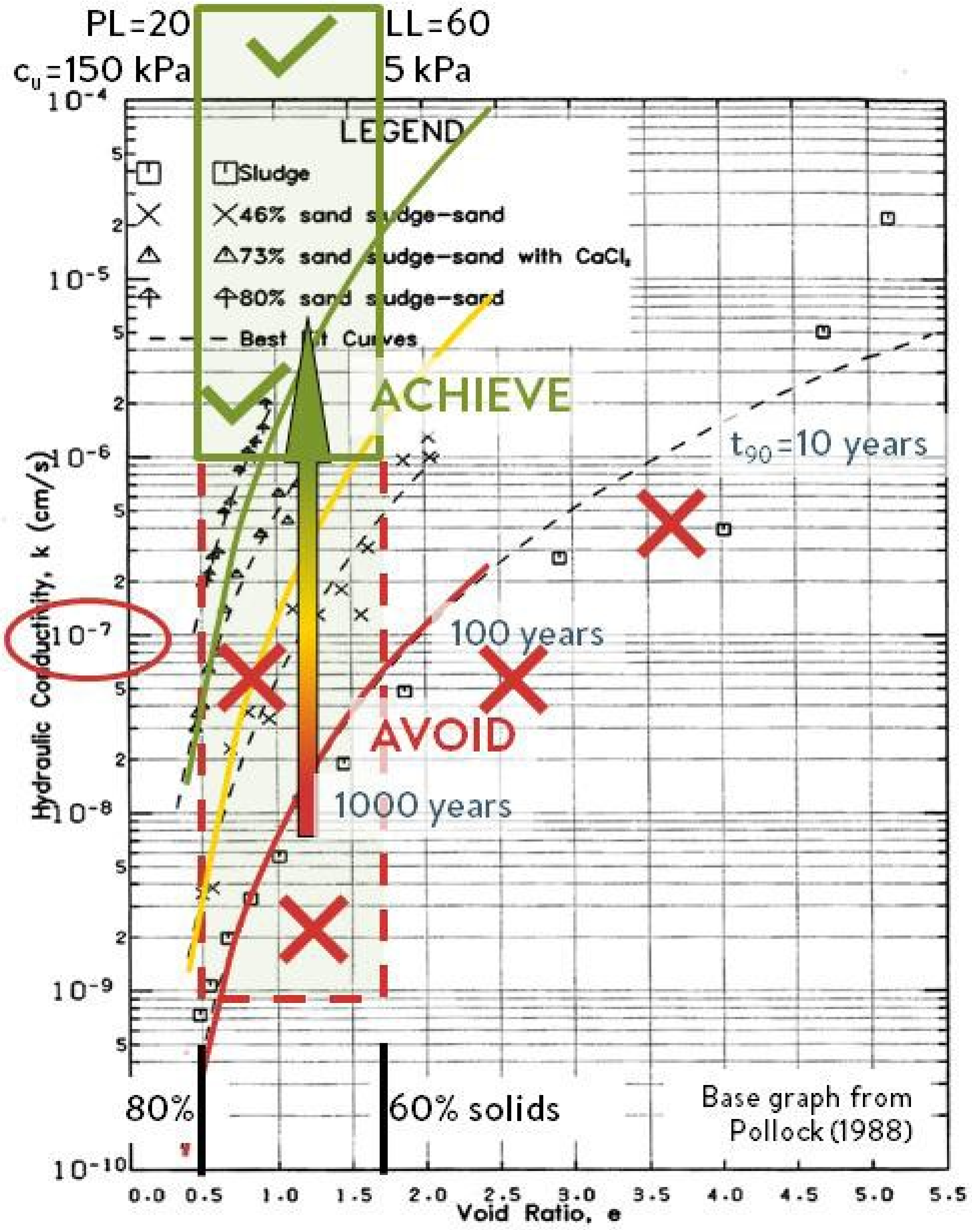

Figure 2-5: Target for tailings consolidation properties (Hyndman et al. 2018)

2.3.3 Tailings Treatment Technologies

The TMF requires that operators explore cost-effective ways to manage oil sands FFT produced during mine operations in order to minimize liability and environmental risk. In fulfilment of this responsibility, the industry has been conducting research and development studies at both laboratory and field pilot scales to develop tailings treatment technologies to speed up water release and consolidation of FFT. These technologies must aim to reduce volumes and increase the density and strength of FFT deposits through dewatering.

Further to the technological advances in fine tailings dewatering reported in the Oil Sands Technology Roadmap and Action Plan (Sobkowicz 2012), research and development have contributed a cumulative total of 981 tailings management technologies in the oil sands industry (Corriveau 2018), which comprise physical or mechanical, natural, chemical, biological, mixtures or co-disposal, and permanent storage treatment processes. Some of these technologies are already in commercial use, while others are at various stages of research and development. Most of these technologies address the tailings processing and deposition or capping challenges but must be combined with one another to meet various performance objectives and regulatory requirements for reclamation (Sobkowicz 2012, McKenna et al. 2012).

Each of these technologies has its advantages and limitations, as well as some knowledge gaps that require further research. For example, Thickened Tailings (TT) was developed by dewatering whole tailings directly from the extraction plant in a tank thickener using polymer flocculants to a target solids content of 45% to 55% (McKenna et al. 2012). However, the resulting treated tailings from the thickener underflow is sensitive to shear and segregates in the pumps and pipeline during transport (Hyndman et al. 2018). Composite Tailings (CT) and Non-Segregating Tailings (NST) transform fluid fine tailings into non-segregating semi-solid deposits of 55% to 65% solids (Mikula 2018) by mixing large amounts of cyclone underflow sand with FFT and TT respectively, along with a coagulant at a sand-to-fines ratio of 4:1 (BGC 2010). CT and NST are readily reclaimable with a terrestrial surface; however, these technologies limit sand availability for dyke construction, beaching and capping activities and leaves a growing inventory of MFT. These limitations led to the development of the in-line thickening, natural drying and centrifugation technologies to manage only FFT for reclamation (McKenna et al. 2012).

As the focus of research gradually shifts from tailings treatment to the long-term performance of tailings deposits and reclamation methods (Corriveau 2018), enhancement of polymer flocculants to optimize FFT dewatering has gained considerable interest within the past decade in the exploration of new and improved treatment methods for FFT management (COSIA 2019, Vajihinejad et al. 2019).

2.4 Polymer Treatment of Fluid Fine Tailings

Chemical amendment of FFT using polymer flocculants effectively enhances particle aggregation and the dewatering performance of fine tailings slurries (Demoz and Mikula, 2012; Farkish and Fall, 2013; Vajihinejad et al., 2019). In the oil sands industry, polymeric flocculants are extensively used in in-line flocculation and tank thickening of FFT, but also have applications in other tailings dewatering technologies, such as centrifugation, rim ditching and atmospheric fines drying (Mikula 2018). These secondary applications require that FFT is first flocculated to improve the dewatering efficiency of the technology. The relevance of polymer treatment in emerging dewatering technologies places polymer development at the core of recent research in the oil sands industry.

2.4.1 Flocculation Process

Flocculation refers to the aggregation of fine tailings particles into larger lumps through chemical bonding between charged surfaces of dispersed particles and the added flocculant (Jeeravipoolvarn 2010, Mewis and Wagner 2012). Anionic polymers with a high molecular weight flocculates FFT particles via a bridging mechanism (Klein 2014, Vajihinejad et al. 2019). The process separates water from the solids, thereby promoting water release. For a given flocculant, FFT flocculation and dewatering performance depend on shear rate, mixing time, and flocculant dosage (Mikula 2018; Vajihinejad and Soares, 2018). Figure 2-6 illustrates a typical aggregate size development with mixing time during FFT flocculation.

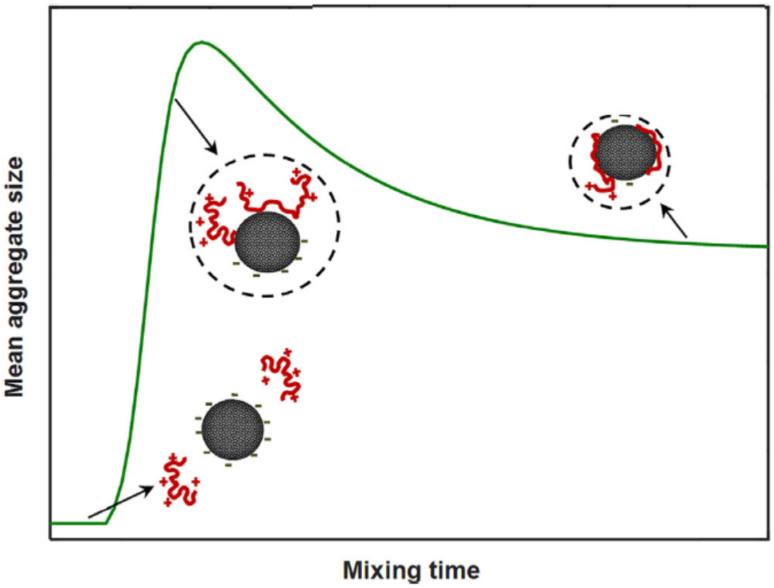

Figure 2-6: Typical FFT flocculation process with mixing time (modified from Vajihinejad and Soares, 2018)

Following the addition of polymer flocculant, proper mixing distributes the flocculant through the FFT and enables the adsorption of flocculant to the surface of tailings particles. The flocculant begins to bond with clay particles to form aggregates that increase in size to a maximum, beyond which further mixing results in irreversible floc breakage due to shear. The increasing aggregate size during flocculation translates into increasing yield stress, which decreases in a similar pattern to a steady-state yield stress after reaching a peak value as mixing continues (Wells et al., 2011; Vajihinejad and Soares, 2018). The formation of large aggregates suggests improved permeability; however, shearing can reduce the dewatering performance and yield stress of flocculated FFT (Wells et al. 2011, Mizani et al. 2016, Derakhshandeh et al. 2016).

2.4.2 Flocculant Effectiveness

Tailings treatment technologies ultimately aim to achieve FFT volume reduction after deposition both in the short term and the long term. The effectiveness of chemical amendments of FFT is assessed based on their initial dewatering performance. For effective dewatering of FFT, polymer amendments must (i) enhance the settling rate of solids, (ii) achieve optimum water recovery, (iii) produce supernatant water of reusable quality, and (iv) increase the solids content of sediments (Gumfekar et al. 2019). Graduated column settling and capillary suction time (CST) are commonly used as characterization tests for assessing the initial dewaterability of polymer treatments (Mikula and Freeman 2016, Gumfekar et al. 2019), while water quality is evaluated based on fines capture (turbidity), ion concentrations, total dissolved solids (TDS), and pH (Vietti 2018).

Synthetic polymers used in FFT treatment are water-soluble and consist of a chain of monomers with a chemical composition, structure and molecular weight designed to achieve a desired flocculation performance. With an average molecular weight that typically ranges in millions, the polymer structure can be either linear, branched, hyperbranched, or grafted, while the charges of the monomers used may classify the polymer as cationic, anionic, non-ionic, or amphoteric (Vajihinejad et al. 2019, Mahmoudkhani et al. 2012). Polyacrylamide flocculants with large molecular weights have been found to be effective in paste and thickened tailings process development (Mikula 2018) and are often used by oil sands operators for FFT treatment because of their performance and cost advantages (Vajihinejad et al. 2019). Mikula (2018) noted that polyacrylamide polymers with medium charge densities have shown optimum flocculation performance.

While the nature of the flocculant is essential for effective dewatering, research has shown that the flocculant dosage, mixing conditions and shear effects affect the polymer performance and must be carefully balanced to optimize the dewatering efficiency of polymer treatments (Mikula 2018, Znidarcic et al. 2016; Yao et al., 2012). As research continues to improve polymer options and behaviour, evaluation of polymer performance must rely on empirical studies (Mikula 2018).

2.5 Hindered Sedimentation

The physical processes that dominate the initial dewatering stage of FFT mainly include particle settling and initial water release. Most studies often rely on graduated column settling to evaluate the dewatering efficiency of chemical additives at the bench scale level (Mikula and Freeman, 2016). This experiment typically utilizes a graduated cylinder to monitor the free and hindered settling of chemically amended and unamended FFT as well as the immediate water release over several days.

Znidarcic et al. (2016) examined the settling behaviour of flocculated FFT prepared in five different conditions of polymer dosage and mixing combinations compared to untreated FFT using settling columns. Figure 2-7 shows the settling profiles observed during sedimentation and demonstrates the effect of polymer dosage and mixing on the settling characteristics of the flocculated FFT. Results suggest that undermixed or underdosed FFT have lower settling rates and immediate water recovery compared to the overdosed condition. The dewatering efficiencies of these three flocculation conditions are lower compared to FFT flocculated at the optimum polymer dosage with optimum mixing conditions. However, further shearing beyond the optimum mixing condition at the optimum polymer dosage slightly increased the initial water release, as was observed by Derakhshandeh et al., (2016) and Wells et al. (2011).

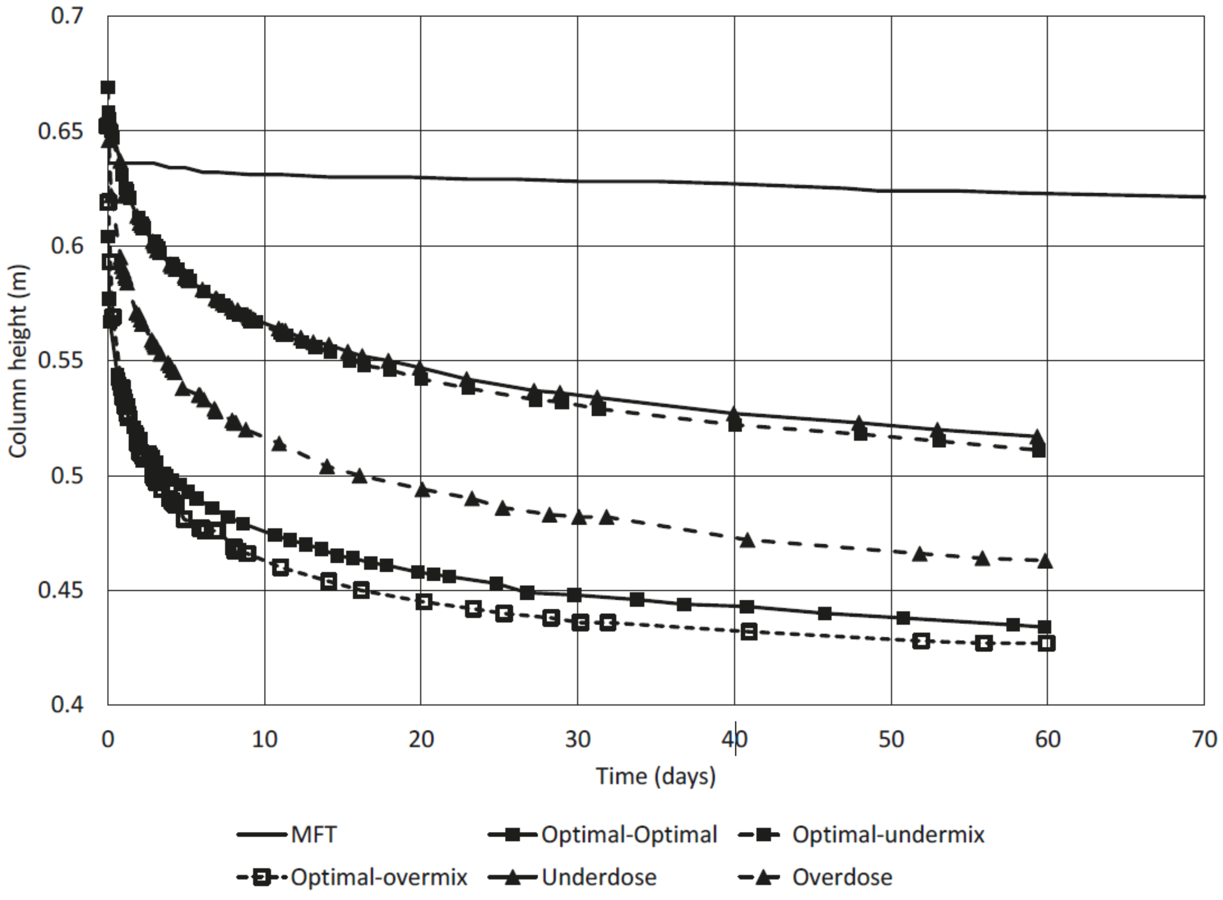

Figure 2-7: Settlement interface heights of FFT flocculated with different polymer dosages and mixing conditions (Znidarcic et al., 2016).

A higher net water recovery during sedimentation results in a higher solids content, which is a key criterion for polymer-based treatment technologies. Some studies indicate that the initial void ratio (or solids content) is influential in reducing tailings volume (Rourke and Hockley, 2018).

However, the time to reach the final void ratio is a function of the settling velocity, which in turn depends on the particle weight. The sedimentation test allows the hydraulic conductivity of tailings at higher void ratios to be determined from the interface settlement curve based on Kynch's (1952) theory. This approach requires the settling velocity of the settlement interface at the height of interest and the surface void ratio. These initial settling properties can be determined using Equation 1 and Equation 2 (Jeeravipoolvarn, 2010).

$$k = v_s(1+e)\gamma_w/(\gamma_s - \gamma_w) \tag{1}$$

$$e = \frac{(1+e_0)\left(h + v_{sp}t\right)}{H} - 1 \tag{2}$$

where,

v_s = the settling velocity,
γ_s = the unit weight of solids,
γ_w = the unit weight of water,
k = the hydraulic conductivity, and
e = the surface void ratio,
e_0 = the initial void ratio,
h = the sediment-water height of interest,
v_{sp} = the tangential settling velocity at the height of interest,
t = the elapsed time, and
H = the initial height of settlement.

2.6 Large Strain Consolidation

Sustainable reclamation of out-of-pit or deep in-pit fine tailings deposits to closure requirements can be achieved with the following objectives (Hyndman et al. 2018):

- the rate of strength development in the deposit should be sufficient for timely capping and reclamation; and,
- the deposit should develop sufficient density and low compressibility to minimize long-term settlement and disturbance to the closure landscape.

These objectives and long-term targets are attainable via consolidation and the development of shear strength within the tailings deposit, which are driven by the compressibility and hydraulic conductivity of the tailings material. These tailings properties are measured in a large strain consolidation test based on a finite strain consolidation theory.

2.6.1 One-dimensional Finite Strain Consolidation Theory

Karl Terzaghi developed the classical one-dimensional consolidation theory in 1923 (Terzaghi and Peck, 1967). The theory, among others, assumes that deformations are very small, and the compressibility and hydraulic conductivity are constant during consolidation under a given load. While these assumptions are applicable to stiff soils, very soft soils, such as FFT, undergo large volume changes in compression and are best modelled by the large strain consolidation theory. To this end, Gibson et al. (1967 and 1981) proposed the finite strain consolidation theory given in Equation 3.

$$\pm\left(\frac{\rho_s}{\rho_f}-1\right)\frac{d}{de}\left[\frac{k(e)}{1+e}\right]\frac{\partial e}{\partial z}+\frac{\partial}{\partial z}\left[\frac{k(e)}{\rho_f(1+e)}\frac{d\sigma'}{de}\frac{\partial e}{\partial z}\right]+\frac{\partial e}{\partial t}=0 \tag{3}$$

where,

ρ_s = solids density,

ρ_f = fluid density,

k = hydraulic conductivity,

e = void ratio,

σ' = effective stress,

z = depth, and

t = time.

Gibson's theory accounts for non-linear changes in both the compressibility and hydraulic conductivity as well as large deformations that occur in very soft tailings deposits as they consolidate. The finite strain theory relates compressibility to a change in effective stress, while hydraulic conductivity is a function of the void ratio. For FFT, these relationships are defined by power-law, modified power-law and Weibull functions (Jeeravipoolvarn 2010). Gibson et al. (1967) maintained the validity of Darcy's law, which relates the flow velocity of water through a porous medium to the hydraulic gradient.

2.6.2 Compressibility

In geotechnical engineering, the change in volume of a material under self-weight and applied stress describes its compressibility. The applied stress is transferred to the soil matrix as the excess pore pressure dissipates, and the effective stress, which refers to the pressure between solid particles, is often used by geotechnical engineers to refer to the material's compressive strength. In tailings management, the compressibility relationship defined across a range of effective stresses determines the tailings deposit volume and density with depth, which is key in assessing the impact of treatment technologies on the rate of FFT accumulation. In addition, long-term settlements are of critical importance to terrestrial reclamation and landform sustainability and can be predicted from the compressibility of the tailings deposit.

Compressibility relationships for polymer amended and unamended FFT determined in various laboratory studies within the past decade are shown in Figure 2-8. These studies employed either the large strain consolidation (LSC) or seepage-induced consolidation testing (SICT) method to measure the consolidation properties of tailings at each load step. FFT were either only flocculated (Boxill 2016, Znidarcic et al. 2016) using different industry polymer flocculants, or coagulated and then flocculated (Jeravipoolvarn 2010, Elias 2019). Both treated and untreated FFT have higher void ratios (lower densities) with greater variability at low effective stresses, where chemical effects and electrostatic repulsive forces between clay particles dominate the tailings behaviour (Hockley 2018a). Jeeravipoolvarn (2010) attributed the observed convergence of compressibility to a narrow range of void ratios as effective stress increases to the structural collapse of clay particles in untreated FFT and the compression of the micro and macro floc structure in polymer amended FFT.

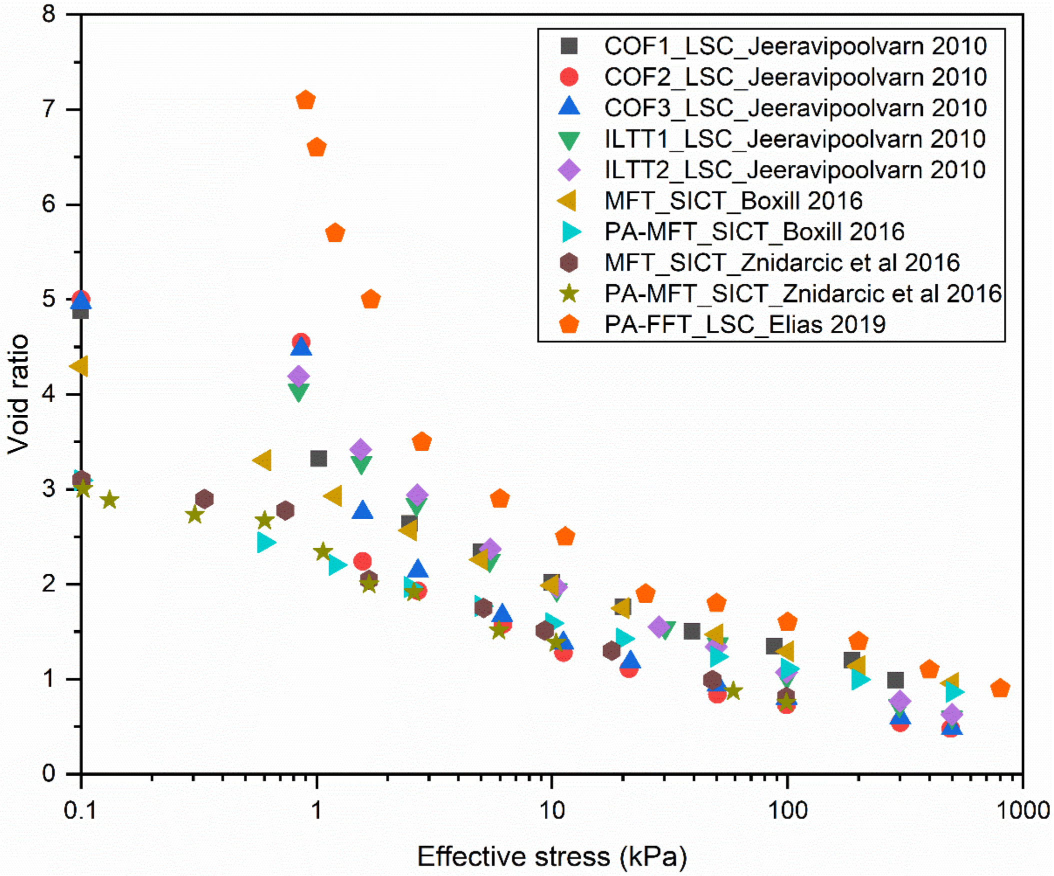

Figure 2-8: Compressibility of polymer amended and unamended FFT

Most laboratory studies have shown that polymer treatment reduces the initial density of oil sands FFT when considering the void ratio achieved at a given effective stress (Jeeravipoolvarn 2010, Yao et al. 2012, Gholami and Simms 2015, Elias 2019). Few studies have indicated an increase or no significant change in density when FFT is flocculated (Boxill 2016, Znidarcic et al. 2016). Although these experimental studies are inconclusive regarding the effect of polymer addition on the compressibility of FFT, the rate of consolidation and actual density of the tailings deposit are a function of the coupled interaction between compressibility and hydraulic conductivity (Hockley 2018a). Constitutive functions such as power law, modified power law, or Weibull functions have been found to be representative fits for the compressibility of FFT in experimental or field studies; however, the power-law function expressed in Equation 4 is widely used in finite strain consolidation modelling of FFT deposits (Rourke and Hockley, 2018).

$$e = A\sigma'^{B} \tag{4}$$

Where:

e = void ratio

σ' = effective stress

A, B = unique material constants.

2.6.3 Hydraulic Conductivity

The rate of settlement of a material under applied stress is a function of its hydraulic conductivity, which controls the rate of expulsion of pore water during consolidation. The porosity of the soil matrix dictates the water expulsion rate, and consequently, the rate of strength gain (Hockley 2018a). Bench-scale studies employ constant-head permeability or seepage techniques to measure the hydraulic conductivity of slurries. For very soft materials like FFT, the hydraulic conductivity over a range of void ratios at different effective stresses is defined by the power-law function expressed in Equation 5, which can be solved together with the compressibility function to determine the long-term consolidation behaviour of the tailings deposit.

$$k = Ce^{D} \tag{5}$$

Where:

k = hydraulic conductivity

e = void ratio

C, D = unique material constants.

Rourke and Hockley (2018) pointed out that increasing the hydraulic conductivity of FFT reduces the time to reach desired deposit densities and shear strength, and consequently shortens the reclamation timeframe. For this reason, polymer-based technologies aim to improve the permeability of FFT through aggregation of fine particles. Figure 2-9 shows the hydraulic conductivity of the polymer amended and untreated FFT tested in the cited studies in Figure 2-8. These studies and others (Yao et al. 2012, Gholami and Simms 2015, Wilson et al. 2018) have demonstrated an increase in the hydraulic conductivity of FFT after polymer addition across the range of void ratios examined. Untreated and polymer amended FFT exhibit divergence in hydraulic conductivity at high void ratios, which may be attributed to either or both the heterogeneity of the tailings structure and the differences in test methods (Hockley 2018a, Hockley 2018b). As the floc structure collapses under high compressive strengths, the hydraulic conductivity of flocculated FFT reduce to rates similar to those untreated FFT.

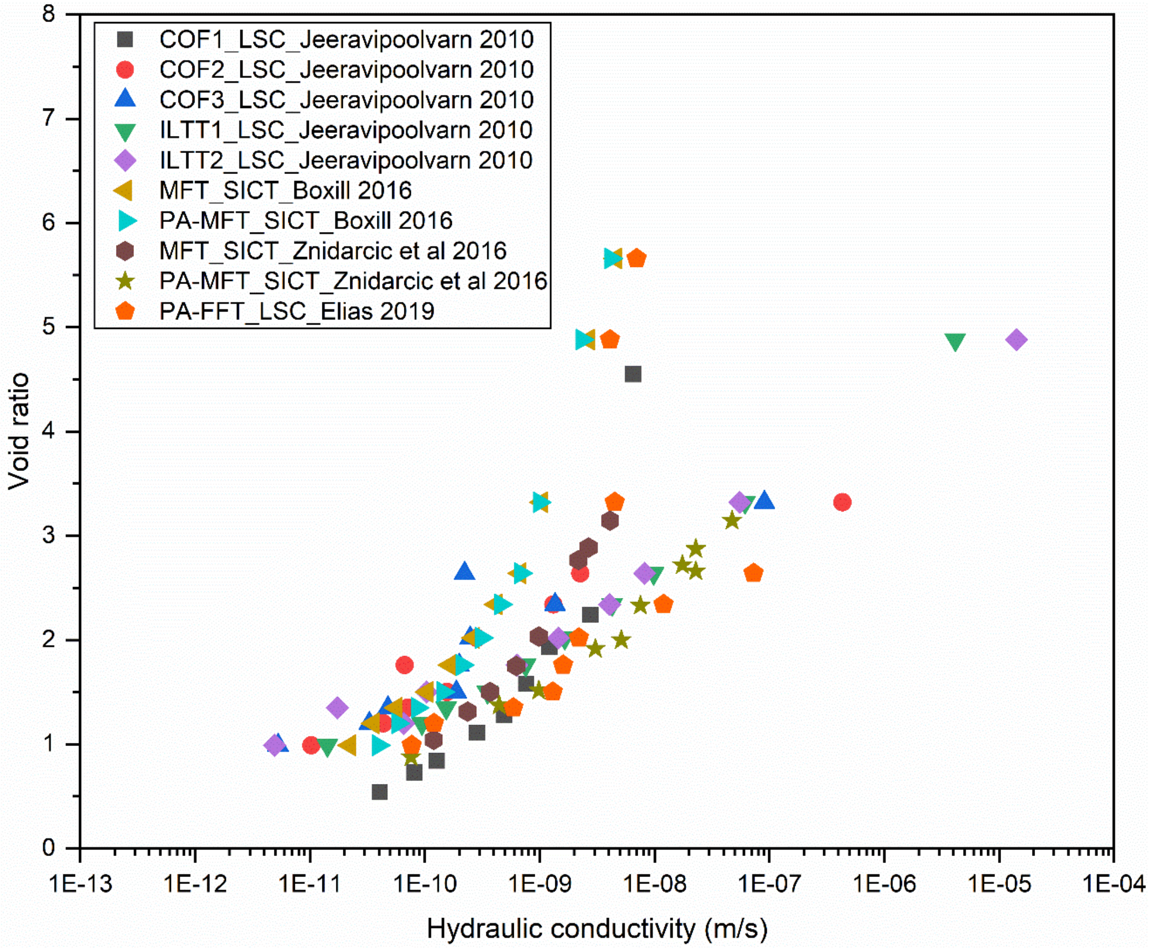

Figure 2-9: Hydraulic conductivity of polymer amended and unamended FFT

2.6.4 Undrained Shear Strength

The undrained strength gain of tailings after deposition is a key performance indicator for evaluating the long-term geotechnical performance of tailings deposits (Hyndman et al. 2018, McKenna et al. 2016). As previously mentioned, the rate of consolidation dictates the rate of strength gain, and the large strain consolidation test method allows the undrained shear strength of tailings to be measured at different consolidation stages by vane shear. Empirical studies have shown that polymer treatment increases the undrained shear strength of FFT at a given void ratio

(Jeeravipoolvarn 2010, Yao et al. 2012, Wilson et al. 2018, Elias 2019). Jeeravipoolvarn (2010) suggested that the impact of polymer addition on the shear strength of FFT is demonstrated by the high undrained strength ratio at high void ratios, as shown in Figure 2-10, which is indicative of strong chemical bonds. However, due to preconsolidation pressure, the shear strength of FFT is lower than that of treated FFT (Jeeravipoolvarn, 2010). These physicochemical effects in the tailings are overwhelmed by frictional interactions between flocs as effective stresses increase, contributing largely to the undrained shear strength gain of the tailings (Hockley 2018a).

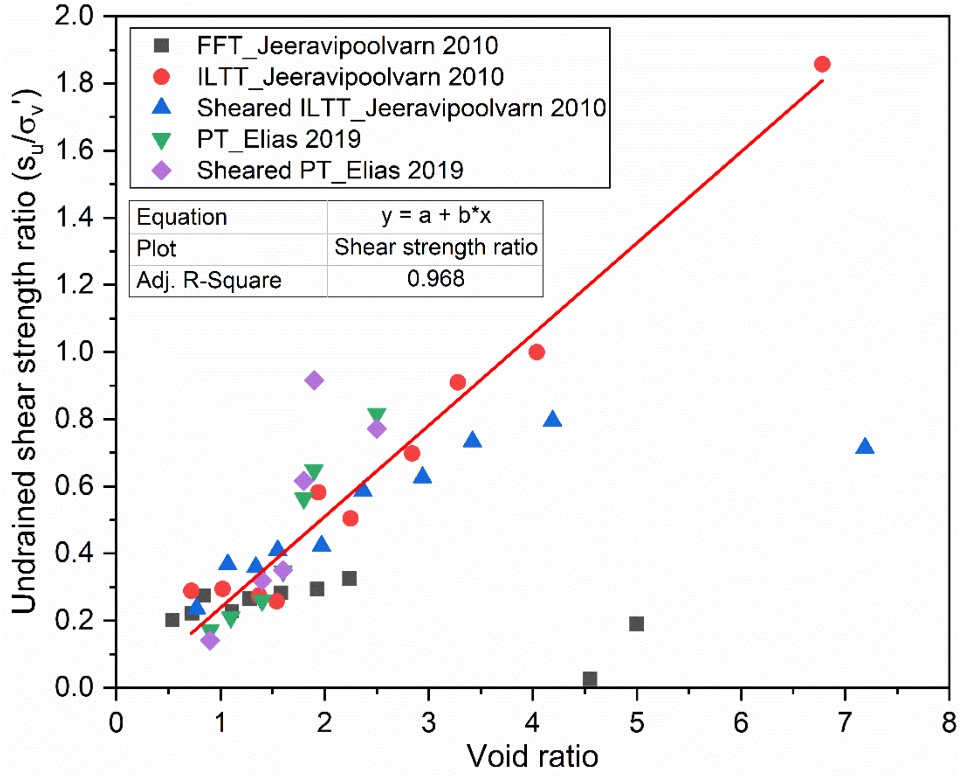

Figure 2-10: Shear strength ratio of polymer amended and unamended FFT

In addition to the consolidation properties, the literature suggests that solids content, particle size distribution, clay content, mineralogy, and water chemistry also influence the undrained shear strength of tailings (Mitchell and Soga 2005; Sobkowicz and Morgenstern 2009). Beier et al. (2013) suggested that the combined influence of these factors can be represented by the liquidity index. A comparison between polymer amended FFT (PT and ILTT) and untreated FFT in their work showed that polymer addition increases the undrained shear strength of FFT at a given liquidity index with a sensitivity ranging from 1 to 10, as shown in Figure 2-11.

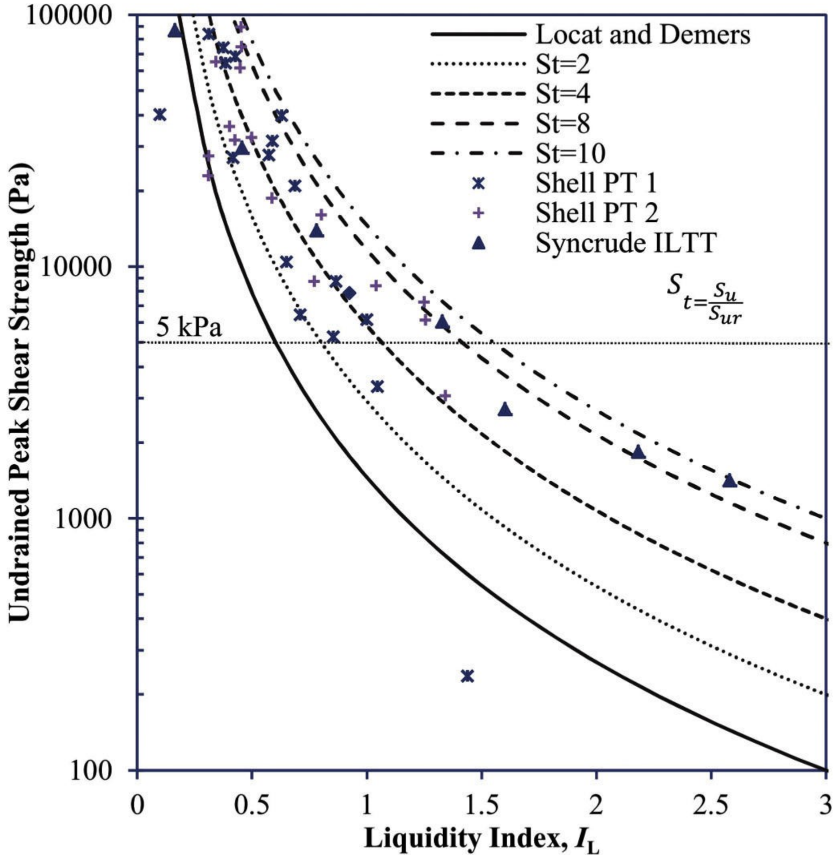

Figure 2-11: Undrained shear strength and sensitivity of oil sands fine tailings (Beier et al. 2013)

More recently, McKenna et al. (2016) provided laboratory and field vane shear measurements for chemically modified oil sands tailings that showed that the undrained shear strength at a given density (solids content) can range from an order of magnitude at higher densities to two orders of magnitude at lower densities. Their work also showed a strong correlation between the undrained shear strength and liquidity index, as suggested earlier by Beier et al. (2013).

2.6.5 Effect of shear on the dewatering and strength of flocculated tailings

The sensitivity of polymer amended FFT to shear during transport or deposition is a concern for mine operators of in-line flocculation technologies (Mizani et al. 2016). Shearing of polymer amended tailings occurs in pumps and pipeline during transport to the tailings pond and is found to affect the rheological behaviour of tailings through aggregate breakdown and restructuring (Neelakantan et al. 2018). Derakhshandeh et al. (2016) also noted that pipeline shearing conditions could reduce the overall performance of polymer-based treatment when they empirically studied the effect of shear in a couette on the dewatering and yield stress of FFT flocculated using three different polymers. Their work concluded that prolonged intense shearing over distances up to 10 km at a shear rate of 63 s^{-1} had little to no impact on the immediate dewaterability of flocculated FFT but improved their long-term dewatering. However, Derakhshandeh et al. (2016) found that pipeline shearing significantly decreased the yield stress of polymer amended FFT.

An earlier study by Jeeravipoolvarn et al. (2014) based on laboratory large strain consolidation testing of sheared in-line flocculated FFT also demonstrated that pipeline shearing reduces the undrained shear strength of flocculated FFT. This finding is evidenced by the reduced shear strength ratio of sheared in-line flocculated FFT (Jeeravipoolvarn, 2010) at void ratios greater than 4, as shown in Figure 2-10. Results from these studies suggest that polymer amended FFT are sensitive to shear, and the impact of pipeline shearing on the immediate and long-term performance of polymer treatment after deposition should be considered in tailings management.

2.7 Thixotropic Strength of Fine Tailings

In geotechnical engineering, thixotropy is an isothermal process of softening due to remolding, followed by the time-dependent recovery of the original strength at a constant water content and porosity in clay-water systems (Mitchell, 1960). This phenomenon occurs through the gradual restructuring of fine clay particles due to electrochemical forces (Mitchell, 1960; Skempton and Northey, 1952). Factors such as clay mineralogy, water content and rate of loading have been identified as directly impacting thixotropy in clay suspensions (Suthaker and Scott, 1997). Although kaolinite does not exhibit thixotropic behaviour, the addition of a dispersing agent such as sodium hydroxide in the bitumen extraction process and the presence of residual bitumen make oil sands fine tailings thixotropic in nature (Mitchell, 1960, Suthaker and Scott, 1997).

The time-dependent thixotropic effects in colloidal suspensions occur at a constant volume and composition (Mitchell and Soga, 2005). Some studies have examined the effect of ageing on the microstructure and compressibility of natural clays from oedometer tests (Delage et al. 2006, Delage et al. 2010). Delage et al. (2010) compared the compressibility curves of three undisturbed samples and a remolded sample of Champlain clay and found that changes in the soil microstructure and strong inter-particle bonding affected the compressibility by increasing the pre-consolidation pressure of the clay.

Research has also shown that thixotropy influences the consolidation and strength behaviour of oil sands fine tailings (Jeeravipoolvarn 2005, Jeeravipoolvarn et al. 2009). Miller (2010) noted that the thixotropic strength gain in FFT is evidenced by the over-consolidation behaviour observed at low effective stresses (or high void ratios), which resists the initial consolidation and dewatering of fine tailings. More recently, Salam et al. (2018) examined the effect of ageing on the shear strength and compressibility of polymer amended FFT. The undrained shear strength of the ageing tailings was measured using the fall cone method. They suggested that the magnitude of the apparent pre-consolidation pressure increases with time and is associated with changes in the tailings microstructure. Results from their work showed significant strength gain in the aged polymer amended FFT under single-drainage conditions, as indicated by a substantial increase in pre-consolidation pressure, compared to the remolded sample. The thixotropic shear strength gain in polymer amended FFT was higher under double-drainage conditions compared to single-drainage. Salam et al. (2018) attributed the observed initial strength buildup and over-consolidation behaviour in the polymer amended FFT to the structuration effect due to thixotropy, as suggested by Miller (2010).

Chapter 3: Experimental Program

3.1 General

This chapter documents experimental procedures, test methods, materials and equipment employed in the laboratory investigations undertaken to achieve the objectives of this body of work. The experimental testing program comprised tailings characterization testing, polymer amendment of FFT, sedimentation, capillary suction time testing, short-term ageing assessment and large strain consolidation testing with shear strength measurement of candidate flocculated FFT. Figure 3-1 illustrates a flow diagram of the experimental program undertaken in this body of work.

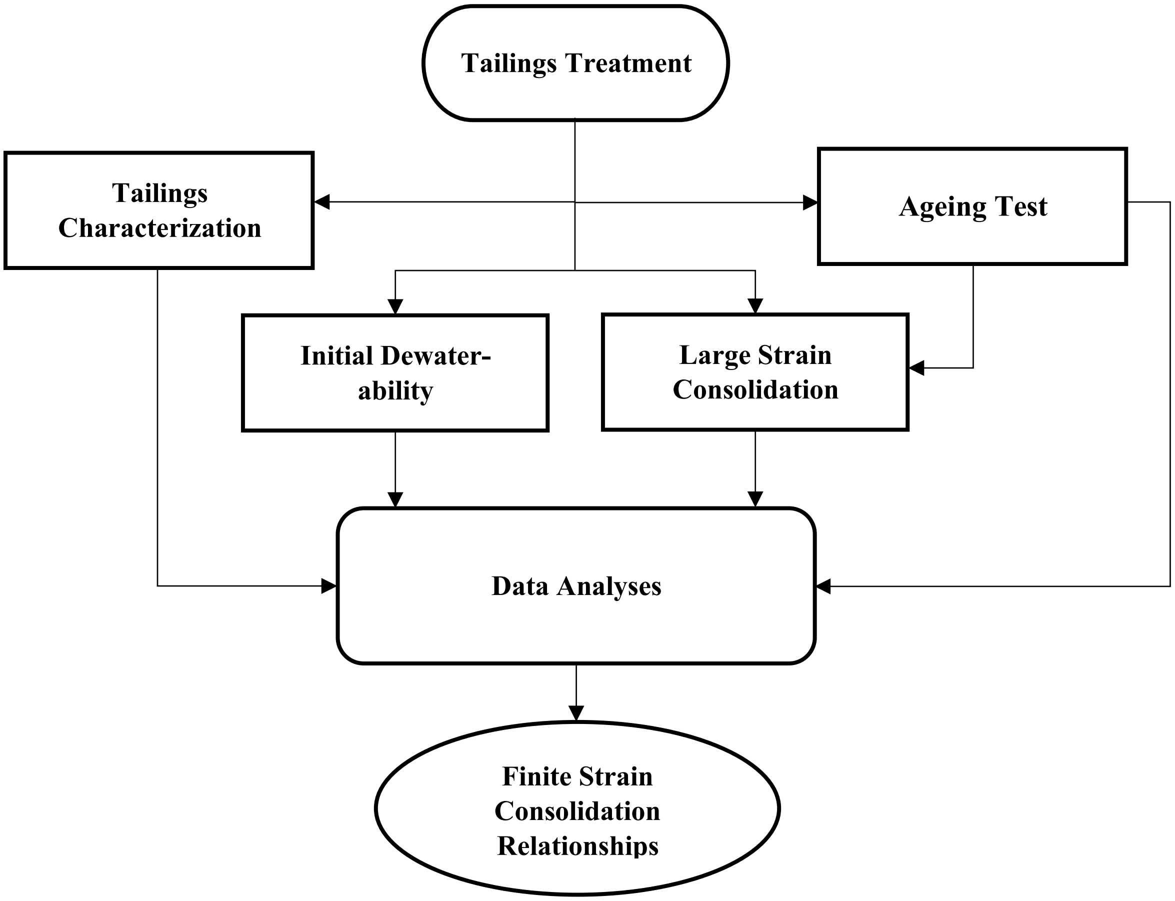

Figure 3-1: Flow diagram of the experimental program

The experimental work was conducted in accordance with standard test methods and procedures, which are described in detail in this chapter. Where necessary, acceptable modifications to standard methods were introduced to achieve successful outcomes. In general, the experiments were performed in a controlled room temperature of 20±0.5°C following standard laboratory practices.

3.2 Materials

3.2.1 Fluid Fine Tailings

Untreated FFT were sourced from Carleton University (CU) to ensure consistency with other Collaborative Research Development (CRD) project studies currently being undertaken. Thus, 40 litres of untreated FFT were received in pails on December 24, 2018, followed by additional 40 litres from the same batch on February 14, 2019. The untreated FFT were homogenized and used as the control sample in all experiments conducted. As with the polymer amended FFT, the control sample was analyzed for basic and advanced geotechnical properties to establish the baseline characteristics and behaviour of the FFT.

3.2.2 Polymers

Three polymer flocculants were used to treat FFT in the laboratory investigation. Two of these polymers, with code names A-1 and B-1, were newly designed to include additional features aimed at improving the dewatering performance of FFT. The third polymer is the FLOPAM^{TM} A3338 manufactured by SNF that has been used as a standard flocculant by oil sands operators.

In terms of chemistry, the polymer A-1 has a brush type structure consisting of linear chains of acrylamide grafted to a main backbone chain made up of amylopectin units. The functional group in this polymer makes it neutral or non-ionic. On the other hand, the cationic polymer B-1 comprises polytrimethylammonium chloride (vinyl benzyl) in a linear structure, while the polyacrylamide A3338 is anionic in nature. The polymers will hereafter be referred to as cationic, anionic and neutral polymers in this thesis. Table 3-1 summarizes the chemical descriptions of the polymers. Further details on the new polymers and their preparation protocol are included in Appendix B.

Table 3-1: Polymer description

Code	Polymer Name	Nature	Type & other details
A-1	Polyacrylamide-g-amylopectin	Neutral	Brush type structure with linear chains of acrylamide are attached to big backbone of amylopectin chain
B-1	Poly (vinyl benzyl) trimethylammonium chloride	Cationic	A linear polymer of Vb+
A3338	Polyacrylamide	Anionic	

For this study, approximately 100 grams of each polymer were sourced. In their dry condition, the neutral polymer is relatively harder and coarser in texture than the cationic polymer. The anionic polymer was received in granular form, sealed in two small plastic containers. Figure 3-2 shows the as-received conditions of the polymers.

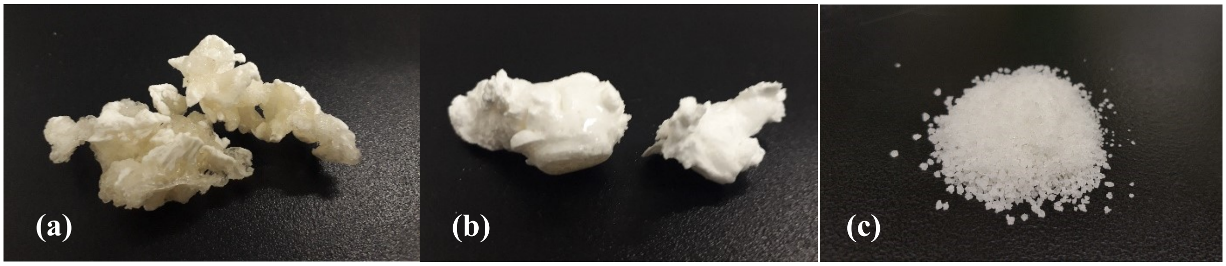

Figure 3-2: As-received condition of polymers (a) neutral, (b) cationic and (c) anionic.

3.2.3 Polymer Amended Fine Tailings

Untreated FFT were amended in the laboratory by adding hydrated polymer flocculants to create flocculated tailings for the experimental study. The addition of the polymer to FFT is a controlled process that is completed at specific dosage and mixing requirements to achieve optimum flocculation. A description of the polymer hydration process and the FFT amendment procedure is provided in Section 3.3.1. For consistency throughout this thesis, the resulting flocculated tailings from the polymer treatment process is referred to as polymer amended FFT.

With each polymer described above, a distinct amended FFT was produced for use in the experimental analyses. Visually, the polymer amended FFT had a relatively thicker consistency compared to the untreated FFT and a noticeable release of clear water at the surface shortly after treatment. The observed initial conditions of the polymer amended FFT are described in Section 3.3.1.2.

Storing bulk quantities of polymer amended FFT for use over several days of testing would have resulted in some disturbance of sensitive floc structure each time the material was re-homogenized. Thus, FFT were amended in batches and quantities required for each day's experiment and were analyzed immediately after treatment.

3.3 Tailings Treatment and Characterization

3.3.1 Fine Tailings Treatment

3.3.1.1 Preparation of polymer solution

The first step in amending fine tailings is to condition the polymers to the right concentrations such that they become readily miscible with the tailings to produce the desired effect. This was achieved through a hydration process to dissolve the solid polymer in distilled water. The same polymer concentrations and preparation protocols were used in the entire CRD project. The target concentrations of the polymer solutions are listed in Table 3-2.

Table 3-2: Polymer solution concentrations

Polymer	Mass of polymer per 500 mL solution (grams)	Concentration (%)
Neutral	1.0	0.2
Cationic	2.0	0.4
Anionic	2.0	0.4

With the exception of the neutral polymer, the polymer solutions were prepared in 500mL beakers. An electric spindle-type mixer was used for homogenizing the flocculant solution, and thus, the size of the spindle was an additional factor in choosing the beaker size. Since the stock solution was prepared in 500 mL volumes, the specified mass of polymer in Table 3-2 was used to achieve the required concentrations.

For the cationic polymer stock, 500 mL of distilled water was added to 2 grams of polymer and stirred with a mixer at 200 revolutions per minutes (rpm) for 5 minutes, and subsequently at 125 rpm for 55 minutes to achieve a solution with 0.4% concentration. To assist the thorough dissolution of the polymer, the polymer was first crushed to smaller fragments before hydrating to increase the overall surface area of the polymer and fragments of the polymer adhering to the walls of the beaker during mixing were manually agitated. At the end of the specified mixing time, a clear solution shown in Figure 3-3(b) was observed, indicating the complete dissolution of the polymer.

Similarly, the anionic polymer solution was prepared to the required concentration based on the respective amounts of polymer and distilled water specified in Table 3-2. To completely dissolve the polymer in water, the same mixing sequence, speeds and time used for the cationic stock were applied, ensuring fragments of the polymer did not remain stuck to the walls of the beaker. As shown in Figure 3-3(a), the resulting solution was sticky and cloudy in appearance.

Figure 3-3: Hydrated polymer after mixing: (a) Anionic; (b) Cationic; (c) Neutral after 2 hours; (d) Neutral after 4 days

The neutral polymer stock was created by dissolving 1 gram of the polymer in 500 mL of distilled water to obtain a concentration of 0.2%. However, the relatively harder neutral polymer presented a challenge during its hydration. In a first trial, the polymer showed little sign of dissolution after an hour of mixing. Even after extending the mixing time to 2 hours, there was no sign of improvement. In a second attempt, the polymer was first crushed in a mortar to nominal sizes in the range of 0.5 to 4 mm before hydrating. Nonetheless, the resulting solution after mixing for 2 hours was similar to that of the first trial, as shown in Figure 3-3(c). These concerns were discussed with the polymer designer, who later succeeded in preparing a litre of the polymer solution at 5 g/L concentration after stirring continuously for approximately 4 days at a faster mixing rate with a magnetic jar mixer (Figure 3-3d). The stock solution was diluted to the specified concentration and homogenized prior to its use in the tailings treatment. Thus, in subsequent polymer solution preparation, the original preparation procedure for neutral polymer was modified to this new procedure. Before using any of the polymer solutions in amending FFT, the stock solution was set aside for a maturation period of at least 15 minutes after mixing.

3.3.1.2 Polymer Amendment of FFT

The tailings amendment process using polymers involves the addition of the flocculant solution to the untreated FFT at a specified dosage to achieve the desired effect. The effectiveness of the amendment in forming the right structure is also dependent on the mixing time during homogenization. The optimal polymer dosage and mixing time for the new polymer treatments used in this study were provided by the polymer designer based on published data by Bazoubandi and Soares (2020) and Vajihinejad and Soares (2018) and are summarized in Table 3-3. The anionic polymer dose used by Salam et al. (2018) was adopted in this work consistency with other concurrent studies under the CRD program.

Table 3-3: Polymer dosage and mixing time for FFT treatment

Polymer	Dosage (ppm or g/ton)	Mixing time
Neutral	8000	2.5 min.
Cationic	4000	1.5 min.
Anionic	800	10 sec.

In tailings treatment, the polymer dosage is administered to the tailings solids, and not the total tailings mass. Thus, for a predetermined mass of fluid fine tailings, the required mass of polymer solids for tailings treatment was calculated based on the tailings solids content and the respective dosage. The required volume of polymer solution for tailings amendment was determined from the calculated mass of the polymer. For effective treatment, the optimal volume of fluid fine tailings for each batch of the amendment was determined based on the size of the spindle and the containing vessel used in the mixing process. That said, 2 L of FFT was found to be just enough to achieve effective homogenization. The flocculation process involved adding the measured volume of the polymer solution to FFT in the container and mixing the entire volume at a speed of 315 rpm for the respective mixing time in Table 3-3.

Figure 3-4 shows the initial condition and fabric of each polymer treatment. The visible striking differences between the polymer treatments are the observed texture and consistency of the resulting amended tailings. Relatively speaking, the anionic polymer created medium-sized flocs with a lumpy, jelly appearance, as shown in Figure 3-4(a). With a consistency, which can be likened to that of cottage cheese, the apparent glassy wet surface of the polymer amended FFT suggests the accumulation of released water on the surface, owing to the increased hydraulic conductivity of the FFT.

The structure created by mixing the cationic polymer with FFT is marked by fine floc sizes, while the neutral polymer produces large flocs. The neutral PT flocs initially developed as stringy particles during mixing and agglomerated into large spongy lumps after settling. The initial particle settling of neutral PT occurred within a couple of minutes, with a large volume of water released and clear water/solids separation. Once settled, the amended tailings could not be re-homogenized to its initial state. This physical behaviour was a challenge in obtaining representative subsamples from a batch of FFT amended with the neutral polymer. Thus, the adopted solution involved mixing only the amount of amended FFT required for each test so that the entire batch can be used for the test.

Figure 3-4: Initial condition and fabric of FFT after polymer treatment. (a) Anionic PT, (b) Cationic PT and (c) Neutral PT

3.3.2 Tailings Characterization

Geotechnical laboratory testing for basic tailings properties was conducted to characterize candidate untreated and polymer amended FFT. Table 3-4 presents a summary of the testing program, with a description of the test procedures in the following subsections of this thesis.

Table 3-4: Basic characterization test program

Test	Untreated FFT	Polymer amended FFT (each)
Solids content	6	3
Bitumen content	2	-
Particle size distribution (PSD)	2	1
Atterberg limits	1	1
Scanning Electron Microscopy	1	1
Specific gravity	2	-
XRD	1	-
MBI	1	1
Water chemistry	1	1

3.3.2.1 Solids content

The percentage of solids and the water content were the first index tests conducted on the untreated FFT. The tests were performed for each pail of FFT following the standard test procedure outlined in ASTM D2216-19. Prior to sampling, the tailings in each pail were homogenized, while ensuring accumulated solids on the walls and bottom corner of the pails were manually agitated. Three subsamples of homogenized FFT were taken from each pail for the test. The samples were weighed and oven-dried at a pre-set temperature of 105°C for 24 hours. The dried samples were weighed, and the solids content of tailings was determined as the percentage of dry mass over the wet mass of the sample. The mass percentage of water to solids of tailings was calculated as the water content.

3.3.2.2 Bitumen content

Dean Stark analysis was performed by AGAT laboratories Ltd on untreated FFT samples to determine the bitumen, mineral solids and water contents of FFT. The test was completed following the standard method used in the oil sands industry. A detailed test procedure is found in Appendix B.

3.3.2.3 Specific gravity

The specific gravity is an essential soil parameter in determining other soil characteristics, such as the particle-size distribution of fine-grained soils, void ratio and dry density. Two subsamples of homogenized FFT were analyzed for specific gravity in accordance with the test procedure described in ASTM D854 – 14. Appendix B outlines the test method used.

3.3.2.4 Particle size distribution

The particle-size distribution of the tailings was analyzed following the hydrometer test method described in ASTM D 422-63(2007)e2. The test was performed for both dispersed and non-dispersed conditions of the untreated FFT, and for polymer amended FFT without adding a dispersant. The test procedure is described in Appendix B.

3.3.2.5 Atterberg limits

The plastic and liquid limits of the untreated and amended FFT (including bitumen) were analyzed by AGAT laboratories Ltd to determine the changes in material behaviour with changing water content. These two limits refer to critical water contents at which FFT would behave as plastic and liquid, respectively. The liquid limit was determined using the Casagrande cup method. The ASTM D4318-17e1 outlines the procedure used for determining the liquid limit and plastic limit of the tailings.

3.3.2.6 Methylene blue adsorption

Replicates of tailings subsamples were prepared and sent to NAIT to determine the clay content by methylene blue adsorption following the test procedure described by Omotoso and Morin (2008). Solids were diluted with de-ionized water and mixed with 1M $NaHCO_3$ to achieve a concentration of 0.015M. The pH of the sample was adjusted to between 8 and 11 by adding 10% w/w NaOH to disperse the solids. Following dispersion, the suspension was acidified by adding 10% v/v H_2SO_4 to reduce the pH to between 2.5 and 3.8 to ensure Fe_2O_3 is positively charged and does not adsorb methylene blue. After sample preparation, the methylene blue titration was carried out until a light blue ring of excess methylene blue is observed around a drop of the prepared sample on a Whatman 42 filter paper (2.5µm pore size), indicating the saturation point was reached. The titration end-point is used to calculate a methylene blue index (MBI) and clay content.

3.3.2.7 Mineralogy

The mineralogical composition of untreated FFT was analyzed using X-ray diffraction (XRD). A dry, homogenous sample of Dean-Stark solids was pulverized to particle sizes less than 5 µm. X-ray diffraction analysis was carried out using a Rigaku Ultima IV X-ray diffraction system equipped with Cu-source. Diffraction data were obtained for incident angles traversing 5° to 80° 2θ. The measured diffraction pattern was described as an intensity vs 2θ plot using 2DP^{TM} data processing software, and subsequently analyzed for mineral identification and quantification.

The major minerals of FFT typically consist of quartz, kaolinite and illite (Kaminsky et al. 2009), while minor phases include carbonates and titanium oxides. Major and minor mineral phases of FFT were identified and quantified using the software Jade™. Minerals were identified by fitting and comparing observable peaks with known patterns of typical minerals of oil sands tailings. Quantification of the minerals was performed with using Rietveld method, which constrains peak positions and intensities for materials with known structures, like the main mineral constituents of oil sands tailings.

3.3.2.8 Scanning electron microscopy

Wet samples of untreated and polymer amended FFT were retrieved at the end of sedimentation and sent to the nanoFab characterization laboratory at the University of Alberta for scanning electron microscopy (SEM) imaging of the tailings microstructure. The samples were dried in a Savant SuperModulyo Freeze Dryer to maintain the material structure before testing. In-lens Field Emission SEM (FESEM) images of the freeze-dried samples were obtained at magnifications of 500×, 8,000× and 20,000× using the Zeiss Sigma FESEM imaging tool.

3.3.2.9 Water chemistry

The supernatant released from untreated and polymer amended FFT at the end of sedimentation were sampled, filtered and analyzed for water chemistry at AGAT laboratories Ltd. The process water samples were analyzed for pH, electrical conductivity, major cations and anions, and Total Dissolved Solids. The measured cations include Na^+, Ca^{2+}, Mg^{2+}, and K^+. Alkanity was measured as the combined concentration of HCO_3^- and CO_3^{2-} and other anions, Cl^- and SO_4^{2-}, were also determined. The ion concentrations were measured in mg/L and the sodium adsorption ratio (SAR) was calculated from the molar concentrations (mol/L) of Na^+ and divalent ions Ca^{2+} and Mg^{2+} using Equation 6. SAR is widely used to indicate, whether or not, the process water will produce dispersive slurries.

$$SAR = \frac{Na^+}{\sqrt{(Ca^{2+} + Mg^{2+})/2}} \tag{6}$$

3.4 Initial Dewatering

3.4.1 Hindered Sedimentation

One way of assessing the initial dewaterability of tailings is by performing a settling test. This test allows the tailings particles in suspension to freely fall and settle under gravity with time, while displacing the pore water to the surface.

The settling test was conducted on all candidate FFT samples (both untreated and amended) to investigate the effect of the polymer addition on the dewaterability of FFT. For each type of polymer amended FFT, a litre of the homogenized sample was transferred into a graduated cylinder immediately after treatment, and the initial time was recorded. With a rubber cap on the cylinder to minimize evaporation, the suspension was allowed to settle while regularly recording the solids/water interface height and the elapsed time. The settling test was allowed to run for several months uninterrupted, with the experimental setup shown in Figure 3-5.

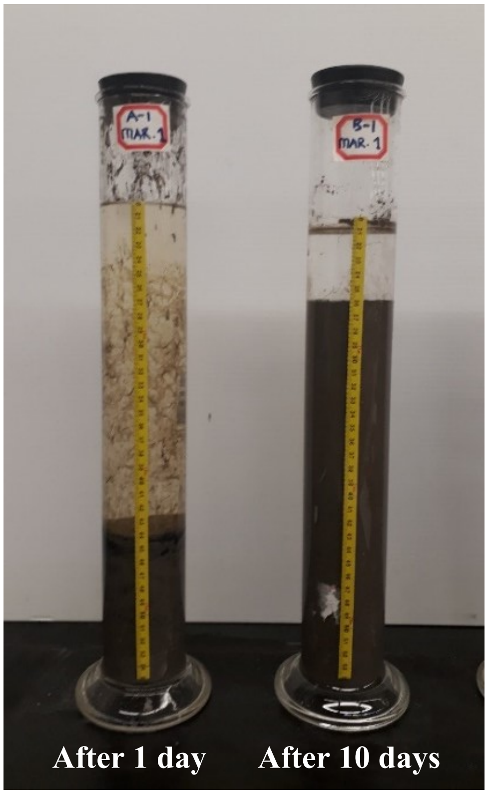

Figure 3-5: Column settling test

3.4.2 Capillary Suction Time

A simple method for assessing the filterability of tailings is by measuring its capillary suction time (CST). For the scope of this study, only the initial CST of the candidate samples was examined. The test was performed using a Triton CST measuring apparatus, equipped with a timing unit, a 50 mm high cylindrical column and two Perspex blocks as shown in Figure 3-6. A Whatman 4 qualitative filter paper with pore sizes ranging between 22-25 microns was used to generate water flow from the bottom of the sample by capillary suction. The upper Perspex block is fitted with two sets of electrodes, approximately 6.5 mm apart, which automatically start and stop an in-built timer once the wetting front reaches the inner and the outer electrodes, respectively. The filter paper provides filtration of the sample, permitting only clear water flow through it.

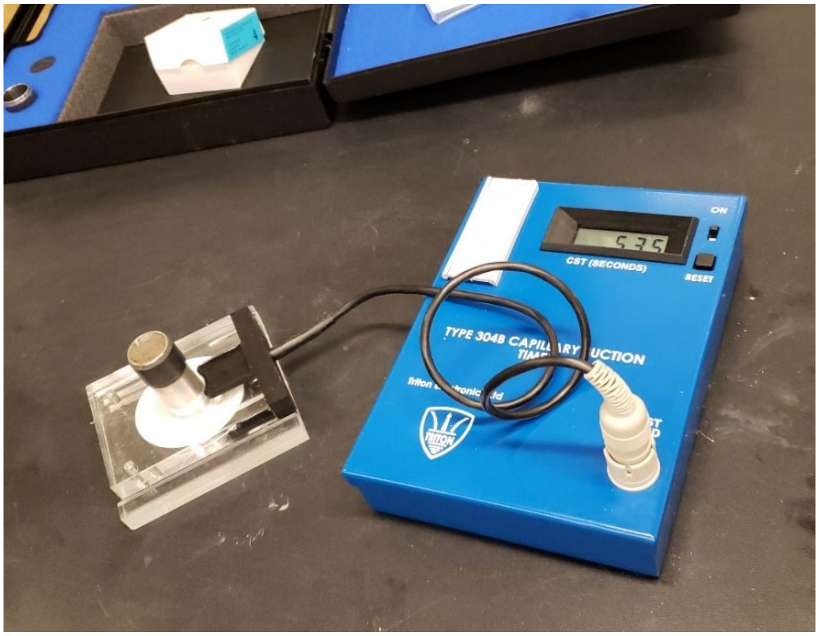

Figure 3-6: Capillary suction time testing apparatus

After setting up the CST apparatus with a new filter paper, the column was filled with a specimen of homogenized untreated FFT or freshly prepared polymer amended FFT. The timer automatically started once the water flow reached the inner electrodes. When the wetting front reached the outer electrode, the timer stopped, and the elapsed time of flow was recorded as the initial CST. The experiment was repeated for at least four additional specimens to obtain an average CST.

3.5 Large Strain Consolidation Testing

The large strain consolidation test (LSC) test yields three critical relationships, compressibility, hydraulic conductivity and shear strength, that describe the changing geotechnical characteristics and behaviour of FFT under different magnitudes of effective stresses. Untreated and polymer amended FFT were examined in a large strain consolidation testing program to determine their long-term consolidation and strength characteristics under incremental loading conditions. For each type of material, both original and duplicate samples were analyzed. Table 3-5 provides a summary of the LSC testing matrix.

Table 3-5: Large strain consolidation testing program

Material type	Sample ID	Vane shear test
Untreated FFT	Untreated FFT	Yes
Polymer A-1 amended FFT	Neutral PT S1	Yes
	Neutral PT S2	No
Polymer B-1 amended FFT	Cationic PT S1	No
	Cationic PT S2	Yes
Polymer A3338 amended FFT	Anionic PT S1	No
	Anionic PT S2	Yes
Aged polymer A3338 amended FFT	Aged anionic PT S1	No
	Aged anionic PT S2	Yes

3.5.1 LSC Setup and Sample Preparation

New 200 mm high by 150 mm diameter cylindrical Plexiglas cells with metal base and valves fittings for drainage were purposely constructed for the large strain consolidation testing program. At the base of each cell, three conduit openings with valve fittings exist; one for pore pressure measurement, another for hydraulic conductivity measurement and the third for deairing. A fourth outlet was located at the upper part of the cell to provide a constant head over the sample. Inside the cell, a porous stone plate, deaired in distilled water, was placed at the base to control and evenly distribute water flow through the bottom of the sample. For sample separation and filtration, the porous stone plate was overlaid with a filter paper (0.22-micron pore size). After flushing the base and ports with distilled water, the cells were filled with candidate samples to the invert level of the top drainage outlet. The total pore pressure in the material was measured with a pressure transducer connected to an electronic data logger. For visual observation of settlement to 1-mm accuracy, the cells were graduated with a metric tape.

LSC testing equipment with a maximum loading capacity of 1,500 kPa was employed in the experimental investigation for the long-term consolidation properties of FFT. The equipment comprises a regulated pressurized air bellofram seated on a loading frame through which effective stresses are applied to the sample in the cell. Measurements of settlement and pressure are respectively taken with a linear variable differential transformer (LVDT) and pressure transducers, while an attached constant head permeability setup provides the measurement of hydraulic conductivity during the consolidation test. Figure 3-7 illustrates the LSC testing apparatus utilized for the experimental work.

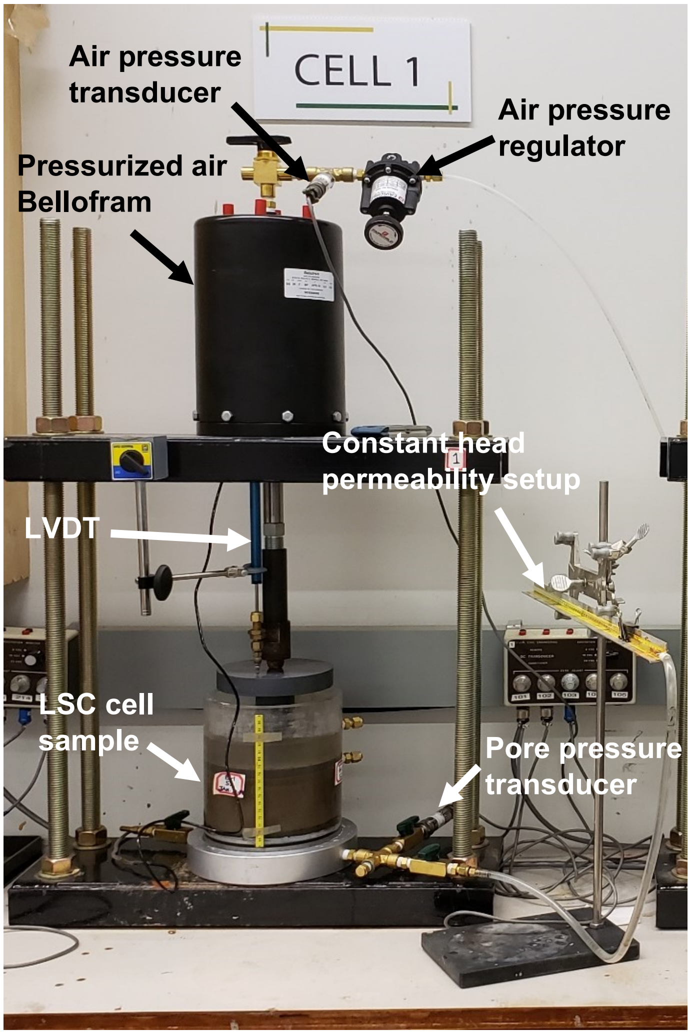

Figure 3-7: Large strain consolidation testing apparatus

3.5.2 Criteria for End of Consolidation

Unlike stiff soils, soft soils like tailings undergo large volume changes under compressive stresses. These large volumetric strains alter the geotechnical properties of the material in a non-linear way (Gibson et al., 1967) and this non-linear behaviour is best determined in an LSC test. Jeeravipoolvarn et al. (2015) summarized the assumptions of the LSC test. One of these assumptions is that, in large strain consolidation, only the primary consolidation of the material, indicated by the complete dissipation of excess pore pressure, is considered. However, the end of consolidation for each LSC load step in this study was determined by the following indicators:

- Vertical deformation of the sample under the applied load is infinitesimal; and,
- Excess pore pressure generated in the material as a result of the applied load is entirely dissipated.

3.5.3 Self-weight Consolidation

After the tailings amendment, the flocs remain in suspension as water is trapped in the pores of the sample. Confinement of pore water generates some excess pore water pressure, which must be dissipated during an initial consolidation/settling process. The initial consolidation occurs under the sample's own weight as the flocs settle under gravity, displacing pore water to the surface.

Prior to loading, the freshly prepared LSC cell samples were allowed to consolidate under their own weight until excess pore pressure has dissipated. While measuring the total pore pressure, the resulting vertical deformation of the samples was monitored by time-lapse photography until the end of self-weight consolidation. In addition to the aforementioned indicators, the settling test served as a guide in estimating the time to reach the end of self-weight consolidation. The measured deformation in this loading stage permitted the initial change in void ratio in the compressibility curve to be calculated.

3.5.4 Multi-step Loading

After deposition, tailings are subjected to different magnitudes of vertical stresses from overlying layers in storage facilities. The imposed stresses vary from self-weight to several hundreds of kilopascals, depending on the height or depth of the deposit. Under these stresses, the deposit undergoes various degrees of consolidation, resulting in an improvement of its geotechnical properties for reclamation purposes.

Subsequent to self-weight consolidation, effective stresses ranging from 0.3 kPa to 900 kPa were incrementally applied to the samples during the LSC experiment. For effective consolidation, each newly applied load was approximately twice the previous load. Two loading systems were adopted in the experiment: dead weight surcharge and pressurized air. Due to air fluctuation, effective stresses less than 10 kPa were imposed on the samples using dead weights equivalent to the desired stress for accuracy. Loads above 10 kPa were applied by pressurized air from a regulated bellofram through a loading frame as shown in Figure 3-7. The bellofram system was equipped with a pressure transducer to monitor the applied air pressure.

3.5.5 Vertical deformation measurement

As one of the indicators of consolidation, vertical deformation of tailings under imposed stresses is indicative of the compressibility of the material and allows the changes in the void ratio of the material during consolidation to be determined. There are two ways of determining the void ratio of soil; either by measuring the soil water content, degree of saturation and specific gravity, or by measuring the volume of voids and the volume of solids. Both methods rely on phase relationships for calculating the void ratio. Prior to consolidation, it was most appropriate to determine the initial void ratio by measuring the water content and assuming the samples are fully saturated. However, since it is impossible to measure the water content of the sample during consolidation, the vertical deformation of the sample under each load was relied on to determine the void ratio at the end of every load step.

A calibrated linear variable differential transformer (LVDT), with a measuring limit of 100 mm, was installed on each LSC sample to measure vertical deformations from imposed stresses. As depicted in Figure 3-7, the LVDT was electronically connected to the data logger to record and monitor readings during consolidation. The deformation was deemed complete only when infinitesimal changes in sample height were observed for the load step. Given the constant cross-sectional area of the LSC cell, the measured deformation is equivalent to the change in volume of voids, from which the void ratio can be determined. The procedure was repeated for each load step until completion of the consolidation test.

3.5.6 Pore water pressure measurement

Measurements of pore water pressure in the samples were required for monitoring the consolidation progress and for determining the end of consolidation. Each LSC cell was equipped with a calibrated positive pressure transducer electronically connected to the data logger for real-time recording and monitoring of the total pore water pressure (excess plus hydrostatic pore pressures) throughout the consolidation process. Excess pore pressure generated in the sample as a result of loading was observed as spikes commensurate with the applied load. After loading, the excess pore pressure dissipates with time until a hydrostatic pore pressure is achieved, indicating the end of consolidation. As a routine quality control practice, the transducers were regularly inspected and replaced, if found faulty.

3.5.7 Hydraulic conductivity measurement

A change in void ratio is understood to be a change in the interparticle pore size of the sample and has a direct effect on the saturated hydraulic conductivity of the material. The initial hydraulic conductivity of the unconsolidated sample was estimated from the settling test using Equation (7) (Pane and Schiffman, 1997; Scott et al. 2008).

$$v_s = -\left(\frac{\gamma_s}{\gamma_w} - 1\right)\frac{k}{1+e} \tag{7}$$

where,

v_s = initial settling velocity,

γ_s = the unit weight of solids,

γ_w = the unit weight of water,

k = the hydraulic conductivity and

e = the initial void ratio.

During consolidation, the saturated hydraulic conductivity of the samples was measured at the end of each load step with the aid of a constant head permeability setup shown in Figure 3-8.

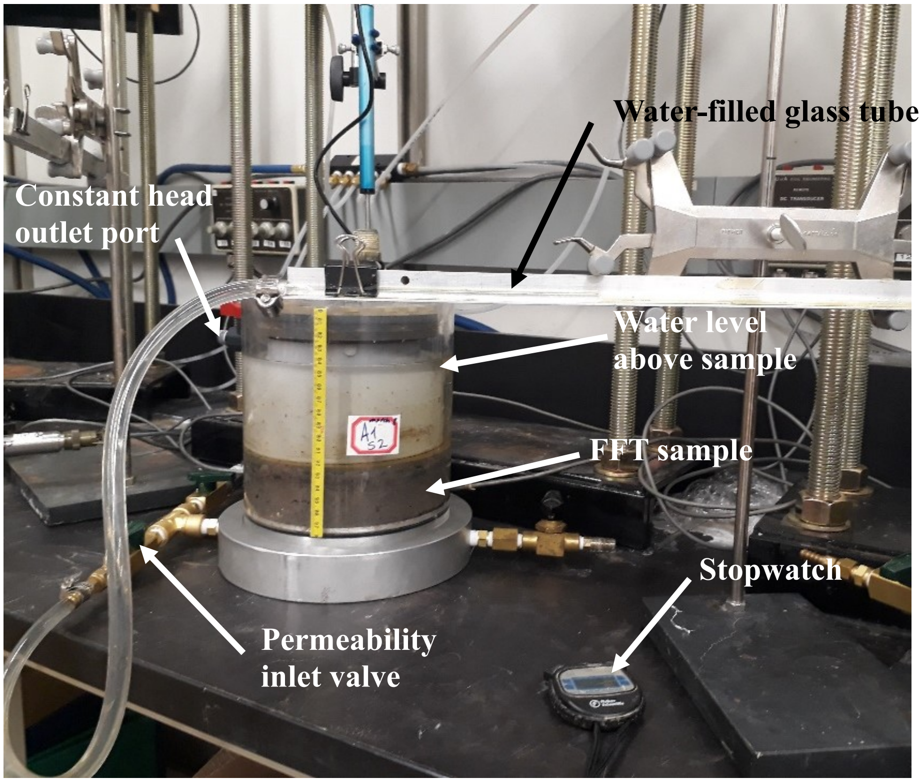

Figure 3-8: Constant head permeability setup for LSC

The setup consists of a transparent glass tube, 4mm in diameter, connected to one of the bottom outlet ports of the cell with a transparent flexible tube. The glass tube is horizontally suspended on a graduated clamp at a height above the LSC cell to establish a constant head between the glass tube and the water surface in the cell. The elevation head difference is kept constant by allowing drainage of excess seepage water through the top drainage port of the cell to maintain upward water flow through the sample.

After deairing the port and tube by allowing downward seepage flow through the sample, the glass tube was filled with distilled water and clamped. The water level in the cell was increased till overflow occurred through the constant head port, and the height of the glass tube was adjusted to create a hydraulic gradient until an upward flow through the sample was observed. While the flow rate steadied, the heights of the glass tube, water and sample were recorded to calculate the actual hydraulic gradient. The hydraulic gradient was kept small enough for each load step to avoid exceeding existing stress and causing a seepage failure. Measurements of the flow distance along the glass tube and elapsed time were recorded to determine the flow velocity, and the saturated hydraulic conductivity was calculated by Darcy’s law. The constant head permeability test was conducted on both original and duplicate candidate FFT samples analyzed in the LSC test.

3.5.8 Undrained shear strength measurement

In addition to the compressibility and hydraulic conductivity, the shear strength development of the materials under the imposed stresses was assessed during consolidation. At the end of each load step, a vane shear test was conducted on the samples to determine the undrained shear strength of the material. In this test, only the duplicate samples were examined to allow the effect of sample disturbance to be evaluated. Soft consistencies (less than 8 kPa) were analyzed with a Brookfield DV3T rheometer, while a motorized vane shear apparatus was used for testing stiffer consistencies, as shown in Figure 3-9. Standard vane sizes and torque springs (for vane tester) by the manufacturer were employed in the shear strength measurement.

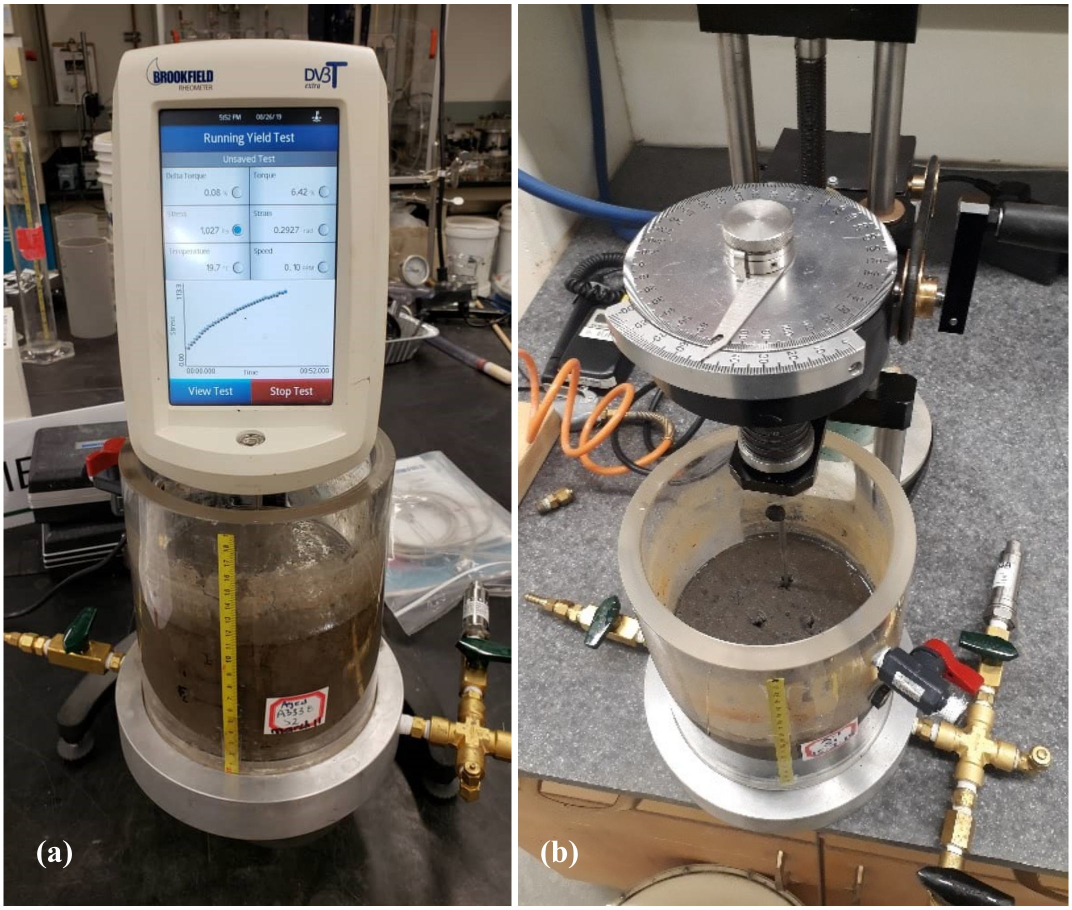

Figure 3-9: (a) Brookfield DV3T rheometer and (b) Motorized vane shear apparatus

Upon completion of the constant head permeability test, the duplicate samples were prepared for shear strength testing by syphoning the supernatant water. Depending on its strength measuring range, a suitable vane blade size was installed on the apparatus and vertically inserted in the sample to a depth about twice the height of the vane blade. The sample was automatically sheared at a constant rate of 0.1 rpm with the rheometer, and 60° per minute with the vane apparatus. In this study, only the peak shear strength of amended tailings was of interest, and thus, the remoulded strength was not measured. With the rheometer, the test automatically stops once the peak shear strength is reached, while the motorized vane apparatus was manually stopped after reaching the peak value. For the vane shear strength, the initial and final angles of rotation were respectively recorded at the start and end of the test, noting the vane size and the spring number. Based on the rotation angle, the measured torque is correlated to the undrained shear strength by applying the corresponding spring and vane calibration factors provided by the manufacturer. The peak shear strength was averaged for two or three shear tests conducted on each sample.

3.6 Thixotropic Behaviour of Polymer Amended FFT

Two LSC cells of FFT amended using the anionic polymer were prepared for evaluating the short-term thixotropic behaviour and effects on the strength and consolidation properties of polymer amended FFT. For a period of 16 weeks, these samples were set aside to age after treatment without loading. On a weekly basis, the surface's undrained shear strength was estimated by the fall cone method (Hansbo, 1957) using a Swedish fall cone apparatus as shown in Figure 3-10, while recording the measured pore pressure from the transducer. Prior to conducting the fall cone test, the cells were emptied of supernatant water in order to access the surface of the solid.

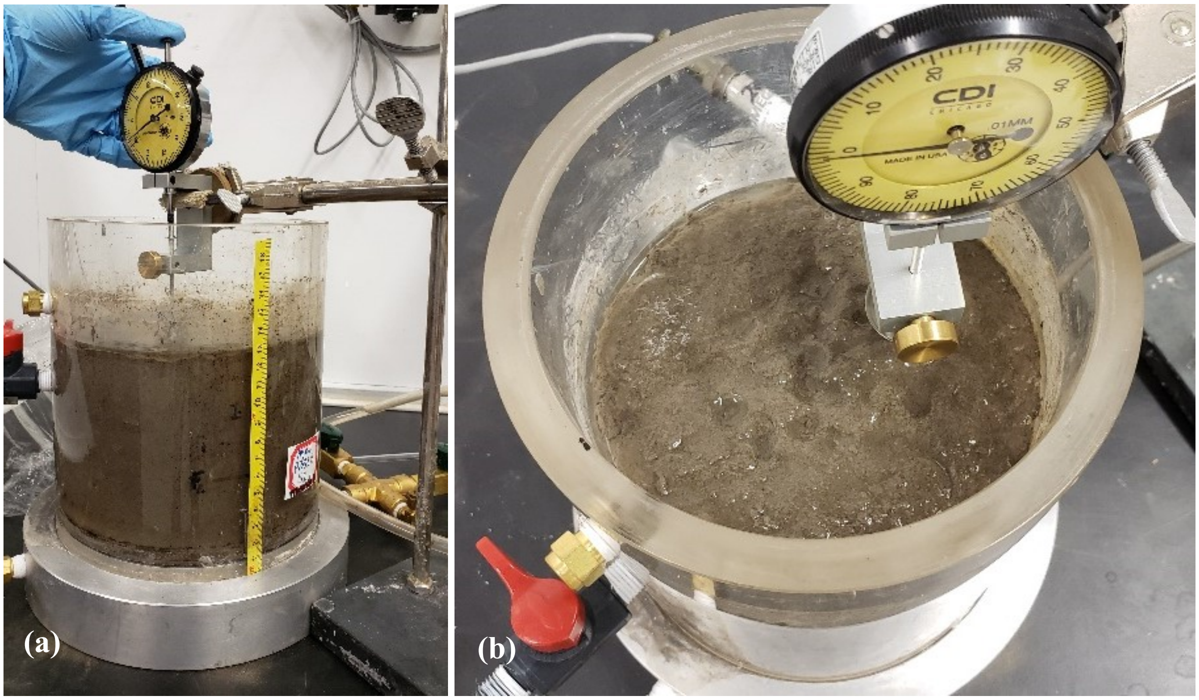

Figure 3-10: Fall cone testing of aged polymer amended FFT:
(a) Side view, (b) Top surface.

The observed surface consistency of the samples allowed the use of only the 10 g cone with 60° apex angle in the fall cone shear strength measurement throughout the ageing period. The shear strength was correlated from the cone penetration in the sample by applying a corresponding cone constant of 0.26 calculated from the device manufacturer's specification. At the end of the 16 weeks of monitoring, the saturated hydraulic conductivity and vane shear strength were measured on the samples prior to the start of the large strain consolidation tests, in adherence to the respective test procedures described in the preceding subsections.

Surface disturbance of the sample observed during the fall cone test after several weeks led to a decision to repeat the test for accurate measurements to be obtained. This time, a total of 16 subsamples of the anionic polymer amended FFT were each prepared in a 250 mL container and allowed to age with minimum evaporation (Figure 3-11). At the end of every week, a subsample was tested for the peak undrained shear strength using both fall cone and rheometer shear testing methods, as shown in Figure 3-12, to obtain a 16-week shear strength profile for the ageing period.

For consistency with the fall cone test, the rheometer shear test was performed within the upper 20 mm of the sample.

Figure 3-11: Ageing of 16 subsamples of polymer amended FFT

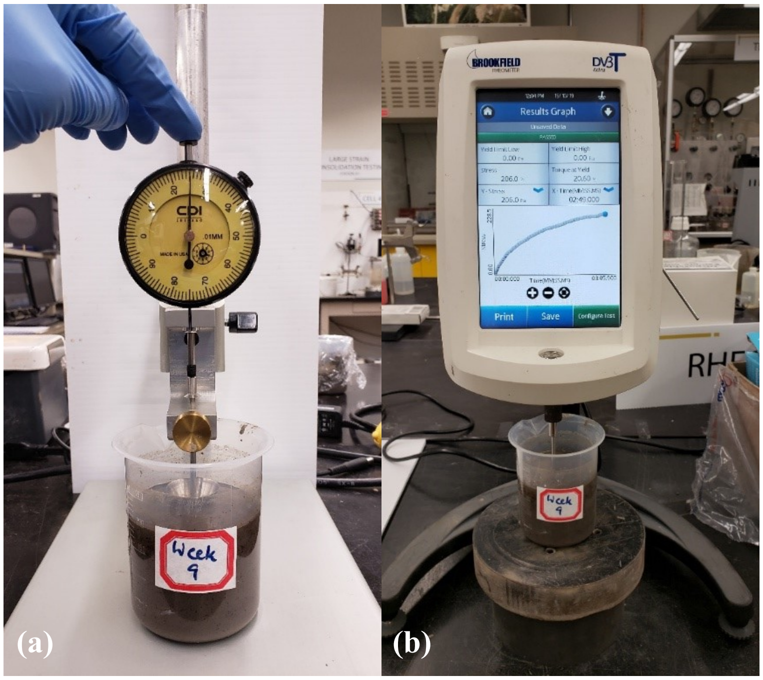

Figure 3-12: Peak undrained shear strength and Yield stress measurement: (a) Fall cone test, (b) Brookfield rheometer.

Chapter 4: Results and Analyses

This chapter presents the results of the experimental testing program completed in this study, including tailings characterization, capillary suction time, hindered sedimentation, ageing and large strain consolidation experiments. The long-term consolidation of a deep in-pit deposit of the different tailings was modelled and analyzed, and the results are also presented.

4.1 Tailings Characteristics

4.1.1 Basic tailings properties

The initial properties of FFT measured before and after flocculation from geotechnical characterization tests are presented in Table 4-1. The untreated tailings had a solids content of 30.5% and bitumen content of 2.4%. With a measured specific gravity of 2.27, the initial void ratio of FFT was 5.17. Fresh samples of anionic, cationic, and neutral polymer amended FFT had solids contents of 28.9%, 23.6%, and 13.7%, respectively, due to the different polymer dosages and the volume of polymer solution added to FFT in each treatment.

Table 4-1: Initial tailings properties

Material	Solids content (%)	Fines content (%)	Sand-fines ratio (SFR)	Initial void ratio
Untreated FFT	30.5	94	0.06	5.17
Neutral PT	13.7	NM	NM	14.25
Cationic PT	23.6	92	0.09	7.44
Anionic PT	28.9	72	0.39	5.63

Note: NM, not measured

4.1.1.1 Particle size distribution

Hydrometer and wet sieve analyses were performed to determine the particle size distribution of untreated and treated FFT. The wet sieve method was used to obtain the coarse grain distribution (>44 microns) of the untreated FFT but was unsuitable for floc size measurements. Figure 4-1 shows the particle size distribution of the tailings. The untreated FFT (including bitumen) was analyzed for both dispersed and non-dispersed conditions, while the tested treated samples were non-dispersed.

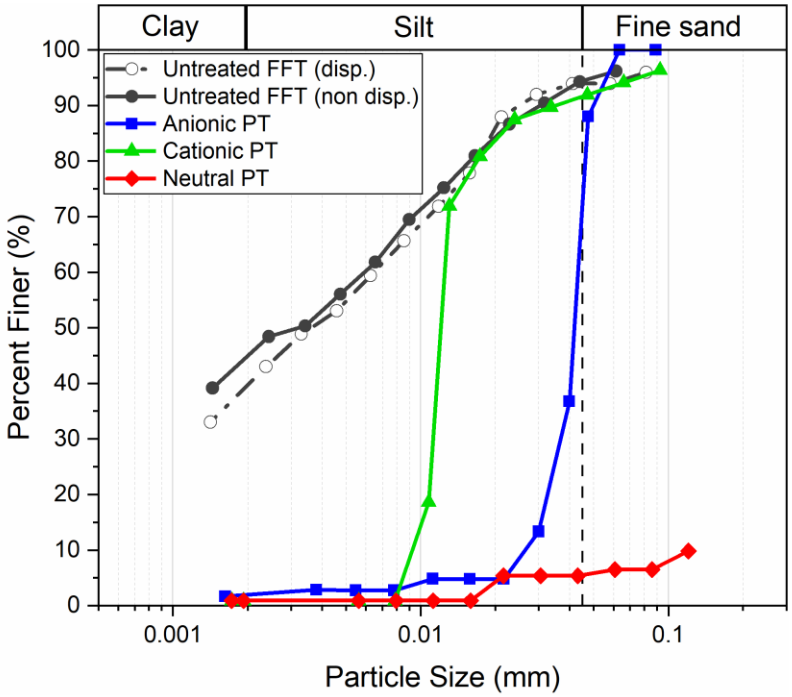

Figure 4-1: Particle size distribution of untreated and polymer amended FFT

The untreated FFT had a fines content (< 44 μm) of 94 %, and 40 % of its total mass consists of clay-sized particles. The dispersed and non-dispersed untreated FFT have a similar, well-graded particle size distribution, which indicates that the as-received condition of FFT was dispersed.

The addition of the neutral polymer to FFT produced approximately 92% of the flocs larger than 0.1 mm and approximately 6% by total mass finer than 44 microns with no apparent clay-sized particles. The distribution of the large floc sizes required optical digital imaging methods, which were not employed in this work.

The anionic polymer treatment produced a uniformly graded floc distribution with approximately 95% of flocs ranging from 0.02 mm to 0.06 mm in size. The flocs finer than 44 microns was 72% of the total mass, of which about 2% are clay-sized. An SFR of 0.39 was calculated based on the proportion of sand size flocs.

The cationic polymer treatment resulted in a uniform aggregation of particles finer than 11 microns, while larger particle sizes were similar to those of the untreated FFT. The treated FFT had a fines content of 92% by total mass, devoid of clay size particles.

4.1.1.2 Atterberg limits

Samples of the untreated and treated FFT were analyzed to determine the liquid limit, plastic limit and plasticity of each type of tailings. Table 4-2 presents the Atterberg limits of the different tailings tested, while Figure 4-2 describes their plasticity.

Table 4-2: Atterberg limits

Material	Liquid limit (%)	Plastic limit (%)	Plasticity index (%)	Initial Liquidity index
Untreated FFT	52	30	22	9.0
Neutral PT	82	46	36	16.2
Cationic PT	76	44	31	8.9
Anionic PT	78	39	38	5.4

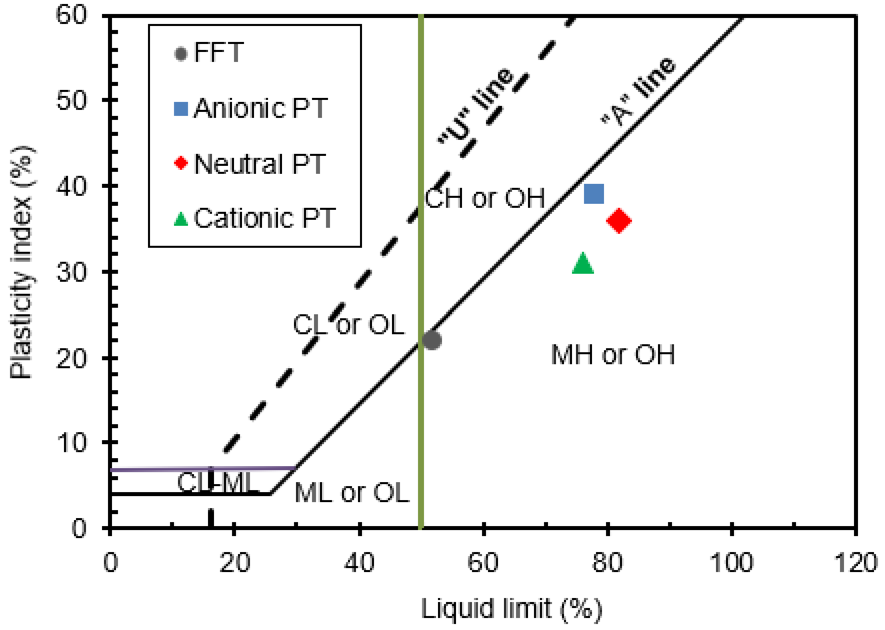

Figure 4-2: Plasticity chart for untreated and polymer amended FFT.

The untreated FFT had a liquid limit of 52% and a plasticity index of 22%, which are within the typical range for MFT (Beier et al. 2013). The anionic, cationic and neutral polymer treatments increased the liquid limit and plasticity index of FFT. The post-treatment water contents and Atterberg limits of the tailings indicate that the cationic polymer-treated tailings and untreated FFT exhibit a similar initial liquidity index. While the liquidity index of FFT reduced after treating FFT with the anionic flocculant, the neutral PT increased the liquidity index to 16.2 due to the volume of polymer solution added. The plasticity chart shows reduced FFT plasticity by all treatments.

4.1.2 Clay content and mineralogy

Three replicates of each tailings type were analyzed to determine the clay content by methylene blue adsorption. Table 4-3 presents the clay content of the tailings as measured by MBI using Equations 8 and 9 (Kaminsky, 2014; Kaminsky and Omotoso, 2018). The initial clay to water ratio (CWR) of the tailings was calculated based on the Dean-Stark extraction and MBI data using Equation 10 and is included in Table 4-3 .

$$MBI\left(\frac{meq}{100g}\right) = \frac{mL\ of\ MB\ \times Normality\ of\ MB}{Mass\ of\ dried\ sample\ (g)} \times 100 \tag{8}$$

$$\%\ Clay = \frac{MBI\left(\frac{meq}{100g}\right) + 0.04}{0.14} \tag{9}$$

$$CWR\ =\ (C\ *\ S)/(1-(S+b)) \tag{10}$$

where: S = mineral solids content (%), C = clay content (%), b = bitumen content (%)

Table 4-3: Clay content of tailings

Material	Clay content by MBI (%)	Average Initial CWR
Untreated FFT	50.6 ± 0.21	0.21
Neutral PT	41.2 ± 2.27	0.05
Cationic PT	40.5 ± 4.57	0.11
Anionic PT	51.8 ± 0.80	0.19

The mineral composition of the untreated FFT was characterized by X-ray diffraction (XRD). The observed XRD pattern is shown in Figure 4-3. The major minerals identified in the FFT are quartz and kaolinite. Minor constituents comprised illite, calcite, siderite with trace amounts of anatase, rutile, pyrite and zircon. The proportions of the minerals identified by total weight are provided in Table 4-4. A clay content of 38.9 % was calculated from the sum of kaolinite and illite fractions.

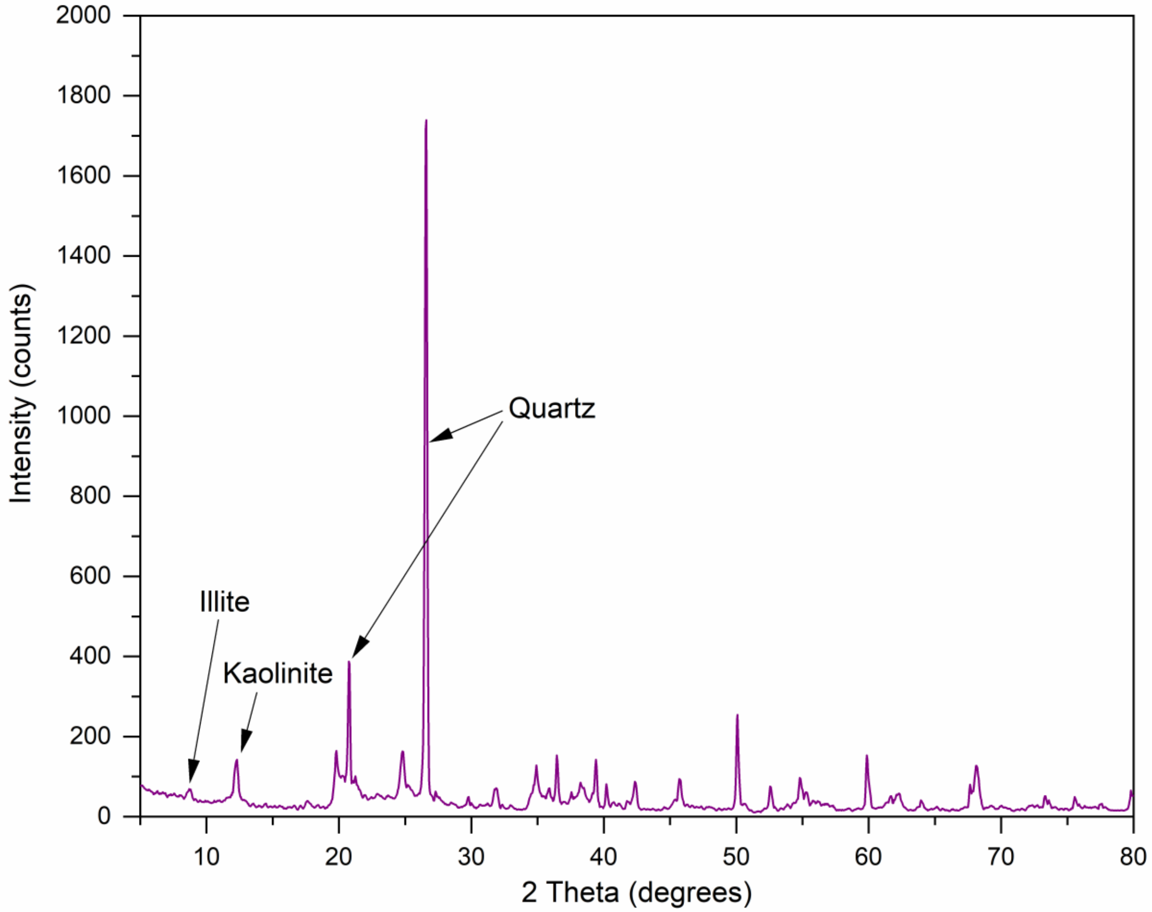

Figure 4-3: XRD pattern for untreated FFT

Table 4-4: Mineral composition of untreated FFT by XRD

	Mineral	% conc. wt./wt.	Standard deviation
Clays	Kaolinite	22.1	0.6
	Illite	16.8	0.3
Carbonates	Calcite	4.7	0.3
	Siderite	4.9	0.3
Titanium oxides (TiO2)	Anatase	2.2	0.1
	Rutile	1.5	0.1
	Pyrite (FeS_2)	1.9	0.1
	Zircon	1.2	0.1
	Quartz	44.7	2.5

4.1.3 Tailings microstructure

Figure 4-4 shows micro- and nano-scale images of the untreated and polymer amended FFT after sedimentation obtained from a scanning electron microscope. The SEM images of the polymer amended tailings reveal that the floc microstructure consists of flocculated clay mineral platelets with ramdom orientations. The flocs are formed by edge-to-edge and edge-to-face associations between clay mineral surfaces. Mineral layering and face-to-face particle association are also seen to contribute to flocculation by the neutral polymer (Figure 4-4E and Figure 4-4I), while edge-to-edge and edge-to-face association of clay mineral booklets can be observed in the cationic and anionic PT flocs. The untreated FFT exhibits a card-house microstructure formed by edge-to-face association of dispersed clay minerals due to interactions between the charged mineral surfaces.

The pore spaces in each tailings type vary in size and are irregularly shaped. The voids observed in the neutral PT range in width from 1μm to 5μm approximately (Figure 4-4A) and a close-up view reveals small pore spaces < 200nm between clay mineral platelets (Figure 4-4I). The pore sizes of the cationic PT are relatively large compared to the neutral PT (Figure 4-4B), which enhance the hydraulic conductivity of the tailings. However, a cluster of fine minerals with pores less than 50nm in size can be observed in Figure 4-4J. The anionic PT flocs exhibit a more compact structure due to its high mineral solids content after treatment. On the other hand, the card-house structure and dispersed state of the untreated FFT create larger pore spaces ranging from about 3µm to 10µm between the clay minerals (Figure 4-4D). It is evident that the addition of the cationic, anionic and neutral polymers to FFT effectively binds clay minerals by neutralizing the mineral surface charges.

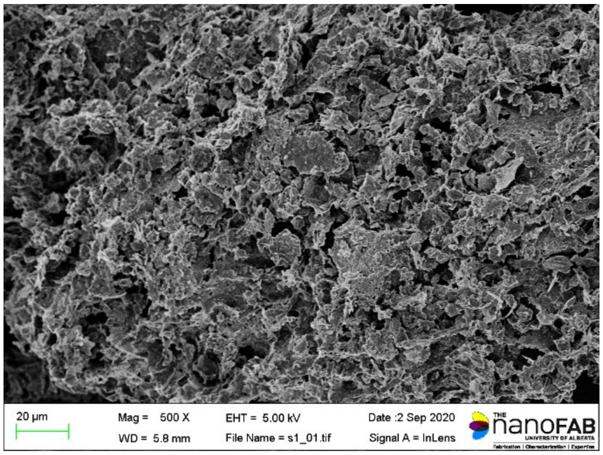

A. Neutral PT ×500 (10µm scale)

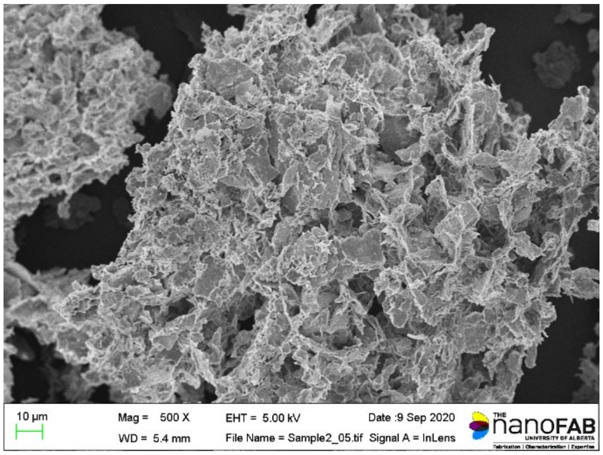

B. Cationic PT ×500 (10µm scale)

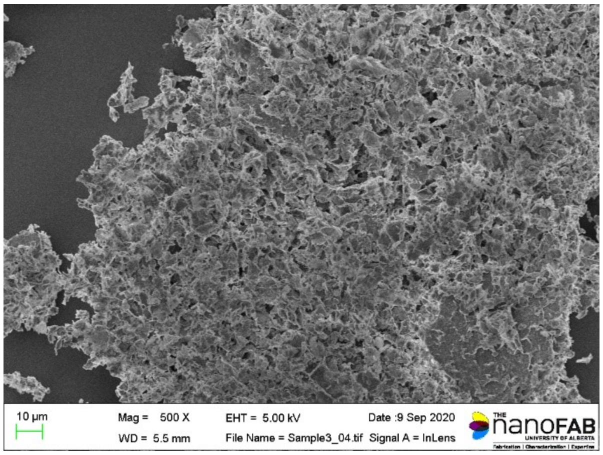

C. Anionic PT ×500 (10µm scale)

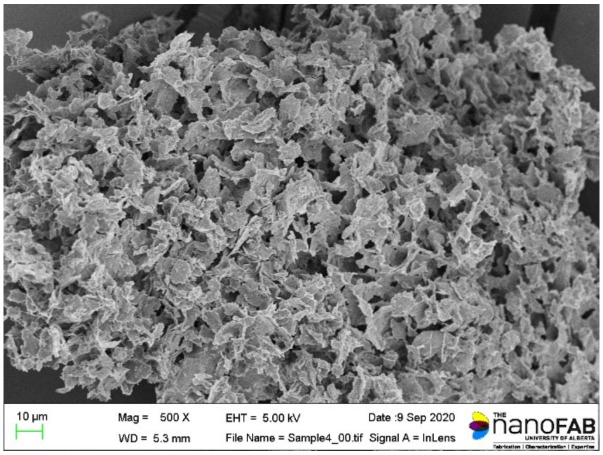

D. Untreated FFT ×500 (10µm scale)

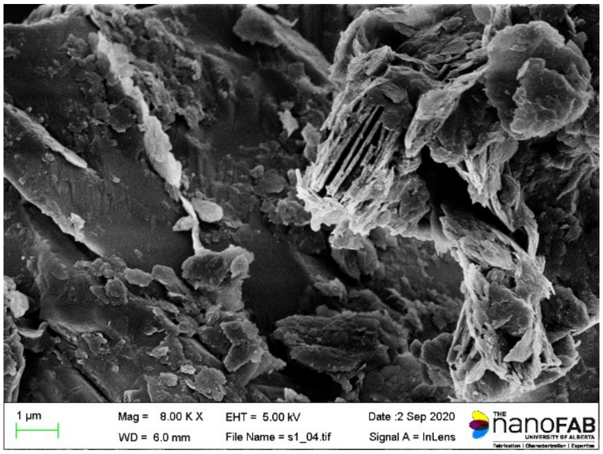

E. Neutral PT ×8000 (1µm scale)

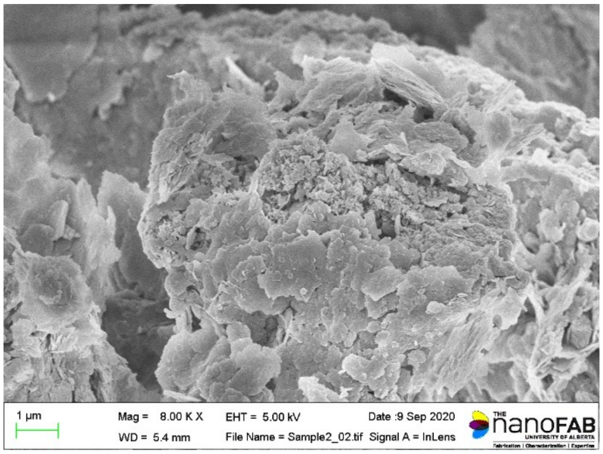

F. Cationic PT ×8000 (1µm scale)

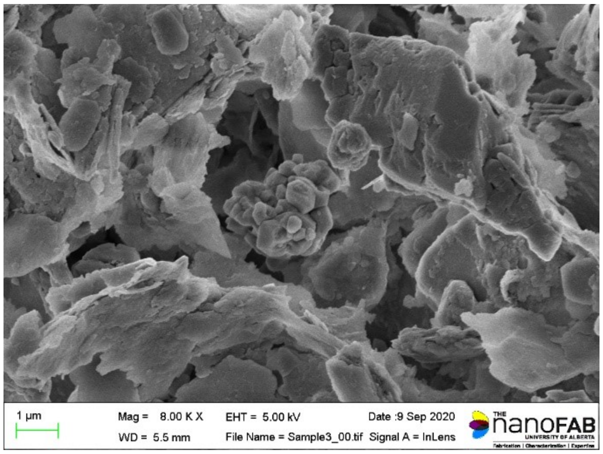

G. Anionic PT ×8000 (1µm scale)

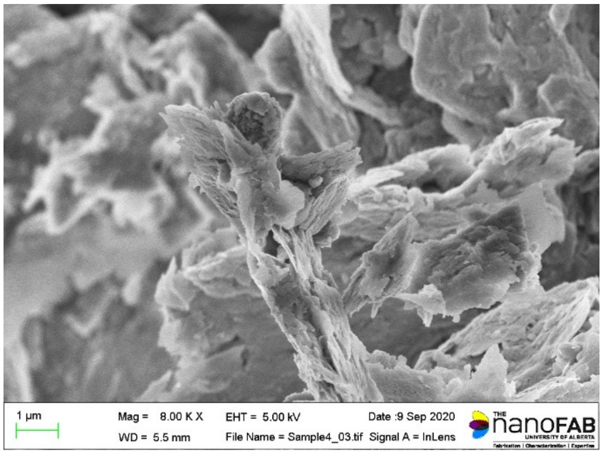

H. Untreated FFT ×8000 (1µm scale)

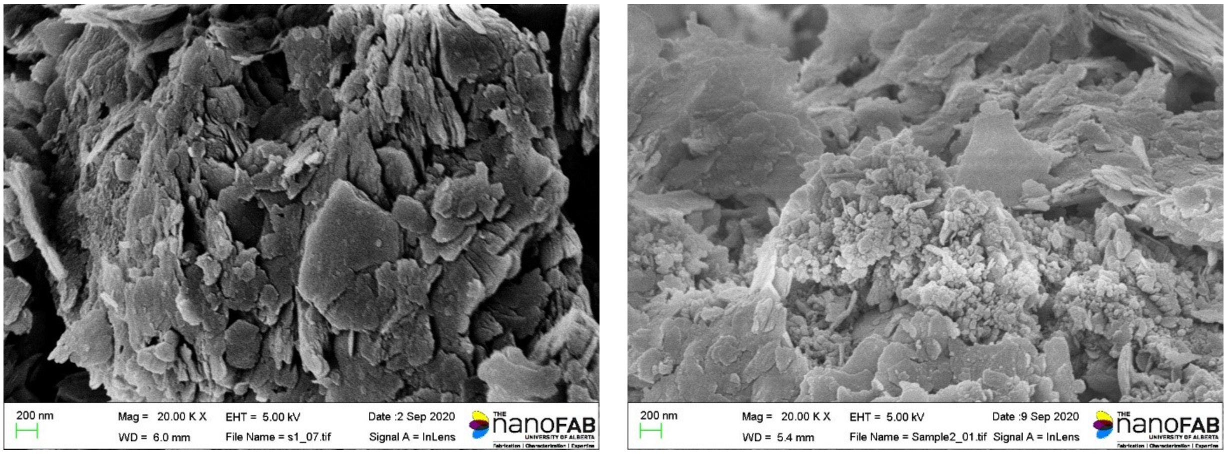

I. Neutral PT ×20000 (200nm scale)

J. Cationic PT ×20000 (200nm scale)

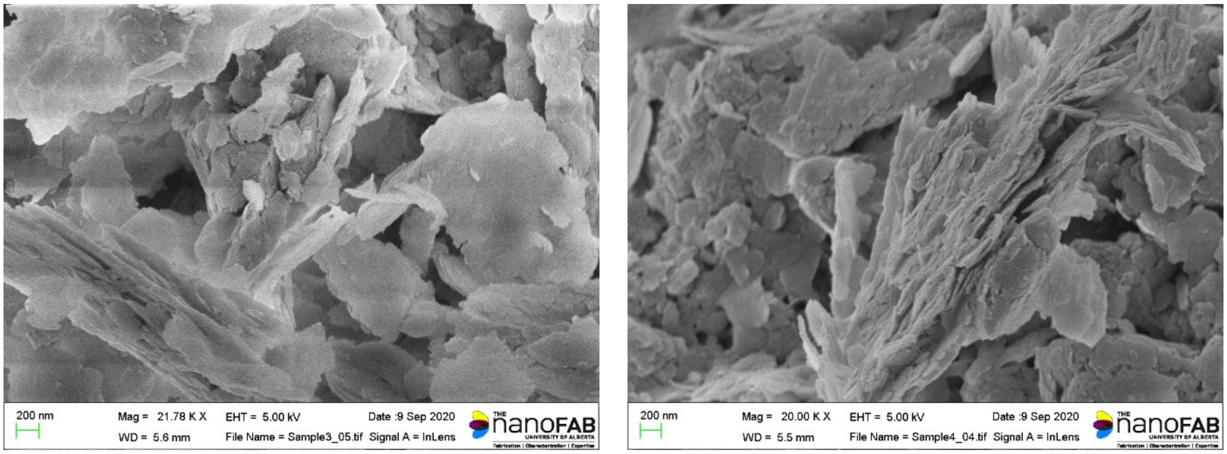

K. Anionic PT ×21780 (200nm scale)

L. Untreated FFT ×20000 (200nm scale)

Figure 4-4: Scanning electron microscope images of untreated and polymer amended FFT after sedimentation.

4.1.4 Water chemistry

Table 4-5 presents the water chemistry of untreated and polymer amended FFT at the end of sedimentation. In general, the measured pH, electrical conductivity and ion concentrations in each tailings type are within the existing ranges compiled by Johnston (2018). The dominant cation in the tailings was sodium (Na^+), while the bicarbonate (HCO_3^-) and sulfate (SO_4^{2-}) concentrations were also high. The anionic PT produced the highest pH, conductivity, and concentrations of Na^+ and SO_4^{2-}. On the contrary, the addition of the neutral polymer to FFT reduces the concentrations of Na^+, Ca^{2+}, Mg^{2+} and Cl^- as well as the conductivity by more than half, with a reduction in alkalinity. The sulfate content in FFT is almost consumed by the neutral polymer, reducing the concentration to 16mg/L. The cationic PT had relatively little effect on the water chemistry of FFT compared to the neutral and anionic PT. The ionic interaction between the polymer and the tailings is beyond the scope of this study. The resulting concentrations of cations in the neutral and cationic PT reduced the SAR value of FFT to 7.03 and 9.17, respectively. However, the anionic PT increased the SAR due to high Na^+, but low Ca^{2+} and Mg^{2+} concentrations. The water chemistry data of the tailings is included in Appendix A.

Table 4-5: Water chemistry of untreated and polymer amended FFT

Tailings	pH	Electrical Conductivity (μS/cm)	Aqueous ion concentration (mg/L)							SAR
			Na^+	Ca^{2+}	Mg^{2+}	K^+	Cl^-	HCO_3^-	SO_4^{2-}	
Untreated FFT	7.96	2370	377	61.2	30.7	19.1	175	512	595	9.82
Neutral PT	7.66	949	167	21.7	12.8	13.1	58	454	16	7.03
Cationic PT	8.02	1890	293	52.3	27.4	18.3	308	361	279	8.17
Anionic PT	8.51	2470	430	35.5	24.6	18.0	194	294	774	13.6

Slurries are likely to be non-dispersive (or settling) if the SAR value of the process water is less than about 10, but dispersive at higher SAR values (Vietti 2018; Mitchell and Soga 2005). The SAR values of the neutral and cationic PT water indicate a flocculated state, which is consistent with the settling behaviour observed during sedimentation. Recycling of the neutral PT supernatant for oil sands processing would require increased amounts of process aids (NaOH) compared to the other polymer treatments to achieve the required clay dispersion for bitumen extraction.

4.2 Initial Tailings Dewatering

4.2.1 Capillary suction time

The initial dewaterability of treated and untreated FFT was assessed by the capillary suction time (CST) test. At least four CST measurements were obtained on each type of tailings tested, and the results are shown in Figure 4-5, with a high CST value indicating low initial dewaterability.

Results show that the polymer treatments enhanced the initial dewaterability of FFT. The addition of the anionic polymer increased the initial FFT dewatering rate by about twice as much. The highest initial dewatering occurred after treating FFT with the cationic polymer, as indicated by a CST of 46 s. With a standard deviation of 7 s, the CST of the cationic PT was more repeatable relative to the mean value compared to the anionic PT and untreated FFT, which showed similar variability. The neutral polymer produced initial dewatering rates somewhat between those of the anionic PT and the cationic PT, but over a much wider range of CST values with a standard deviation of 91s. This large variability is attributed to the fact that the subsample of the neutral PT used in the CST test was unable to representatively capture the macrostructure of the neutral PT due to the size of the CST column, hence the large error.

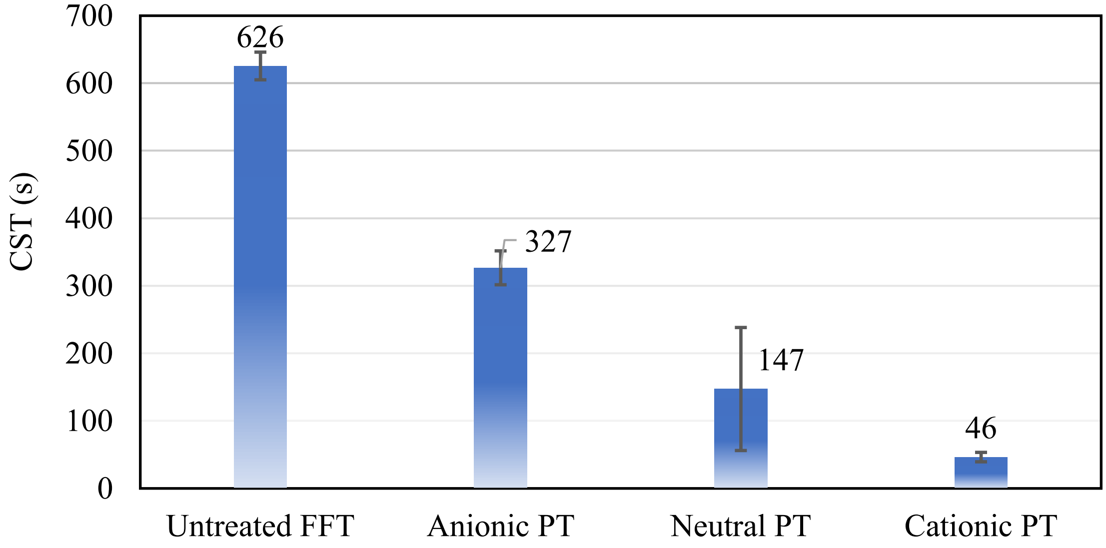

Figure 4-5: Initial capillary suction time of polymer amended and untreated FFT

4.2.2 Hindered settlement

Particle settling of a litre of each tailings type was monitored in a graduated transparent column using time-lapse photography. The sediment-water interface height was measured to the nearest millimetre, and the corresponding elapsed time was recorded. Figure 4-6 shows the profile of the interface settlement normalized to the initial sample height with time for the treated and untreated FFT.

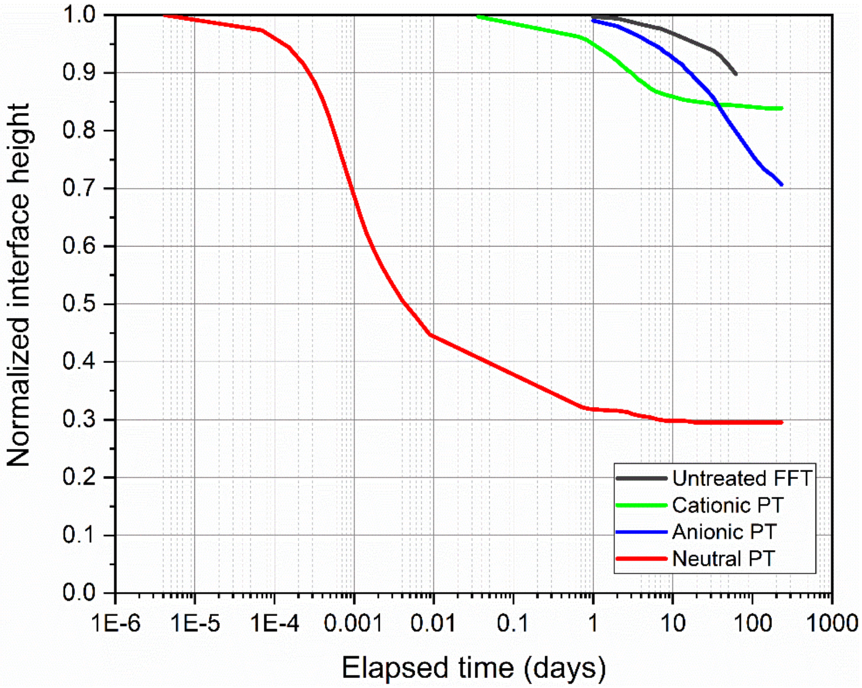

Figure 4-6: Settlement interface height of polymer amended and untreated FFT

Clear water separation from solids was observed during sedimentation in all three polymer treatments. Figure 4-6 shows a settling time difference of 3 days between the neutral and cationic treatments, and about 17 days between the neutral and anionic PTs for a 10% settlement of the total sample height. The neutral PT completed approximately 90% of the total settlement after 2.5 hours with little or no further settlement observed after 24 hours. The cationic PT settled by 5% after 24 hours, increasing to a final settlement of 15% after 10 days. The interface settlement of the anionic PT was relatively slower compared to the other polymer treatment.

The initial settling velocity and hydraulic conductivity of the different tailings were determined from the linear portion of the interface settlement profiles using Equation 1 in Section 2.5 and are presented in Table 4-6.

Table 4-6: Initial settling velocity and hydraulic conductivity of tailings

Material	Initial void ratio	Initial settling velocity (m/s)	Initial hydraulic conductivity (m/s)	Period
Untreated FFT	5.17	1.16E-08	5.62E-08	1 day
Anionic PT	5.63	4.05E-08	2.11E-07	1 day
Neutral PT	14.25	1.43E-03	1.72E-02	41 sec
Cationic PT	7.44	1.38E-07	9.17E-07	2 days

4.2.3 Immediate water release

As indicated by the measured initial solids content provided in Table 4-1, the amount of solids in the settling column differs for each treatment, owing to the different polymer dosages used in the FFT treatment. For proper comparison of results, the volume of FFT for each polymer treatment was rescaled to 1000 ml to match the analyzed volume of untreated FFT. Figure 4-7 shows the volume of polymer solution required to treat 1000 ml of FFT.

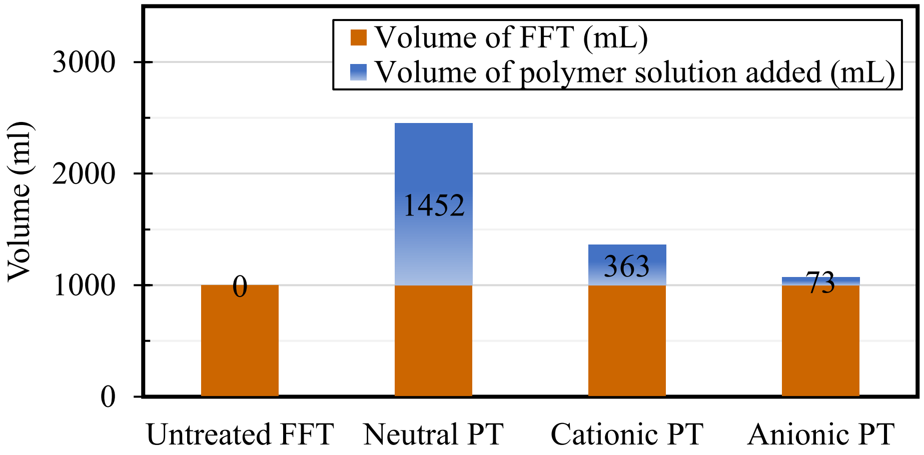

Figure 4-7: Volume of hydrated polymer to treat 1000 ml of FFT

The net water release from treating 1000 ml of FFT with the polymers, as determined using Equation (11), is shown in Figure 4-8. In addition, the proportion of the net water release relative to the volume of water in 1000 ml FFT before treatment is indicated on the left vertical axis. The negative values indicate the volume of polymer water remaining in the treated tailings at a given time, while the positive net water is the volume of the original FFT water released.

$$NWR = V_{wr} - V_p \tag{11}$$

where,

NWR = net water release,

V_{wr} = total volume of water released, and

V_p = volume of hydrated polymer added to FFT during treatment.

Figure 4-8 shows that the polymer water in the anionic PT was released after 9 days with a gradual release of an additional 218 mL of water, representing 26 % of the pore water volume in the original FFT. The cationic PT accumulated total supernatant water of 200 mL within 14 days and reached a peak of 212 mL after 34 days. The first 10 days of water release occurred rapidly, but the total volume of water released during settling was less than the volume of hydrated polymer added to the FFT during treatment. A more rapid water release was observed in the neutral PT as the added polymer water was recovered after 18 minutes of settling. Moreover, dewatering of the original FFT water by the neutral polymer reached a maximum of 32% after 18 days without further settlement.

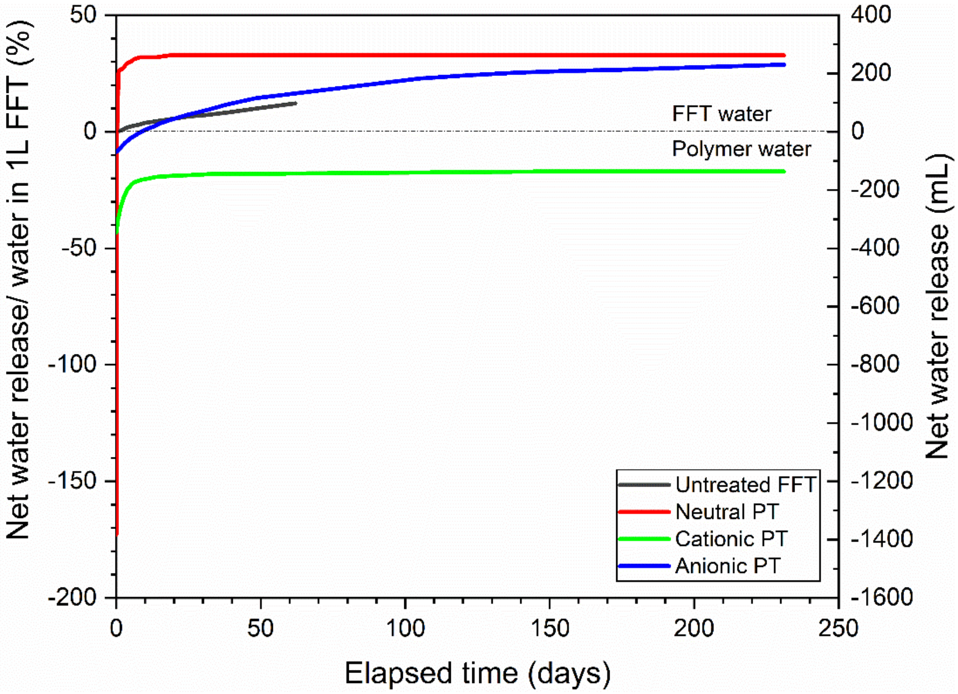

Figure 4-8: Net water release in untreated and polymer amended FFT

4.3 Large Strain Consolidation with Shear Strength Measurement

This section reports the results of the large strain consolidation tests completed in this study. Following self-weight consolidation, samples of polymer amended and untreated FFT were surcharged with incremental loads ranging from 0.3 kPa to 900 kPa in the LSC test. Measurements taken from the LSC test were analyzed to understand the compressibility, hydraulic conductivity and undrained shear strength behaviour of the tailings. The large strain consolidation test results are presented in Table A-1 to Table A-7 in Appendix AAppendix A:.

4.3.1 Compressibility

Changes in the void ratio of the tailings under the range of applied effective stresses were determined from the measured consolidation settlements during the LSC test. Figure 4-9 shows the compressibility of the different tailings, defined by the void ratio-effective stress relationship. The total experimental time of the large strain consolidation of the tailings for the range of effective stresses applied is presented in Table 4-7.

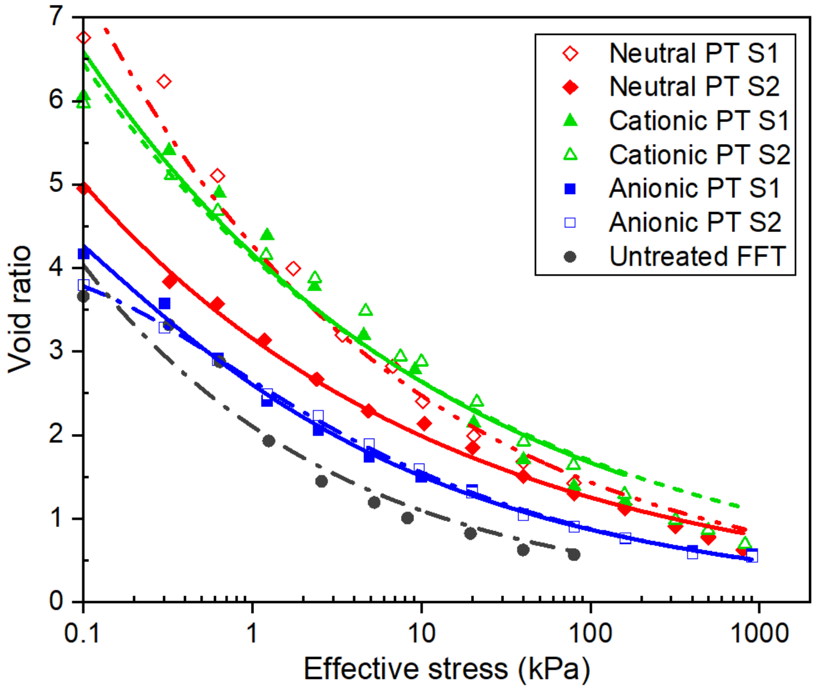

Figure 4-9: Void ratio-effective stress relationship for untreated and polymer amended FFT.

Table 4-7: Experimental large strain consolidation time of tailings

Material	Range of effective stress (kPa)	Total consolidation time based on load steps (weeks)
Untreated FFT	0 – 80	51
Neutral PT	0 – 900	17
Cationic PT	0 – 900	26
Anionic PT	0 – 900	44

The larger part of the self-weight consolidation was dominated by hindered settling of particles in suspension at different rates based on aggregate sizes in each treatment. The void ratio of the neutral PT reduced from an initial 14.25 to 4.95 (31% solids) after self-weight consolidation. This occurred within 10 hours after treatment, with little to no further settlement observed. The void ratios of the cationic PT and anionic PT after self-weight consolidation were 6.06 (27% solids) within 11 days and 4.17 (35% solids) after 47 days respectively, while the untreated FFT attained a void ratio of 3.66 (38% solids) after 8 weeks.

A final void ratio of 1.20 (65% solids) was achieved in the cationic PT at 160 kPa, after which no further compression was observed. Further compression was observed in the duplicate sample of the cationic PT until a final void ratio of 0.70 (77% solids). With or without vane shear testing, the neutral PT and anionic PT had final void ratios of 0.63 (78% solids) and 0.58 (80% solids), respectively, with measured settlements under each load.

The polymer-treated and untreated tailings exhibit a normally consolidated behaviour with a decreasing compression index with effective stress. The compressibilities of the treated tailings do not show pre-consolidation behaviour in the material. Moreover, it can be seen that the compressibilities of the optimum and overmixed neutral PT samples converge at effective stress of 10 kPa. A similar convergence is observed in the compressibility of the cationic and neutral PTs under a vertical effective stress of 20 kPa.

4.3.2 Hydraulic conductivity

Constant head permeability measurements were taken during consolidation to assess the effect of volume change on the saturated hydraulic conductivity of the untreated and polymer amended FFT. The hydraulic conductivity at a given stress was averaged for five to ten measurements, with a standard deviation ranging between 2 % and 23 % of the mean value. Hydraulic gradients ranging from 0.06 to 31.27 were applied across the tested tailings samples in order to observe seepage flow through the tailings. The stress induced by the gradient at a given load did not exceed the applied stress – to ensure that all loading of the samples were accounted for.

Figure 4-10 and Figure 4-11 show the hydraulic conductivity as a function of effective stress and void ratio, respectively. By the end of the LSC test, the hydraulic conductivity of the anionic and cationic PTs decreased by four orders of magnitude, as against five orders of magnitude in the case of the neutral PT. Almost 40 % of the change in the hydraulic conductivity of the neutral PT occurred between 0.3 kPa and 0.6 kPa effective stress, with corresponding void ratios of 3.8 and 3.6. With the exception of the neutral PT, the hydraulic conductivity-void ratio relationships of the cationic and anionic PTs can be described with power functions.

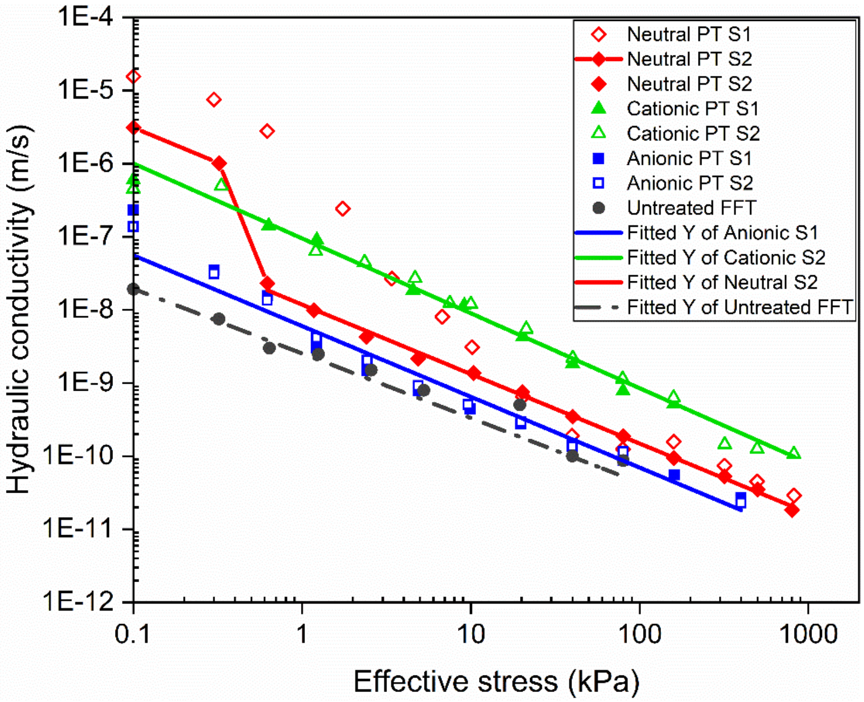

Figure 4-10: Hydraulic conductivity-effective stress relationships of untreated and polymer amended FFT.

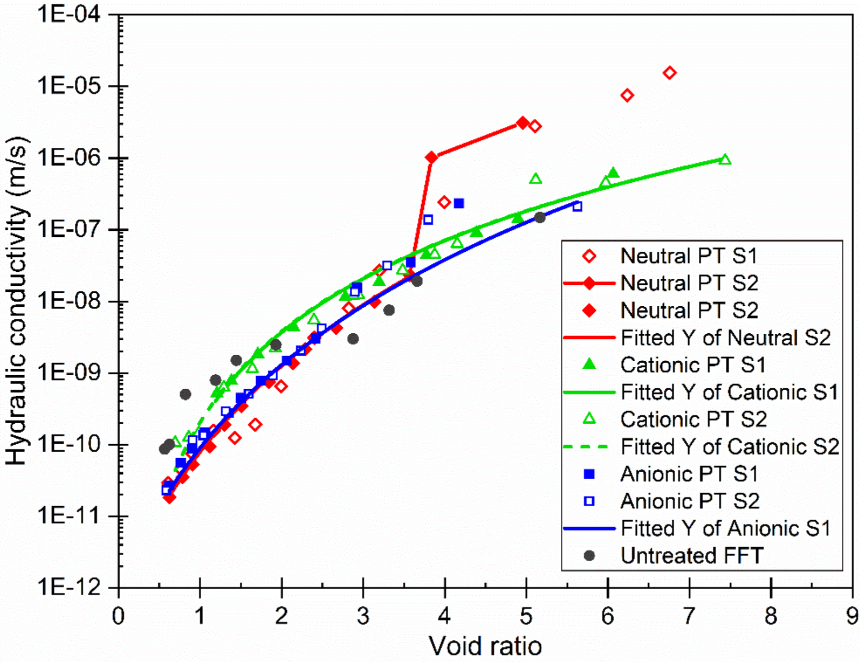

Figure 4-11: Hydraulic conductivity-void ratio relationship for untreated and polymer amended FFT.

4.3.3 Undrained shear strength

The peak undrained shear strength of the tailings was measured using a laboratory vane shear apparatus and a rheometer. Two to four yield stress or vane shear strength measurements were averaged for each load step, as provided in Appendix A. Figure 4-12 shows the relationship between the peak undrained shear strength and effective stress of untreated and polymer amended FFT that indicates an exponential gain in the undrained shear strength of the tailings, which can be described by a power function. The range of measured shear strengths for a given effective stress is indicated by the error bar. The undrained shear strengths of the cationic and anionic PTs are similar within experimental error, with slightly higher average values in the anionic PT at given effective stresses less than 200 kPa. The neutral PT produced the highest undrained shear strength in the FFT among the polymer treatments, with a rapid initial strength gain at effective stresses less than 10 kPa.

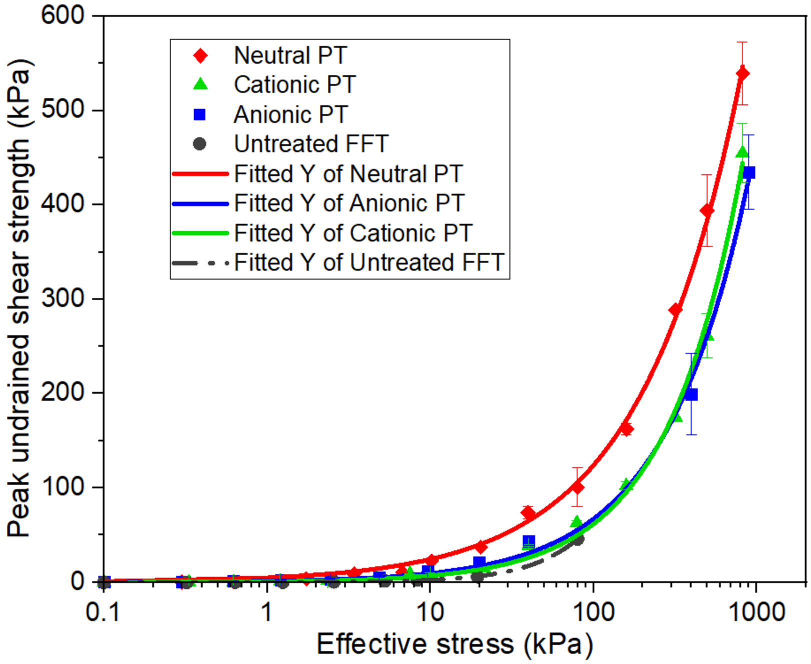

Figure 4-12: Undrained shear strength-effective stress relationship for untreated and polymer amended FFT.

Figure 4-13 and Figure 4-14 relate the peak undrained shear strength to the void ratio and solids content of the different tailings, respectively. The results show that the undrained shear strength achieved at a given void ratio in the neutral and cationic PTs is about an order of magnitude higher than that of the anionic PT and about two orders of magnitude higher compared to that of untreated FFT. The neutral PT, however, exhibits a distinctly higher undrained shear strength at void ratios higher than 3.5 and solids content lower than 35% compared to the other polymer treatments. Figure 4-15 shows the relationship between the undrained shear strength, effective stress and the density of the tailings. The correlation between the undrained shear strength and the increasing effective stress with depth for the different tailings is described by normalizing the undrained shear strength by the effective stress.

The water content of the tailings at a given stress was calculated from the corresponding void ratio achieved in the LSC test. The liquidity index was then calculated for the given effective stress to scale the water content relative to the liquid and plastic limits of the tailings and to account for the combined effect of the grain size, plasticity, and water chemistry on the geotechnical behaviour of the tailings. Figure 4-16 shows the relationship between the undrained shear strength and the liquidity index of the untreated and polymer amended tailings compared with a general fit for sensitive clays proposed by Locat and Demers (1988).

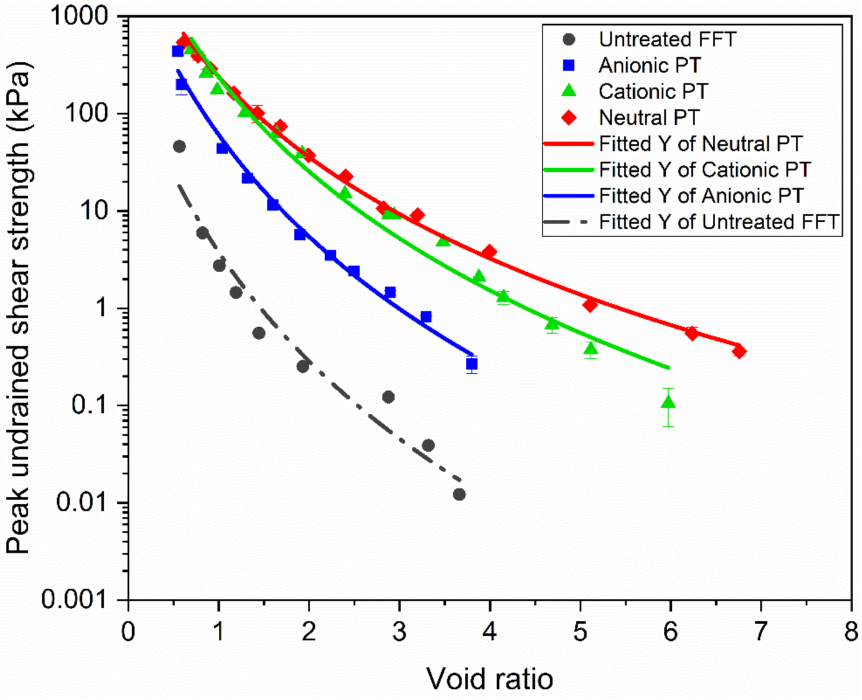

Figure 4-13: Void ratio-undrained shear strength relationship for untreated and polymer amended FFT.

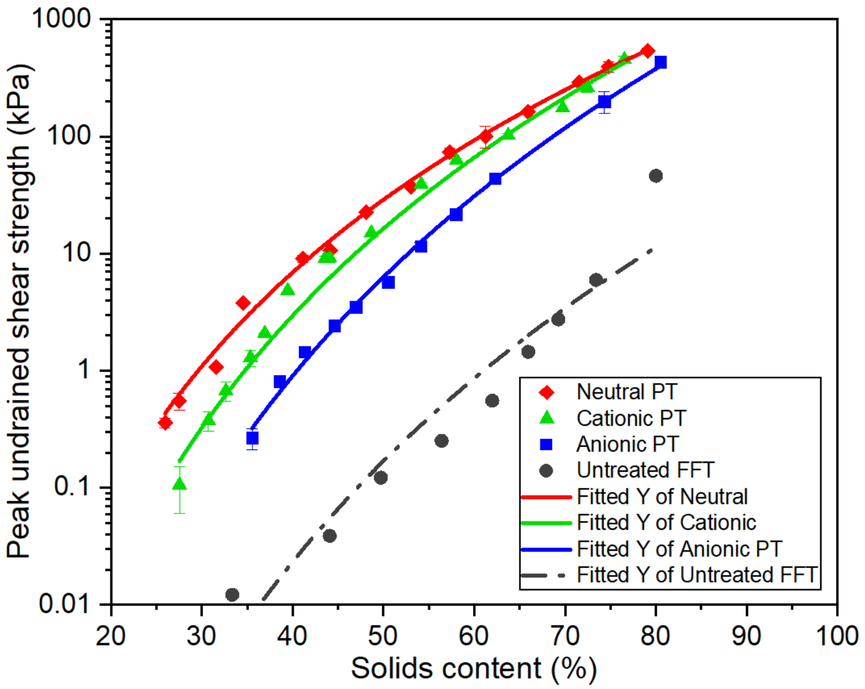

Figure 4-14: Undrained shear strength-solids content relationship for untreated and polymer amended FFT.

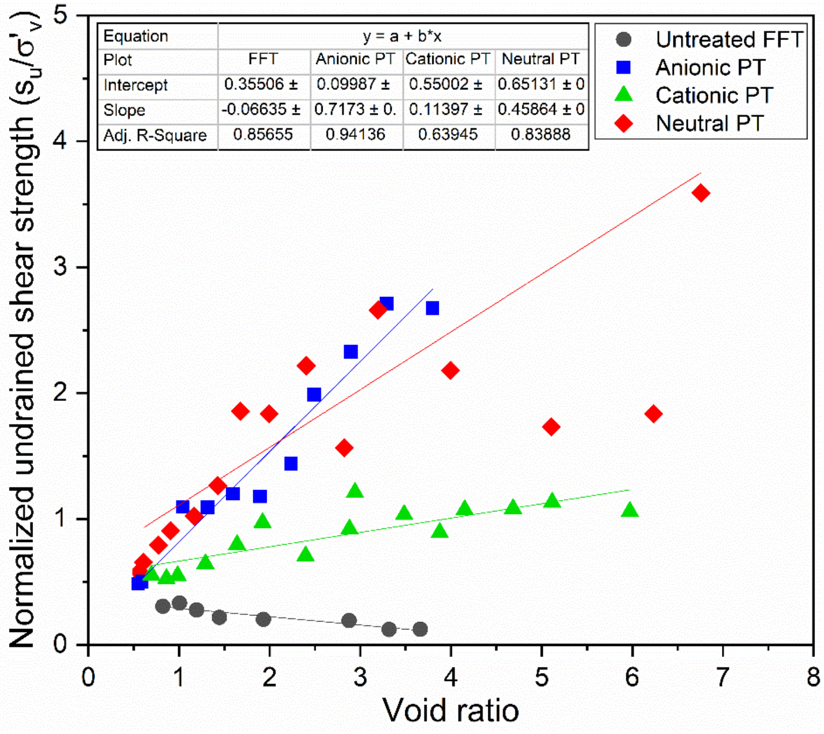

Equation	y = a + b*x			
Plot	FFT	Anionic PT	Cationic PT	Neutral PT
Intercept	0.35506 ±	0.09987 ±	0.55002 ±	0.65131 ± 0
Slope	-0.06635 ±	0.7173 ± 0.	0.11397 ±	0.45864 ± 0
Adj. R-Square	0.85655	0.94136	0.63945	0.83888

Figure 4-15: Normalized undrained shear strength-void ratio relationship for untreated and polymer amended FFT.

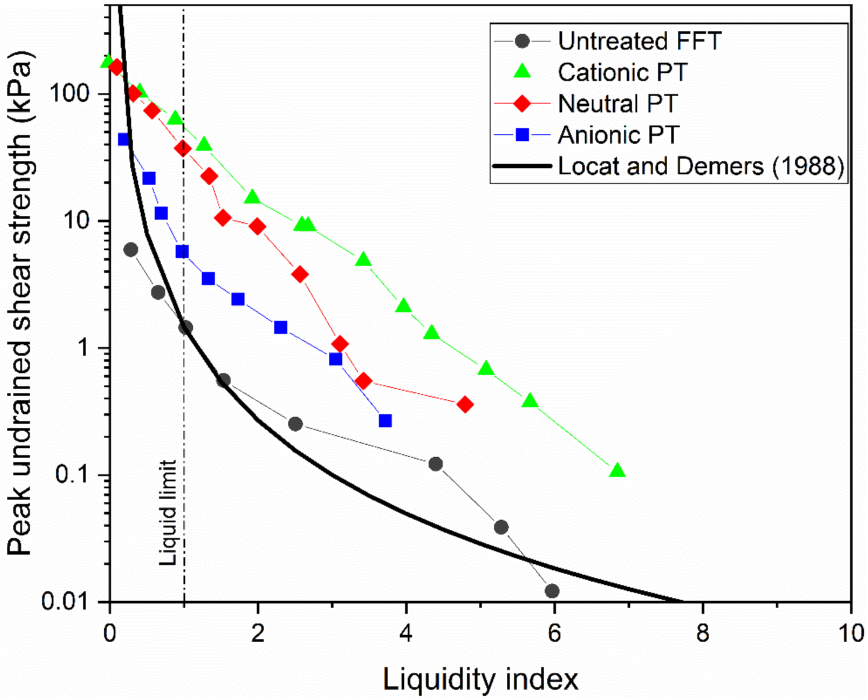

Figure 4-16: Undrained shear strength-liquidity index relationship for untreated and polymer amended FFT.

4.4 Thixotropic Strength of Polymer Amended FFT

As part of this study, ageing experiments were conducted to assess the thixotropic shear strength development at the surface of anionic polymer amended FFT over a short-term period. Large strain consolidation tests were subsequently performed to evaluate the effect of ageing on the long-term consolidation of the polymer amended FFT. This section presents the results of the ageing and large strain consolidation tests completed. The results include surface settlements, pore water pressure, and undrained shear strength measurements recorded over the ageing period. The large strain consolidation properties and undrained shear strength of the aged material are also presented.

4.4.1 Ageing experiments

The thixotropic strength behaviour of the polymer amended FFT was examined from the pore water pressure and the surface undrained shear strength of the two LSC cell samples. The initial sample heights were 146 mm and 141 mm for sample 1 and sample 2, respectively. A cone factor (*k*) of 0.26 was calculated for the 10 g cone based on the fall cone apparatus manufacturer's specifications and applied in the calculation of the undrained shear strength using Equation 12. Figure 4-17 shows the weekly pore water pressure and surface undrained shear strength of the LSC cell samples over a period of 17 weeks.

$$s_u = k\frac{d^2}{mg} \tag{12}$$

where,

s_u = undrained shear strength in kPa,

k = cone factor,

d = cone penetration in mm.

m = mass in grams.

g = acceleration due to gravity.

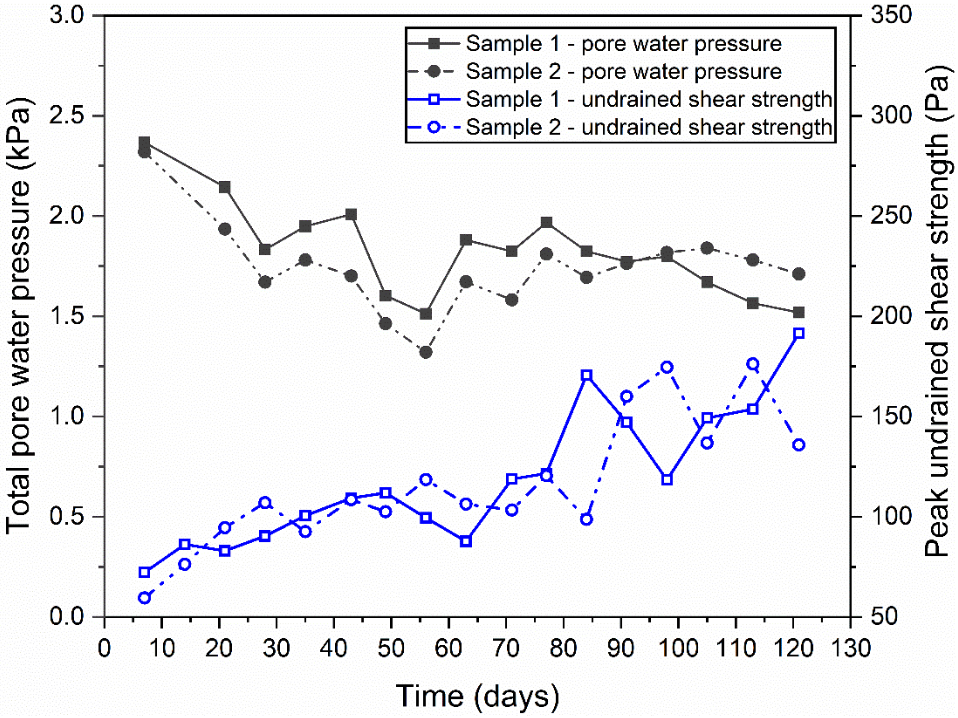

Figure 4-17: Pore water pressure and surface undrained shear strength of ageing polymer amended FFT in LSC cells.

A gradual buildup in the undrained shear strength of the treated tailings was observed with time. As shown in Figure 4-17, the undrained shear strength of the flocculated tailings increased from 72.2 pascals (Pa) in week 1 to 191.5 Pa after 17 weeks in sample 1. Sample 2 shows a similar shear strength gain from 59.5 Pa to a maximum of 176.2 Pa over the same period. The large scatter in the surface shear strength of the two samples after 50 days was attributed to the retesting of disturbed surface locations tested in previous weeks due to limited undisturbed tailings surface in the LSC cell. The corresponding pore water pressures in both samples show a gradual excess pore water pressure dissipation in the tailings over the test period.

The ageing experiment was repeated using 16 subsamples of 250 mL of flocculated tailings each to eliminate surface disturbance due to multiple testing. The measured settlement height was normalized to the initial sample height for each subsample and averaged for the remaining subsamples in a given week. A fall cone test was performed on each subsample per week. Figure 4-18 shows the 16-week profile of the normalized sample height and the peak undrained shear strength of the tailings. The range of sample heights is indicated by the error bars.

Shear strength gain, similar to that of the LSC samples, was observed in the 250-mL tailings samples over the study period. The sample settled approximately 21 %, and the surface strength of the tailings increased by 71 Pa over 16 weeks of ageing.

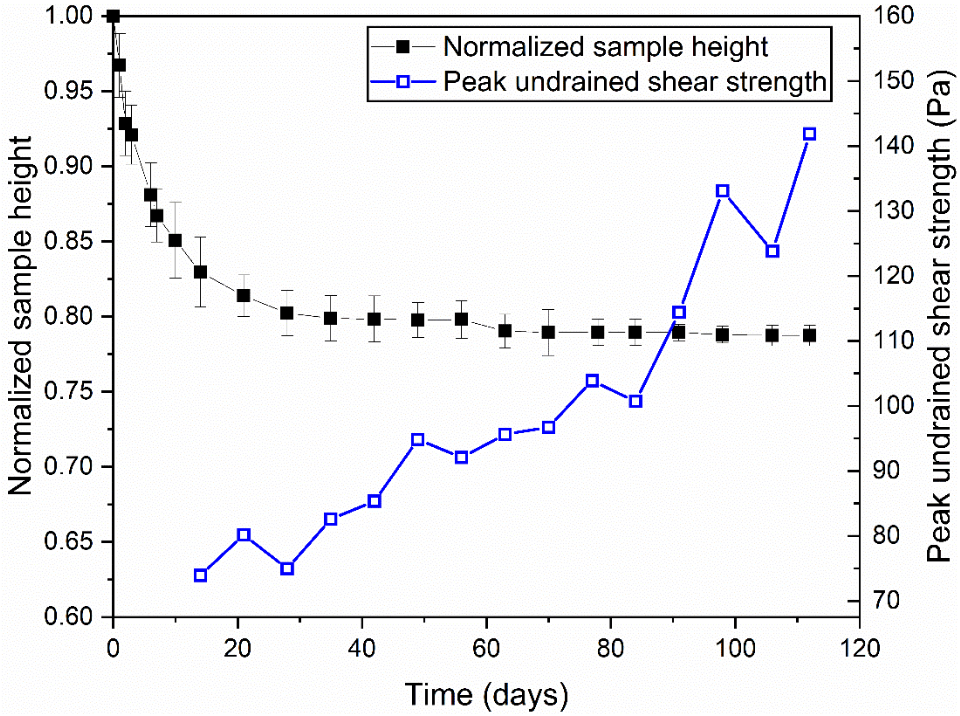

Figure 4-18: Normalized height and undrained shear strength of 250-mL ageing polymer amended FFT

4.4.2 Large strain consolidation of aged polymer amended FFT

After ageing, the LSC cell samples were subjected to incremental multi-step loading from 0.3 kPa to 200 kPa. The void ratio of the tailings at the start of the LSC test was 3.72 for sample 1, and 3.54 for sample 2. Table A-8 and Table A-9 in Appendix A present the results of the large strain consolidation tests conducted on the polymer amended FFT after ageing. The compressibility, hydraulic conductivity and undrained shear strength relationships from these results are shown in Figure 4-19, Figure 4-20, Figure 4-21 and Figure 4-22, respectively.

The hydraulic conductivity was measured at hydraulic gradients ranging from 0.23 to 13.63, as effective stresses increased. The coefficient of variation for at least five measurements taken per hydraulic gradient ranged from 2% to 28%. For the undrained shear strength, the vane shear test was limited to three or four measurements of the peak value to prevent excessive disturbance of the tailings' microstructure. The range of measured peak undrained shear strength at a given density is indicated by the error bars.

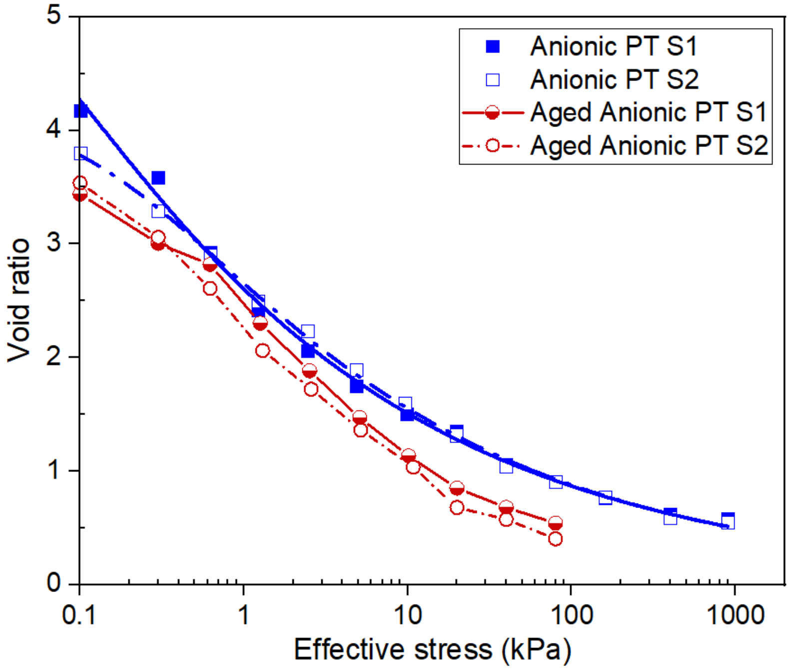

Figure 4-19: Compressibility relationship of aged polymer amended FFT

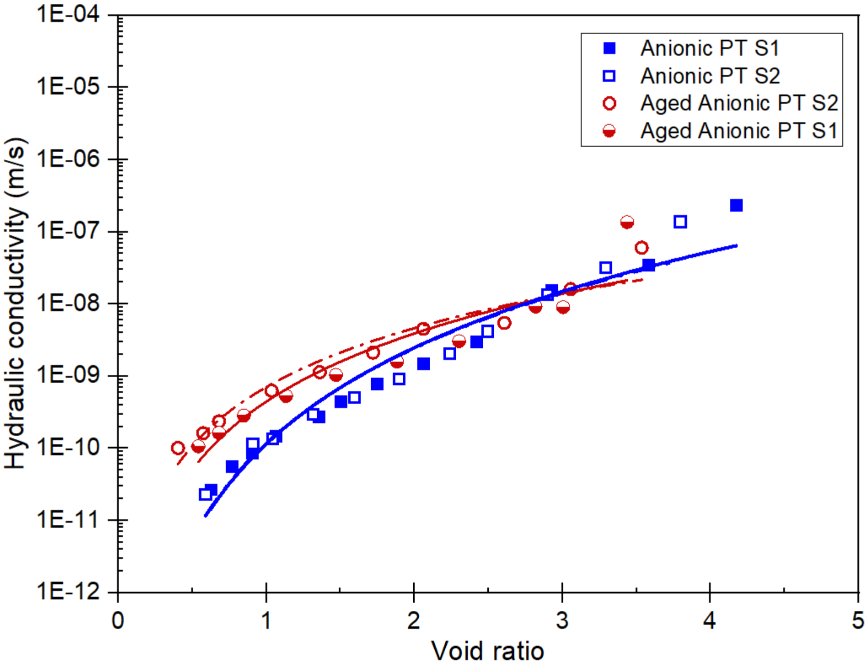

Figure 4-20: Hydraulic conductivity-void ratio relationship of aged polymer amended FFT

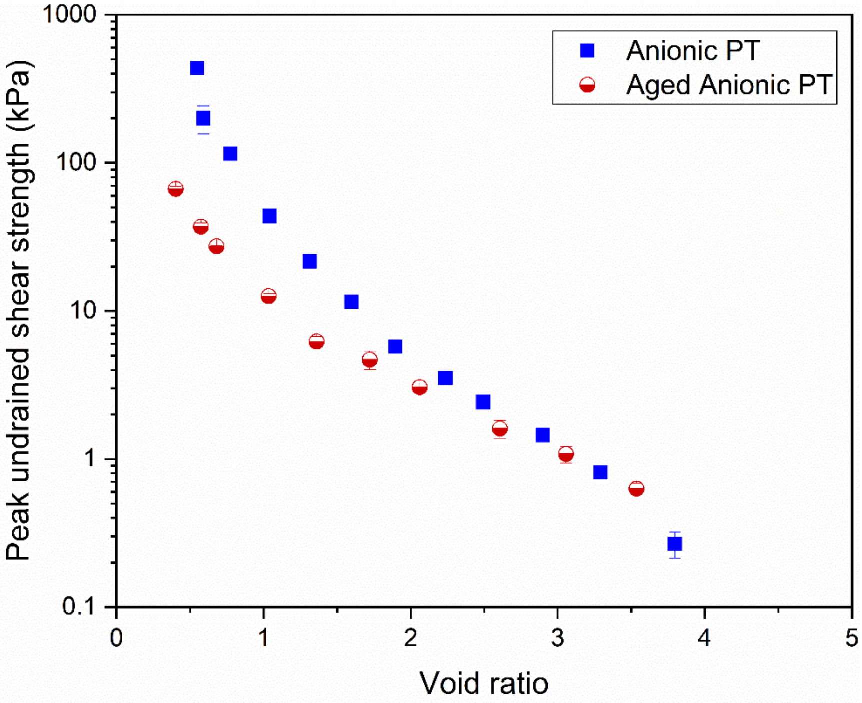

Figure 4-21: Undrained shear strength-void ratio relationship of aged and unaged polymer amended FFT

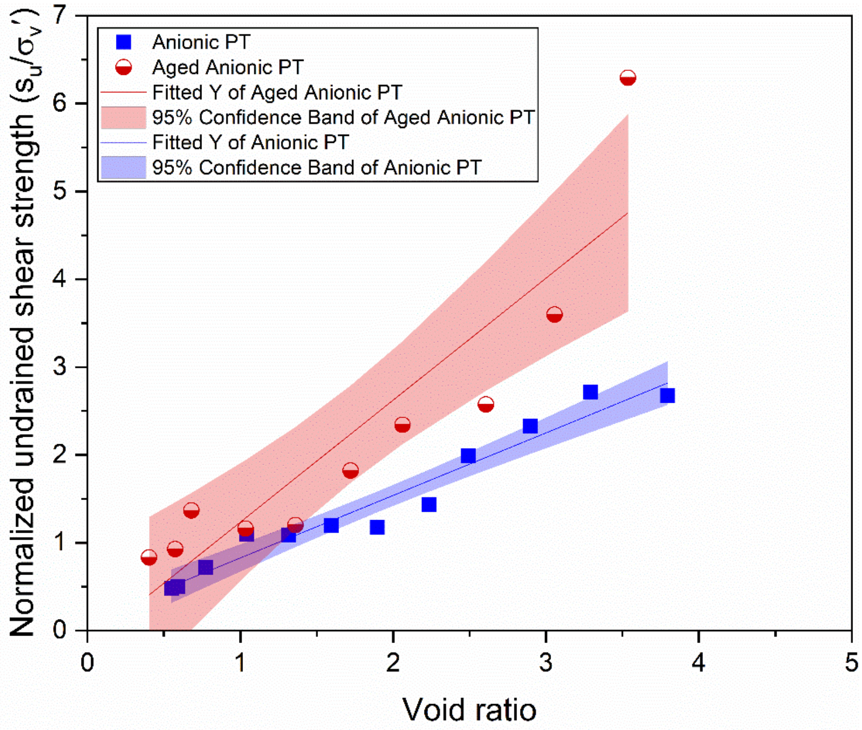

Figure 4-22: Normalized undrained shear strength-void ratio relationship of aged and unaged polymer amended FFT

4.5 Finite Strain Consolidation Modelling

A deep in-pit deposit of FFT treated with either the anionic, cationic and neutral polymers was modelled using the 1-D large strain consolidation computer program FSConsol version 3.49 (GWP Geo Software) to predict the long-term consolidation behaviour of the polymer amended tailings after deposition. The objective of this modelling work is to compare the long-term field-scale settlement, density and strength development of the polymer-treated tailings deposits over reclamation and post-closure timelines to support the experimental study conducted in this body of work.

The FSConsol program can simulate the deposition and consolidation processes of fine-grained soils like FFT that undergo large deformations by solving Gibson's finite strain consolidation equation in one dimension. The consolidation model relies on the deposition conditions, basic material properties and the compressibility and hydraulic conductivity relationships obtained from experimental large strain consolidation tests as parametric inputs to predict the deposit behaviour with time.

This section presents the results of the one-dimensional finite strain consolidation model (hereafter referred to as "the model") of the anionic, cationic and neutral polymer amended FFT over extended timeframes. The input parameters used in the model, including the analysis conditions, material properties, boundary conditions, initial conditions and analysis time, are presented.

4.5.1 Deposition and analysis conditions

A mined-out pit with a surface area of 5 km^2 and depth of 75 m with vertical side slopes was assumed for the purpose of modelling. Two different analyses can be performed using FSConsol: a tank analysis, which simulates an instantaneous deposition of tailings without consolidation, followed by consolidation after complete filling, and a pond analysis that allows consolidation while tailings are gradually deposited. With an average mine life of 40 years, it is estimated that treatment and re-disposal of accumulated FFT at a mine site would commence 20 years before the end of mining at a reasonable deposition throughput. Therefore, the pond analysis was selected for this model to simulate the gradual filling of the pit with treated tailings for the first 20 years, followed by 280 years of quiescent conditions, during which the deposit was allowed to consolidate under self-weight without additional filling. This filling scheme was adopted from

Hyndman et al. (2018), but the analysis period was limited to 300 years. The incremental mass of dry solids (in kg/day) to be discharged into the pond was calculated based on the total volume of the pit using the corresponding dry density of the untreated tailings assuming full saturation to determine the filling rate, as given by Equations 13 to 15. Based on Figure 4-7, the same dry solids mass of 20,000 tons was used for the treated tailings deposits for comparison.

The mined-out pit considered in this model has no pre-existing tailings stored in it, and thus, no initial conditions were specified. The deposit was analyzed under single-drainage conditions by allowing free drainage at the top boundary and no flow across the bottom boundary (impermeable bottom). In this drainage condition, water released by consolidation only travels upwards.

$$\rho_d = \frac{\rho_w}{\left(\frac{1}{G_s} + \frac{\left(\frac{1}{s} - 1\right)}{G_w \times S_r}\right)} \tag{13}$$

$$\rho_d = \frac{M_s}{V} \tag{14}$$

$$\text{Filling rate (kg/day)} = \frac{M_s\,[kg]}{filling\ duration\ [days]} \tag{15}$$

where,

ρ_d = dry density of tailings

ρ_w = density of water

G_s = specific gravity of solids

G_w = specific gravity of water

S_r = degree of saturation

s = initial solids content

M_s = mass of solids deposited

V = total volume of tailings deposited

4.5.2 Material properties

The large-strain consolidation model requires the constitutive void ratio – effective stress relationship (e-σ', compressibility) and hydraulic conductivity – void ratio relationship (k-e) as input to describe the consolidation properties of the tailings. The coupled effects of these non-linear relationships determine the consolidation behaviour of the deposit under increasing effective stress as the model solves the governing equations of large-strain consolidation.

FSConsol allows the dataset or the power-law fit parameters for the consolidation properties of tailings to be entered to define the constitutive relationships. In this model, the effective stress versus void ratio and the corresponding hydraulic conductivity data sets provided in the large strain consolidation test results in Appendix A were entered to describe the compressibility and hydraulic conductivity relationships of the tailings.

In addition to the consolidation properties, the initial solids content and specific gravity of the tailings were specified to enable the computer program to calculate the initial void ratio and the dry density of deposited tailings.

4.5.3 Numerical settings

Additional numerical settings in FSConsol include indicating the time step, maximum stress difference between nodes and the number of nodes per meter for a more accurate solution. To obtain accurate results within reasonable time, a calculation time step of 1 day and 20 nodes per meter were specified for all analyses performed. The maximum stress difference between nodes was maintained at 100 kPa in all cases, as recommended in the FSConsol manual.

4.5.4 Consolidation model results

Figure 4-23 shows the predicted settlement profile of the model deep in-pit deposit over time using the compressibility and hydraulic conductivity datasets. The deposit height is normalized by the height of the untreated FFT deposit at the end of deposition. The discharged tailings begin to consolidate under self-weight during filling, and the deposit height at the end of filling indicates the cumulative amount of water released for each type of tailings. The predicted settlement of the deep deposit during self-weight consolidation under quiescent conditions after 300 years varies for each polymer treatment.

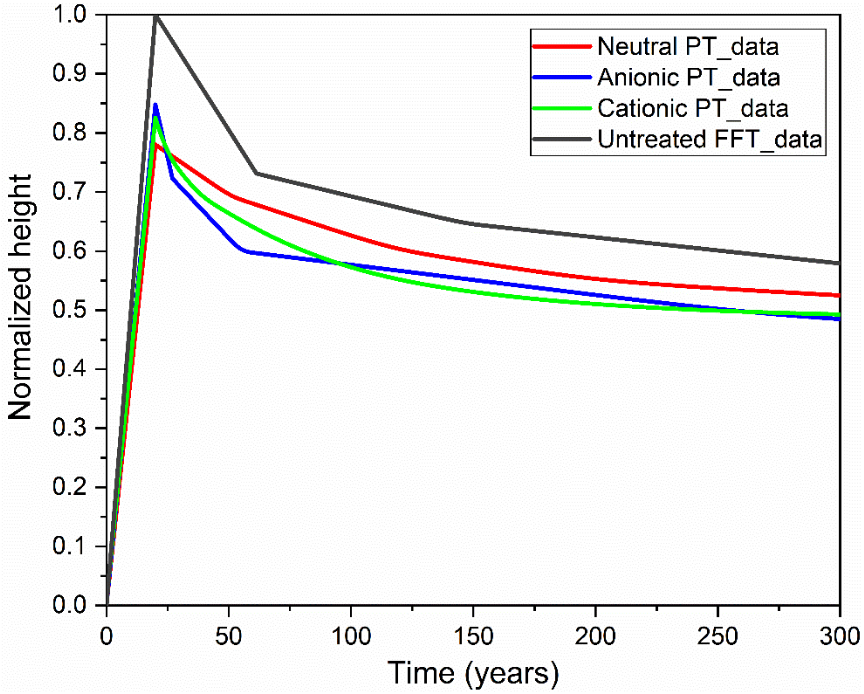

Figure 4-23: Settlement over time for the model deep deposit

Figure 4-24 shows the average solids content of the tailings deposit over time. The solids content of the neutral PT increases rapidly within the first 5 years of filling from 13.7% to about 40%, where it plateaus until deposition ends. After tailings deposition, the overall solids content of the deposit increases gradually under self-weight consolidation. A similar pattern is observed for the cationic PT deposit, where a maximum average solids content of approximately 39% is achieved during deposition, followed by further densification at a relatively higher rate. The solids content profile of the anionic PT deposit after deposition almost coincides with that of the cationic PT, but attains a higher solids content at the early periods of filling. The predicted solids content profile with the depth of the tailings deposit at the end of filling and at year 30, year 100 and year 300, are shown in Figure 4-25 to Figure 4-28. A detailed discussion of these results is presented in the next chapter.

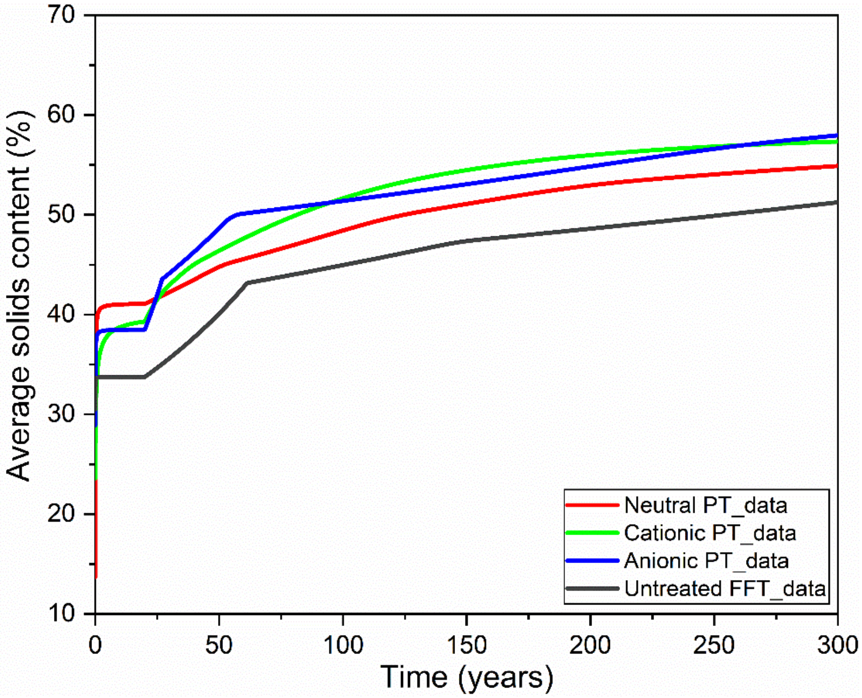

Figure 4-24: Average solids content over time for the model deep deposit

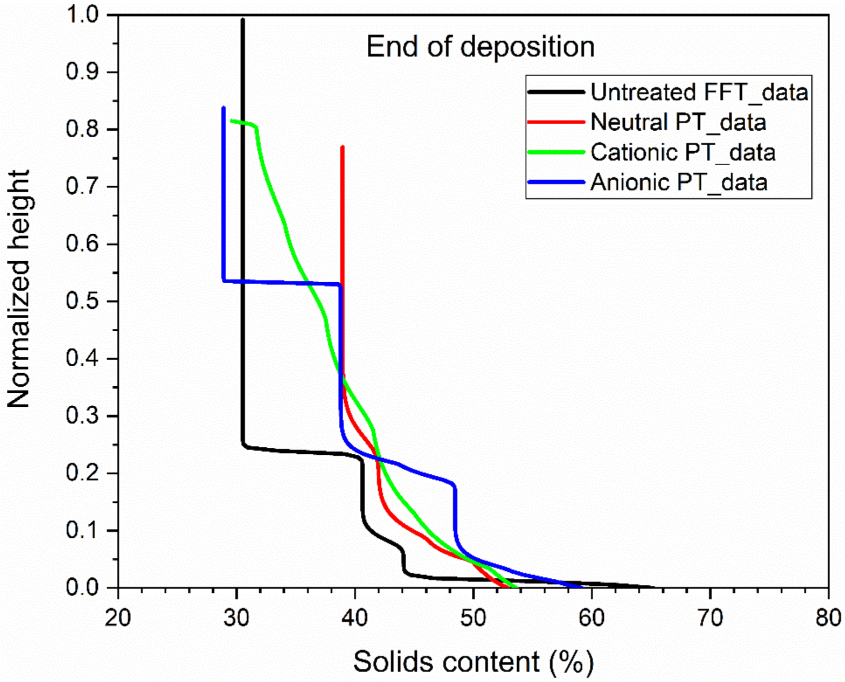

Figure 4-25: Solids content profile of the model deep deposit at the end of the deposition

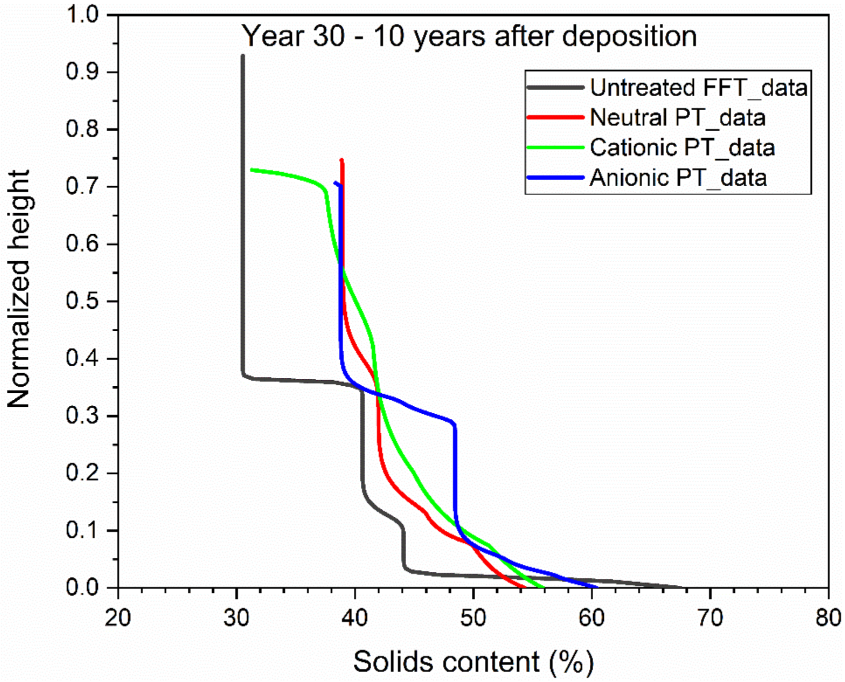

Figure 4-26: Solids content profile of the model deep deposit 10 years after deposition

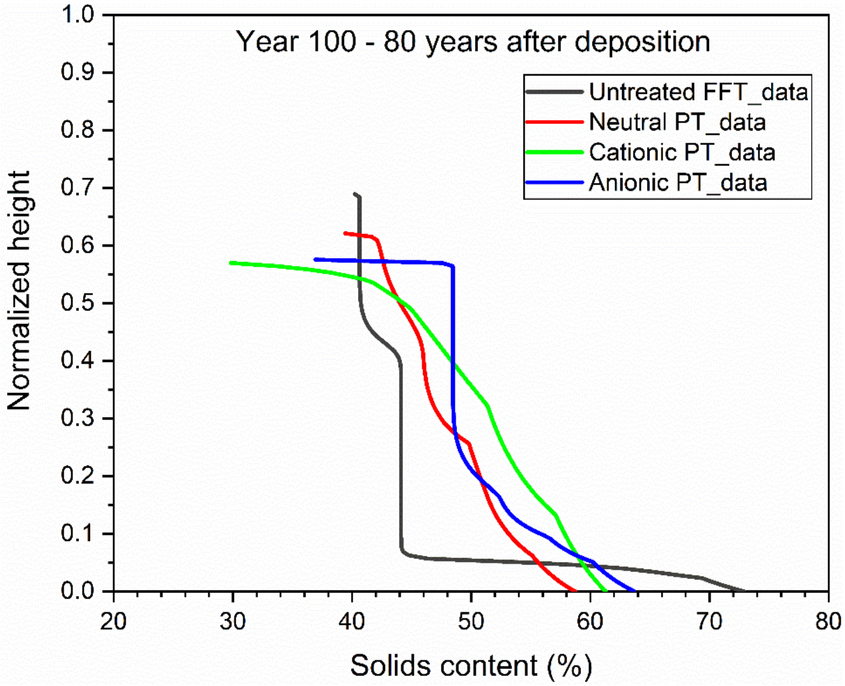

Figure 4-27: Solids content profile of the model deep deposit 80 years after deposition

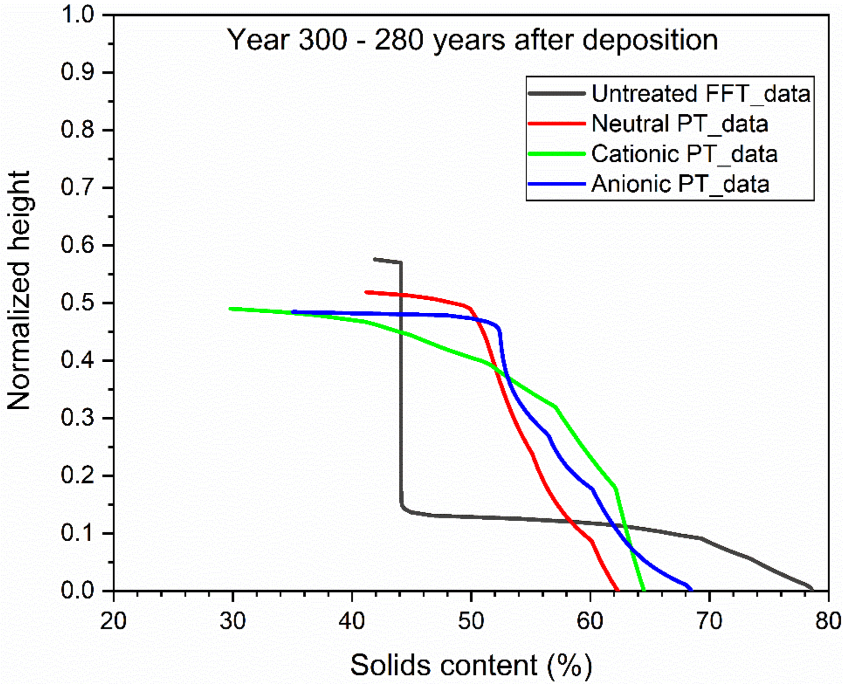

Figure 4-28: Solids content profile of the model deep deposit 280 years after deposition

Chapter 5: Discussion

5.1 Effect on material properties

Flocculation processes aim to increase the settling and consolidation rates of FFT by modifying the material properties. The particle size distribution of the tailings in Figure 4-1 suggests that polymer addition increased the weight of solids through flocculation, thereby accelerating the tailings settling rate. The cationic PT produces sandy silt floc sizes, which are relatively fine and light in weight compared to the anionic PT flocs, while the larger and heavier flocs of the neutral PT explain the rapid settling rate observed during hindered settling. The liquid limit and plasticity index of the flocculated tailings are consistent with the expected ranges suggested by Beier et al. (2013). From the plasticity chart in Figure 4-2, the polymer treatments produced tailings with high plastic silt behaviour, which suggests the effectiveness of the polymers in neutralizing the active sites of clay particles through bridging and chemical bonding.

The consolidation properties of polymer amended FFT and untreated FFT are compared to evaluate the effect of the cationic, neutral and anionic polymer treatments on the consolidation behaviour of FFT. The compressibility curves in Figure 4-9 show that the treated tailings settled to distinct void ratios at the end of self-weight consolidation (0.1 kPa), indicating the tailings deposit density after the initial water release. With the final void ratios achieved by the three polymer treatments ranging between 0.55 and 0.70, the void ratio attained under self-weight (or solids content) appears to have an effect on the compression index and the rate of volume reduction of the tailings deposit.

The neutral and cationic PTs converge to similar densities at vertical effective stresses greater than 20 kPa. The treated tailings are normally consolidated, with the cationic PT being slightly more compressible after self-weight consolidation, compared to the anionic and neutral PTs. This compression behaviour is attributed to the resistance of the floc structure to compression as the compressive strength of the tailings increases. The higher void ratios measured in the neutral PT compared to the anionic PT is due to the presence of large pores between the flocs created, whereas the cationic PT exhibit a higher water retention capacity due to its fine and light flocs. By the end of consolidation, the void ratio of the original cationic PT sample was 1.20, but continued in the duplicate sample to a final void ratio of 0.70. The reason for this difference in the final void ratio is unknown, but may be attributed to further compression due to the closure of the holes created in the sample after the vane shear tests.

The initial settling velocities of the treated tailings in Table 4-6 obtained from the hindered sedimentation results in Figure 4-6 demonstrate the effect of the polymer treatments on the settling behaviour of FFT. The neutral PT increased the initial hydraulic conductivity of FFT by six orders of magnitude, which remained high through the sedimentation and self-weight consolidation stages, while a two-order-of-magnitude increase in the permeability of FFT was observed in the cationic PT. The hydraulic conductivity of the neutral PT remains high at effective stresses less than 0.3kPa, where void ratios are greater than 3.8 as shown in Figure 4-9 and Figure 4-10, as long as the pore spaces between the large flocs permit higher fluid flow through the tailings. A sudden reduction of about two orders of magnitude in the hydraulic conductivity of the neutral PT occurs when the effective stress exceeds 0.3kPa. This reduction in the hydraulic conductivity of the neutral PT is attributed to the collapse of macropores due to floc compression under increased load, forcing fluid flow through the floc microstructure.

Figure 4-10 shows that the hydraulic conductivities of the cationic and anionic PTs decrease by about four orders of magnitude and that of the neutral PT by five to six orders of magnitude from an effective stress of 0.1 kPa to about 900 kPa. The cationic PT exhibits higher hydraulic conductivities compared to the other polymer treatments, while the lowest hydraulic conductivity is recorded in the untreated FFT. It is evident from Figure 4-11 that the void ratio at a given effective stress is different for each tailings type. The cationic and anionic PTs exhibit somewhat similar hydraulic conductivities, within experimental error, at void ratios higher than 2.8. Below a void ratio of 3.8, the hydraulic conductivity of the neutral PT significantly reduces to rates similar to that of the anionic PT, while the hydraulic conductivity of the cationic PT is three times higher at lower void ratios. Since the hydraulic conductivity mostly controls the consolidation rate of tailings deposits (Rourke and Hockley, 2018), it is anticipated that the neutral PT deposit will consolidate rapidly immediately after deposition, but dewatering at greater depths will occur at a much slower rate. The cationic PT is expected to consolidate relatively faster in the long term compared to the other tailings. The long-term consolidation behaviour of deep deposits of the treated tailings is discussed in Section 5.6.

5.2 Dewatering efficiency of polymer treatments

The CST was used as a metric in this study to assess the initial dewatering performance of the polymer treatments. Figure 4-5 shows that cationic PT exhibits a faster initial dewaterability compared to the anionic PT, which is consistent with the initial hydraulic conductivities calculated from the sedimentation test. The relatively high initial void ratio of the cationic PT provides less tortuous flow paths for fluid flow through the floc structure due to its fine flocs. The measured CST of the neutral PT indicates a lower initial dewaterability compared to the cationic PT, which is inconsistent with its initial hydraulic conductivity and void ratio. This inconsistency results from the use of selected flocs that fitted the CST test column, but were not representative of the macrostructure of the neutral PT. Thus, the measured CST of the neutral PT reflects the dewaterability of the floc microstructure instead of the macrostructure, and the high variability in the values is due to the heterogeneity in the selected floc sizes.

One of the main objectives of tailings treatment is to reduce FFT volume through dewatering. The sedimentation and consolidation results provide information about the amount of water released from the treated tailings. The efficacy of the polymer treatments is evaluated based on the net water release, which is the amount of water removed from the original FFT used in the treatment. Table 5-1 summarizes the calculated water contents and net water release per litre of FFT in the polymer amended tailings after sedimentation and consolidation. The difference between the initial water content of the treated tailings and that of the untreated FFT represents the proportion of the added polymer solution in the total tailings volume.

Table 5-1: FFT water release by polymer treatments

Treatment	Initial water content	End of hindered Sedimentation		End of large strain consolidation		Overall net water released at final load (%)
		Water content (%)	Net water released (%)	Final water content (%)	Net water released (%)	
Neutral PT	627.6	218.5	32.8	27.6	53.7	86.5
Cationic PT	323.0	267.0	0*	30.8	85.0	85.0
Anionic PT	247.8	178.4	28.8	25.4	60.2	87.4
Untreated FFT	227.6	161.2	28.7**	35.2	54.5	87.6

Note: * 40% of added polymer water volume remaining in treated tailings
** FFT water released after 8 weeks of self-weight consolidation

Results in Section 4.3 and Table 5-1 indicate considerable dewatering of FFT by the polymer treatments. In addition to the polymer water added during treatment, the neutral PT rapidly released 32.8% of the pore water volume in FFT at the end of sedimentation, while the anionic PT achieved 4% less, at a relatively slow rate. On the contrary, FFT treated using the cationic polymer retained 40% of the polymer solution added and was unable to dewater FFT by the end of sedimentation. These results show that the neutral PT dewaters FFT more efficiently immediately after deposition compared to the other treatments and attains a relatively high density after settling. The anionic PT also produces considerable FFT water release, but at a slower settling rate. Although, the cationic PT settles faster than the anionic PT, the retention of some of the polymer solution by the cationic PT at the end of sedimentation indicates a negative initial dewatering efficiency. This means that further dewatering of the cationic PT requires a surcharge to recover the remaining polymer solution and to dewater FFT. Therefore, large amounts of process water will be irrecoverable during deposition until sufficient effective stresses develop within the tailings deposit to promote further water release.

Table 5-1 shows that the majority of the tailings dewatering occurs during consolidation. The anionic PT released 5% more FFT water at effective stresses close to 900 kPa compared to the neutral PT. Remarkably, the cationic PT demonstrates a higher compression index, as 86.7% of FFT water and the retained polymer water are all released under the same vertical effective stress. The total net water released by the three polymer treatments during sedimentation and consolidation (~900 kPa effective stress) ranges between 86.7% and 89%. Although the dewatering efficiencies of the polymer treatments converge at greater depths, the net amount of water that can be removed by each polymer treatment vary considerably at any given effective stress, depending on the height (or depth) of the tailings deposit.

It is therefore evident that the neutral PT exhibits better immediate dewaterability than the anionic PT, with a higher initial net water release after deposition. Further dewatering occurs in the long term as the deposit depth increases. Although the cationic PT has a poor initial dewatering efficiency, it consolidates faster with depth as effective stresses develop, owing to its relatively high hydraulic conductivity.

5.3 Effect on shear strength

A key reclamation requirement is the shear strength that can be achieved in the tailings deposit for trafficability and cover system construction. The undrained shear strength relationships of polymer amended FFT in Figure 4-12 show that the neutral PT produces considerable shear strength gain of approximately 40 percent over the anionic and cationic PTs at effective stresses higher than 10 kPa. While the shear strength development produced by the anionic and cationic PTs are similar at given effective stresses, the undrained shear strength of the neutral and cationic PTs is about an order of magnitude higher than the anionic PT and about two orders of magnitude more compared to untreated FFT at given densities. The undrained shear strengths of the polymer treatments begin to converge at void ratios less than 1.0 or solids contents above 70%. At void ratios greater than 3.5 where solids contents are less than 35%, the shear strength of the neutral PT is distinctly higher compared to the other treatments.

The effect of water content and plasticity on the undrained shear strength of the tailings in Figure 4-16 suggests that the cationic PT is more resistant to shear at a given liquidity index compared to the neutral and anionic PTs. This is because, for a given liquidity index, the anionic and neutral PTs require higher water contents due to their relatively high plasticity index, which consequently reduce the undrained shear strength of these tailings. Using the now-defunct directive 074 as a guide, it can also be seen that the minimum undrained shear strength of 5 kPa can be achieved at higher water contents (solids content of 40%) with cationic and neutral polymer addition to FFT compared to the anionic polymer (solids content of 50%) and untreated FFT (solids content of 73%). Model predictions of the average deposit solids content suggest that these water contents can be achieved after 1, 21 and 57 year(s) in the neutral, cationic and anionic PT deposits, respectively. For a bearing strength of at least 25kPa with limited settlement, terrestrial reclamation will require dewatering the anionic PT to water contents below its liquid limit, while this can be achieved at a liquidity index higher than 1 in the cationic and neutral PTs. However, this amount of dewatering is only possible at greater deposit depths over long consolidation timeframes.

The effect of the polymer treatments on the shear strength of the tailings becomes more prominent when the undrained shear strength is normalized by the effective stress for a given density, as shown in Figure 4-15. Results show a decrease in the normalized shear strength of the treated tailings from a high void ratio, where effective stresses are low and physicochemical forces dominate, to high densities, where the shear strength is controlled by frictional interactions. The neutral and anionic PTs exhibit similar undrained shear strength ratio within experimental errors at given void ratios less than 4, although these void ratios were not achieved at equal effective stresses. The neutral PT exhibits a higher normalized shear strength up to 4 at effective stresses close to self-weight, which suggests stronger floc bonds. It is noted that the undrained shear strength of the neutral PT was measured in the sheared sample, and thus, the reduced undrained shear strength ratio at void ratios between 4 and 6.5, where effective stresses are still low, can be attributed to shear effects as observed by Jeeravipoolvarn et al. (2014). The undrained shear strength of the cationic PT relative to effective stress is comparatively lower at given void ratios due to its fine floc fabric, which offers less resistance to shear. Notwithstanding, Jeeravipoolvarn (2010) indicates that strong floc bonds are responsible for the high shear strength of in-line flocculated FFT at high void ratios, where chemical forces dominate. This observation holds true in the present study, as the neutral PT creates large flocs with high solids content that draw their strength from the stiff amylopectin backbone and long polyacrylamide grafts of the neutral polymer, to which FFT particles are bonded. Thus, the flocs of the neutral PT appear to be the most resistant to shear at higher void ratios. The cationic polymer, on the other hand, is relatively softer, and the post-treatment flocs are less strong at high void ratios compared to the anionic and neutral PTs.

5.4 Post-treatment shear sensitivity of tailings

In addition to the above effects, the large strain consolidation results of the overmixed neutral PT (labelled neutral S1) in Figure 4-9 to Figure 4-11 indicate that shearing can significantly affect the compressibility and hydraulic conductivity of the neutral PT. Additional mixing of the neutral PT after the flocs settled resulted in floc breakage, which substantially increased the tailings void ratio after self-weight consolidation from 4.95 to 6.48, as well as the compression index of the tailings. Consequently, the hydraulic conductivity of the overmixed neutral PT increased accordingly at effective stresses lower than 10 kPa, but the sudden reduction in the hydraulic conductivity observed at a void ratio of 3.8 was no longer apparent as the macro floc structure was destroyed by shear. Jeerapoolvarn (2010) observed a similar macrostructure breakdown in sheared ILTT, except that the resulting compression index was lower at void ratios higher than 5 compared to the non-sheared ILTT and only the material compressibility was affected.

The compressibilities of the sheared and non-sheared neutral PTs converge at an effective stress of 10 kPa. This behaviour suggests that the flocs created by the neutral PT are sensitive to shear, and if sheared, the deposit volume at shallow depths will increase substantially. However, the sheared material will consolidate more rapidly due to its higher hydraulic conductivity and achieve the same density as the non-sheared tailings at depths where effective stresses exceed 10 kPa. Although the properties of the resulting sheared material depend on the FFT properties, polymer type, chemical bonding between polymer and clay particles, floc structure and strength and degree of shearing, it can be concluded that excessive shearing affects the consolidation properties of FFT treated with the neutral polymer at low effective stresses (below 10 kPa). The cationic and anionic PTs exhibit a relatively more stable floc structure compared to the neutral PT.

Considering that additional mixing considerably influenced the compressibility of the neutral PT as discussed above, the difference in void ratio at stresses below 10 kPa suggests a difference in the undrained shear strength achieved in the sheared and non-sheared materials. The observed shear effect on the consolidation properties of the neutral PT in this study suggests that shearing also reduced the undrained shear strength of the neutral PT. Thus, a higher undrained shear strength is expected in the non-sheared neutral PT below 10 kPa effective stress. However, since pipeline shearing is an inevitable operational condition, its effect on the geotechnical behaviour of the new polymer treatments requires investigation.

5.5 Effect of thixotropy on the consolidation and shear strength of flocculated FFT

Ageing experiments, followed by large strain consolidation testing, explored the effect of thixotropic processes on the shear strength of polymer amended FFT. Undrained shear strength measurements from the fall cone tests in Figure 4-17 and Figure 4-18 show a continual increase in the surface strength of tailings with time as excess pore pressure dissipates, even after final settlement. This is attributed to ongoing, time-dependent structuration processes caused by electrochemical forces within the tailings, which are independent of effective stress. These findings agree with observations by Salam et al. (2018) that indicate a similar decline in excess pore water pressure with undrained shear strength gain using a large column and single-drainage replicate columns. Drying at the tailings’ surface may potentially have occurred during the fall cont test, but its effect on the results was minimized by maintaining a water cover above the tailings during the ageing and LSC tests. It is noted that considerable thixotropic strength gain in the amended tailings at the polymer dose used would require extended ageing time and/or optimization of polymer dose and mixing protocol.

The compressibility of the aged polymer amended FFT in Figure 4-19 shows a different response to compression compared to the unaged tailings. The void ratio of 3.5, attained after ageing at 0.1 kPa effective stress, indicates a reduced tailings volume. This appears to increase the compressibility of the tailings, resulting in higher densities, as demonstrated by relatively lower void ratios at given stresses. In addition, the compressibility curve shows an apparent pre-consolidation pressure at about 0.6 kPa, indicating an increase in the tailings stiffness and resistance to compression developed during ageing. Beyond this stress, electrochemical forces are overcome in compression, resulting in a normally consolidated behaviour. Furthermore, the aged and unaged polymer amended FFT exhibit similar hydraulic conductivities at void ratios greater than 1.8, within experimental error, as shown in Figure 4-20. However, the aged tailings are up to an order of magnitude more permeable than the unaged tailings at lower void ratios. Thus, the aged amended FFT is less compressible, but more permeable, at higher densities compared to the unaged tailings, indicating a denser but more porous structure that enhances the long-term dewatering of the amended tailings.

The thixotropic strength gain of the polymer amended FFT is more evident when the undrained shear strength is normalized by the effective stress, as shown in Figure 4-22. The results indicate that the undrained shear strength of the amended tailings increased by over 2.5 times after ageing under self-weight. The thixotropic strength at a given density reduces during compression as effective stresses develop in the aged tailings until a void ratio of 1.4 is reached, where the thixotropic effects on the shear strength of the polymer amended tailings are considerably overcome by frictional forces.

5.6 Evaluation of long-term consolidation of model deep tailings deposits

Deep deposits of in-line flocculated tailings in mined-out pits undergo large settlements over an extended time. Figure 4-23 shows the predicted long-term settlement of model deep deposits of FFT amended with the anionic, cationic and neutral polymers compared to the untreated FFT, filled to a depth of 70 m. After treating and depositing the same mass of solids in the FFT, the anionic, cationic and neutral PT deposits settle by 10 m, 12 m, and 15 m, respectively, more than the untreated FFT at the end of deposition (year 40 - end of mining). The neutral PT deposit attains an average solids content 40% within the first year of deposition, increasing to 41% at fill completion, while approximately 39% and 38% solids contents, on average, are gradually achieved in the cationic and anionic PT deposits, respectively, by the end of deposition (Figure 4-24). The neutral PT deposit settles rapidly with little change in the average solids content between year 1 and year 20, which indicates a low excess pore pressure buildup in the deposit during deposition compared to the other deposits. This can be attributed to its high initial hydraulic conductivity, suggesting that the hydraulic conductivity and the rate of rise directly affect the rate of consolidation of tailings during deposition. It is noted that the high hydraulic conductivity of the untreated FFT at lower void ratios provides considerable dewatering and settlement in the long term. Duplicates of untreated FFT were analyzed to confirm the LSC data and similar results were found. However, this peculiar performance cannot be generalized for other FFTs.

The anionic and cationic PT deposits settle faster within the first 40 years (year 20 to year 60) following deposition, but attenuate in their rate of settlement with time as the deposit densifies. The settlement of the neutral PT is relatively slower during year 20 to year 50, owing to its high solids content and reduced hydraulic conductivity at lower void ratios below 3.6. Both the anionic and cationic PT increase FFT settlement by 12%, 80 years after deposition. Over the same period, the neutral PT adds 7% more in settlement, decreasing to about 5% at year 300, which is relatively low compared to the 9% increase achieved by the anionic and cationic PT. Regardless, the anionic and cationic PTs attain a similar average solids content at the end of deposition, which increases to about 57 to 58 %, at year 300. The average solids content of the neutral PT deposit at this time is 2 to 3% lesser, and 5 to 7% lesser for the untreated FFT deposit. The concentration of solids increases with depth at a given time, and the entire density profile progressively grows over time as the deposit consolidates.

The difference in the initial solids contents and the compressibilities of the different polymer treatments indicates that the dry density at a given depth varies between the deposits. The relatively higher density of the anionic PT deposit at a given stress during consolidation is an advantage that contributes to its shear strength gain and volume reduction. However, the latter occurs after deposition, when sufficient excess pore pressure has dissipated. The anionic PT requires a much lower water input during treatment and lower supernatant reclaim energy requirement compared to the cationic and neutral PTs.

Although the neutral PT has a low initial solids content, its high initial hydraulic conductivity is responsible for the rapid shear strength gain during deposition due to its high settling rate. However, the deposit density achieved by this initial settling process reduces the long-term rate of settlement and strength gain, as further dissipation of excess pore pressure is hindered by the reduced hydraulic conductivity of the deposit at higher densities. Nonetheless, the neutral PT deposit has the advantage of providing more storage for treated FFT during deposition if the water released is reclaimed. In addition, the neutral PT deposit attains a higher undrained shear strength at a given solids content, which is valuable when compared to the cationic and anionic PT within the range of average solids contents predicted (Figure 4-14). A disadvantage of the neutral PT is that large volumes of water are required for FFT treatment and must be reclaimed during deposition to create storage, which increases costs and energy requirements compared to the anionic and cationic PTs.

The cationic PT deposit has a slight advantage over the anionic PT in terms of the additional storage it provides during deposition despite its relatively lower initial solids content. This is attributed to the high hydraulic conductivity of the cationic PT at higher densities, which enhances dewatering at greater depths as the deposit height increases. The cationic PT deposit exhibits higher dewatering rates following deposition, resulting in greater long-term settlement and higher deposit density compared to the neutral PT. This advantage is, however, leveled by the higher solids content of the anionic PT deposit at a given stress, resulting in a more or less similar long-term settlement and volume reduction for both treatments. Nonetheless, the cationic PT exhibits a higher undrained shear strength at a given density compared to the anionic PT (Figure 4-14), which is an additional advantage within the range of predicted average solids contents. Also, the treatment process and management of the water release to create storage during deposition will require lesser water input and costs compared to the neutral PT.

The step shapes seen in the model data for the untreated FFT and anionic PT in Figure 4-25 and Figure 4-26 arise from the compressibility and hydraulic conductivity dataset coupling at the void ratios achieved along the deposit depth at the end of deposition. It is noted that, by this time, the tailings density with depth remains constant until further compression occurs due to an increase in vertical effective stress. The sudden increases in density at certain depths are because the discrete data points, especially at high void ratios, do not describe a smooth curve that agrees with the power function fits for the compressibility and hydraulic conductivity datasets. Thus, the coupling of the datasets does not provide smooth model curves at low densities, but improves as the deposit densifies (Figure 4-27 and Figure 4-28).

Chapter 6: Conclusions

The objective of this research was to investigate if amending FFT using two novel cationic and neutral polymers, developed through specific modification of the polymer structure, would enhance the long-term dewatering performance of oil sands fluid fine tailings. To this end, this study has completed a laboratory geotechnical testing program to determine the effects of the new polymer treatments at specific doses on the material characteristics, large strain consolidation properties and shear strength of FFT in the immediate and long term, compared to an existing anionic polymer.

Basic characterization tests provided an understanding of the physical and mineralogical characteristics of the tailings products resulting from the polymer treatments compared to the untreated FFT. The initial volumes and solids contents of the amended tailings reflect the polymer doses applied and the amount of FFT solids that can be treated by each polymer in a given volume. Each polymer produced a distinct range of floc sizes, from fine flocs in the cationic polymer treatment to large flocs in the neutral polymer treatment, that had a considerable impact on the initial settling rates of tailings. Changes in the material properties following polymer addition were also evident in the liquid limit and plasticity of the tailings.

The initial dewatering efficiency of the polymer treatments was evaluated from hindered sedimentation tests carried out on the treated and untreated FFT. The effectiveness of the polymers in capturing fines was demonstrated by clear water release. CST also served as a useful method for evaluating the improvement made in the initial dewaterability of FFT by each polymer treatment. Large strain consolidation testing with vane shear tests was carried out on the treated and untreated FFT to determine the compressibility, hydraulic conductivity and undrained shear strength that would control their long-term dewatering performance.

The neutral PT settles rapidly after treatment at the specified polymer dose and releases approximately 33% of the original FFT water shortly after deposition. However, once the flocs settle, the dewaterability of the neutral PT is low. On the other hand, the cationic polymer treatment exhibits rapid initial dewaterability with better CST, but poor initial dewatering as 40% of the added polymer solution remains in the amended tailings after settling. The initial dewaterability of the anionic PT is slower compared to the new polymer treatments; albeit, an appreciable net water is ultimately released during settling, indicating a better dewatering efficiency in the immediate term compared to the cationic PT. Therefore, the neutral PT will help operators to maximize initial dewatering, increase early water recycling for mining operations, and consequently maximize tailings storage in the short term.

The neutral PT produces high dewatering rates at lower densities (void ratio higher than 3.8) due to its distinct floc structure characterized by large pores. Further densification of the tailings reduces its dewatering rate dramatically, impacting long-term dewatering. The cationic polymer treatment provides higher dewatering rates at higher densities compared to the neutral and anionic polymers, leading to continual long-term dewatering.

The neutral and cationic polymer treatments exhibit higher undrained shear strength at a given density compared to the anionic PT. The undrained shear strength produced by the neutral polymer is distinctively high at void ratios higher than 3.5 due to strong floc bonds. Nonetheless, the higher hydraulic conductivity and considerable strength gain of the cationic PT at higher densities are favourable to reducing reclamation timelines in the long term.

The floc structure of the neutral PT is shear sensitive, such that the compressibility and hydraulic conductivity of this treated tailings at void ratios greater than 2 are significantly impacted. Evaluation of the long-term dewatering performance of this polymer treatment should consider the effect of pipeline shearing.

Thixotropic strength buildup measured in polymer amended FFT demonstrated that time-dependent structuration processes could be harnessed to enhance the trafficability and long-term dewatering of chemically-amended tailings after deposition. This strength gain can be maximized by optimizing flocculation.

Model predictions of deep deposits using FSConsol provided additional information in support of the evaluation of long-term dewatering of the polymer treatments. Rapid initial dewatering, higher early strength and small long-term settlement are predicted for the neutral PT deposit, while long-term dewatering, large long-term settlement, and a continual increase in deposit density and strength are anticipated for the cationic PT deposit. From a geotechnical perspective, these predictions suggest that the new polymer treatments would support aquatic reclamation of FFT. The neutral PT can be potentially useful in the development of terrestrial landforms but would require additional engineering to be trafficable and geotechnically stable with reduced risk.

It can be concluded that the new neutral and cationic polymers considerably enhanced the dewatering performance of FFT in different respects compared to the existing anionic polyacrylamide. However, the amount of polymer and water input in the new polymer treatments add increased energy and operational costs.

6.1 Recommendations for Future Work

This research has completed its objective of evaluating the effects of two novel polymer treatments on the immediate and long-term dewatering performance of oil sands fluid fine tailings. This was achieved by:

- Characterizing fine tailings amended using the new polymers at specific dosages and mixing protocols provided by the polymer designer.
- Conducting bench-scale hindered sedimentation and large strain consolidation tests with vane shear tests on the amended FFT to determine the consolidation properties and shear strength of the tailings.
- Evaluating and comparing the effects of the new polymer treatments to an existing polymer treatment used in the industry.
- Assessing the effects of thixotropy on the trafficability and large strain consolidation properties of polymer amended FFT.

While doing so, several new questions that require investigation arose and include the following recommendations:

1. Assess optimum dosage and mixing conditions for each polymer treatment based on the long-term dewatering performance
2. Assess the effect of pipeline shearing under operational conditions on the long-term dewatering performance of the new polymer treatments.
3. Evaluate the thixotropic strength gain on polymer amended FFT at realized optimum dose.

Bibliography

Alberta Energy Regulator (AER) 2017. Directive 085: Fluid Tailings Management for Oil Sands Mining Projects. Available from: https://www.aer.ca/documents/ directives/Directive085.pdf. Accessed on April 10, 2020.

Alberta Energy Regulator (AER) 2019. State of fluid tailings management for mineable oil sands, 2018. Available from: https://www.aer.ca/documents/oilsands/2018-State-Fluid-Tailings-Management-Mineable-OilSands.pdf. Accessed on April 11, 2020.

Alberta Government 2015. Lower Athabasca Region – Tailings Management Framework for the Mineable Athabasca Oil Sands.

ASTM D2216-19, Standard Test Methods for Laboratory Determination of Water (Moisture) Content of Soil and Rock by Mass, ASTM International, West Conshohocken, PA, 2019, www.astm.org

ASTM D422-63(2007)e2, Standard Test Method for Particle-Size Analysis of Soils (Withdrawn 2016), ASTM International, West Conshohocken, PA, 2007, www.astm.org

ASTM D4318-17e1, Standard Test Methods for Liquid Limit, Plastic Limit, and Plasticity Index of Soils, ASTM International, West Conshohocken, PA, 2017, www.astm.org

ASTM D854-14, Standard Test Methods for Specific Gravity of Soil Solids by Water Pycnometer, ASTM International, West Conshohocken, PA, 2014, www.astm.org.

Government of Alberta 2020. Oil sands 101, https://www.alberta.ca/oil-sands-101.aspx. Accessed on April 23, 2020.

Bajwa, T. and Simms, P. 2013. Influence of dewatering and desiccation on microstructure and vane strength of polymer amended oil sand fine tailings. *In GeoMontreal 2013*, pp. 8.

Beier, N.A., and Sego, D.C. 2008. The oil sands tailings research facility. Geotechnical News, June 2008, pp. 72–77.

Beier, N., Wilson, W., Dunmola, A., and Sego, D. 2013. Impact of flocculation-based dewatering on the shear strength of oil sands fine tailings, Canadian Geotechnical Journal, **50**(9): 1001-1007.

BGC Engineering Inc. 2010. Oil sands tailings technology review. Oil Sands Research and Information Network, University of Alberta, School of Energy and the Environment, Edmonton, Alberta.

Bazoubandi, B. and Soares, J.B.P. 2020. Amylopectin-graft-polyacrylamide for the flocculation and dewatering of oil sands tailings, Minerals Engineering, **148**: 106196.

Boxill, L. E. 2016. The impact of fabric and surface characteristics on the engineering behavior of polymer-amended mature fine tailings. PhD thesis, University of British Columbia, Vancouver, Canada. pp.230

CEMA – Cumulative Environmental Management Association 2012. Oil sands End Pit Lake Guidance Document. CEMA. Fort McMurray, Alberta, Canada.

Chalaturnyk, R.J., Don Scott, J., and Özüm, B. 2002. Management of oil sands tailings, null, **20**(9-10): 1025-1046.

Corriveau, D. 2018. Keynote Address. In Sixth International Oil Sands Tailings Conference. December 9-12, 2018. Edmonton, Alberta, Canada.

COSIA – Canadian Oil Sands Innovation Alliance 2012. Technical Guide for Fluid Fine Tailings Management. Oil Sands Tailings Consortium, August 30, 2012, 131 pp.

COSIA – Canadian Oil Sands Innovation Alliance 2014. A Guide to Audit and Assess Oil Sands Fluid Fine Tailings Performance Management. Canada's Oil Sands Innovation Alliance. Calgary. August 2014, 18p.

COSIA 2019. 2018 Tailings research report. Available from: https://cosia.ca/sites/default/files/attachments/2018%20Tailings%20Research%20Report_FINAL%2003Jun2019.pdf. Accessed on April 9, 2020.

Delage, P. 2010. A microstructure approach to the sensitivity and compressibility of some Eastern Canada sensitive clays. Géotechnique, 60(5), 353-368.

Delage, P., Marcial, D., Cui, Y. J. and Ruiz, X. 2006. Ageing effects in a compacted bentonite: a microstructure approach. Géotechnique, 56(5), 291-304.

Demoz, A. and Mikula, R. 2012. Role of mixing energy in the flocculation of mature fine tailings, Journal of Environmental Engineering, **138**: 129-136.

Derakhshandeh, B., Junaid, A., and Freeman, G. 2016. Effects of shearing and shearing time on dewatering and yield characteristics of oil sands flocculated tailings. In Fifth International Oil Sands Tailings Conference, pp. 416-421.

Elias, J. A., 2019. Measurement of floc size and the influence of size distribution on geotechnical properties of oil sands fluid fine tailings. Master of Science thesis, University of Alberta, Edmonton.

Energy Resources Conservation Board (ERCB) 2009. Directive 074: Tailings Performance Criteria and Requirements for Oil Sands Mining Schemes. (Rescinded July 14, 2016).

Energy Resources Conservation Board (ERCB) 2013. 2012 Tailings Management Assessment report. June 2013, pp. 4.

Farkish, A. and Fall, M. 2013. Rapid dewatering of oil sand mature fine tailings using super absorbent polymer (SAP), Minerals Engineering, **50-51**: 38-47.

Fine Tailings Fundamentals Consortium, (FTFC). 1995. Advances in oil sands tailings research. Edmonton, Alta. : Alberta Dept. of Energy, 1995.

Gibson, R.E., England, G.L. and Hussey M.J.L. 1967. The theory of one-dimensional consolidation of saturated clays. I. Finite non-linear consolidation of thin homogeneous layers. Géotechnique, **17**(3): 261–273.

Gibson, R.E., Schiffman, R.L., and Cargill, K.W. 1981. The theory of one-dimensional consolidation of saturated clays. II. Finite nonlinear consolidation of thick homogeneous layers. Canadian Geotechnical Journal, **18**: 280-293.

Gholami, R & Simms, P 2015, 'Shear behaviour in element testing of polymer amended mature fine tailings', *Proceedings of the 68th Canadian Geotechnical Conference*, Canadian Geotechnical Society, Richmond.

Government of Alberta (2020). Oil sands 101. https://www.alberta.ca/oil-sands-101.aspx. Accessed April 23, 2020.

Gumfekar, S.P., Vajihinejad, V., and Soares, J.B.P. 2019. Advanced polymer flocculants for Solid–Liquid separation in oil sands tailings, Macromolecular Rapid Communications, **40**(1): 1800644.

Hansbo, S. 1957. A new approach to the determination of the shear strength of clay by the fall cone test. Swedish Geot. Inst. Pub. No.14, Stockholm

Hockley, D. 2018a. Clay effects on geotechnical properties of tailings. *In* Introduction to Oil Sands Clays *Edited by* D. Hockley and O. Omotoso. Clay Minerals Society, pp. 183-211.

Hockley, D. 2018b. Mescoscale phenomena. *In* Introduction to Oil Sands Clays *Edited by* D. Hockley and O. Omotoso. Clay Minerals Society. Vol. 22, pp. 91-108.

Hyndman, A., Sawatsky, L., McKenna, G., and Vandenberg, J. 2018. Fluid fine tailings processes: disposal, capping, and closure alternatives. International Oil Sands Tailings Conference December 9-12, 2018, Edmonton, Alberta, Canada.

Jeeravipoolvarn S., Masala, S., Zhang, C. and Moore, T. 2015. Revisiting the large strain consolidation test for oil sands. *In* Proceedings of Tailings and Mine Waste 2015, Vancouver, BC, October 26 to 28, 2015

Jeeravipoolvarn, S., Scott, J.D., Chalaturnyk, R., and Shaw, B. 2014. Effect of pipelining shear on consolidation properties of oil sands fine tailings. In Tailings and Mine Waste '14, pp. 495-506.

Jeeravipoolvarn, S. 2010. Geotechnical behavior of in-line thickened oil sands tailings. PhD thesis. University of Alberta. Edmonton. [electronic resource]. 2010.

Jeeravipoolvarn, S., Scott, J.D., and Chalaturnyk, R.J. 2009. 10 m standpipe tests on oil sands tailings: Long-term experimental results and prediction, Canadian Geotechnical Journal, **46**(8): 875-888.

Jeeravipoolvarn, S. 2005. Compression behaviour of thixotropic oil sands tailings. Master's thesis, University of Alberta, Edmonton, Alberta.

Kaminsky, H.A.W., Etsell, T.H., Ivey, D.G., and Omotoso, O. 2009. Distribution of clay minerals in the process streams produced by the extraction of bitumen from Athabasca oil sands, The Canadian Journal of Chemical Engineering, **87**(1): 85-93.

Kaminsky, H. 2014. Demystifying the methylene blue index. *In* Proceedings of the Fourth International Oil Sands Tailings Conference, Banff, Alberta. pp. 221-229.

Kaminsky, H. and Omotoso, O. 2016. Variability in fluid fine tailings. *In* Fifth International Oil Sands Tailings Conference, pp. 178-183.

Kaminsky, H.A. and Omotoso, O. 2018. Clay measurement methods in oil sands. *In* Introduction to Oil Sands Clays *Edited by* D. Hockley and O. Omotoso. Clay Minerals Society, pp. 75-89.

Kynch, E.J. (1952) A theory of sedimentation. Transactions of the faraday Society, **48**, 168-176.

Klein, C. 2014. Effect of Residual Bitumen on Polymer-assisted Flocculation of Fluid Fine Tailings (Master's thesis, Department of Chemical Engineering), Edmonton: University of Alberta.

Locat, J., and Demers, D. 1988. Viscosity, yield stress, remolded strength, and liquidity index relationships for sensitive clays. Canadian Geotechnical Journal, **25**(4): 799‑806. doi:10.1139/t88-088.

MacKinnon, M. and Zubot, W. 2013. Water management. *In*: Handbook on Theory and Practice of Bitumen Recovery from Athabasca Oil Sands, Volume II: Industrial Practice. *Edited by* Jan Czarnecki, Jacob Masliyah, Zhenghe Xu, and Marta Dabros. Kingsley Knowledge Publishing, Canada.

Mahmoudkhani, A., Tellakula, R., Watson, P, Fenderson, T., Stewart, K., & Wu, Y. (2012). Consolidation of oil sands process tailings by enhanced coagulation – flocculation. *3rd International Oil Sands Tailings Conference*, Edmonton, December 2-5.

McKenna, G., Dawson, R., Hyndman, A., LeSueur, P., and Sobkowicz, J. 2012. The oil sands tailings technology roadmap and action plan: Oil sands tailings state of practice overview. *In* International Oil Sands Tailings Conference 2012, pp. 205-212.

McKenna, G., Mooder, B., Burton, B., and Jamieson, A. 2016. Shear strength and density of oil sands fine tailings for reclamation to a boreal forest landscape. *In* Fifth International Oil Sands Tailings Conference, pp. 130-153.

Mercier, P.H.J., Omotoso, O., and Hockley, D. 2018. Oil-sands clays. *In* Introduction to Oil Sands Clays *Edited by* D. Hockley and O. Omotoso. Clay Minerals Society, pp. 9-32.

Mewis, J. & Wagner, N. 2012. Colloidal Suspension Rheology. Cambridge: Cambridge University Press.

Mitchell, J. M. 1960. Fundamental aspects of thixotropy in soils. Journal of the soil mechanics and foundations division, **86**(3), 19-52.

Mitchell, J.K., and Soga, K. 2005. Fundamentals of soil behavior. 3rd ed. John Wiley and Sons, Hoboken, N.J.

Miller, W.G. 2010. Comparison of geoenvironmental properties of caustic and noncaustic oil sand fine tailings. PhD Thesis, University of Alberta, Edmonton, Alberta.

Mikula, R. and Freeman, G., 2016. Chemical amendment of fluid fine tailings and related laboratory performance tests. *In* Fifth International Oil Sands Tailings Conference, pp. 251-260.

Mikula, R. and Omotoso, O. 2006. Role of clays in controlling tailings behaviour in oil sands processing, Clay Science, **12**: 177-182.

Mikula, R. 2018. The role of clays in the performance of oil-sands tailings management options. *In* Introduction to Oil Sands Clays *Edited by* D. Hockley and O. Omotoso. Clay Minerals Society, pp. 129-181.

Mizani, S., Simms, P., Wilson, G.W., and Beier, N. 2016. Thixotropic effects on the rheology of polymer amended mature fine tailings implications for surface deposition control. In Fifth International Oil Sands Tailings Conference, Lake Louise, Alberta, Canade. pp. 60-67.

Neelakantan, R., Vaezi G, F., and Sanders, R.S. 2018. Effect of shear on the yield stress and aggregate structure of flocculant-dosed, concentrated kaolinite suspensions, Minerals Engineering, **123**: 95-103.

Norwest Corporation (Norwest) 2018. Fluid Fine Tailings Management Methods. Report prepared in June 2018.

Omotoso, O., and Melanson, A., 2014. Influence of clay mineralogy on the behavior of oil sands tailings. PASTE pp. 31-42. Vancouver: InfoMine Inc.

Omotoso, O. and Morin, M. 2008. Methylene blue adsorption procedure for Dean Stark solids. Canmet ENERGY, Devon, Canada.

Pane, V. and Schiffman, R.L. 1997. Permeability of clay suspensions. Géotechnique, **47**: 273-288.

Rourke, H. and Hockley, D. 2018. Assessing oil sands tailings consolidation parameters relative to long-term reclamation. *In* Proceedings from Tailings and Mine Waste 2018. Keystone, Colorado, USA. pp. 127-138.

Salam, A. M., Simms, P. H., & Örmeci, B. 2018. Evidence of creep & structuration in polymer amended oil sands tailings. *Proceedings of the 6th International Oil Sands Tailings Conference*. Edmonton, Alberta.

Scott, J.D., Jeeravipoolvarn, S., and Chalaturnyk, R. 2008. Tests for wide range of compressibility and hydraulic conductivity of flocculated tailings. Proceedings of GeoEdmonton'08 Conference, Edmonton, Canada. September 2008.

Skempton, A. W. and Northey, R. D. 1952. The sensitivity of clays. Géotechnique 3, No.1, 30-53.

Sobkowicz, J.C., and Morgenstern, N.R. 2009. A geotechnical perspective on oil sands tailings. *In* Proceedings of the 13th International Conference on Tailings and Mine Waste, Banff, Alta., 1–4 November 2009. University of Alberta. pp. xvii–xli.

Sobkowicz, J. 2012. The oil sands tailings technology roadmap and action plan: Introduction and key recommendations. *In* International Oil Sands Tailings Conference 2012, pp. 13-23.

Suthaker, N.N. and Scott, J.D. 1997. Thixotropic strength measurement of oil sand fine tailings, Canadian Geotechnical Journal, **34**(6): 974-984.

Terzaghi, K. & Peck, R. (1967). *Soil Mechanics in Engineering Practice*. 2nd Ed., Wiley: New York.

Vajihinejad, V. and Soares, J.B.P. 2018. Monitoring polymer flocculation in oil sands tailings: A population balance model approach, Chemical Engineering Journal, **346**: 447-457.

Vajihinejad, V., Gumfekar, S.P., Bazoubandi, B., Rostami Najafabadi, Z., and Soares, J.B.P. 2019. Water soluble polymer flocculants: Synthesis, characterization, and performance assessment, Macromolecular Materials and Engineering, **304**(2): 1800526.

Vedoy, D.R.L. and Soares, J.B.P. 2015. Water-soluble polymers for oil sands tailing treatment: A review, The Canadian Journal of Chemical Engineering, **93**(5): 888-904.

Vietti, A. 2018. Clay–water interactions. *In* Introduction to Oil Sands Clays *Edited by* D. Hockley and O. Omotoso. Clay Minerals Society, pp. 61-74.

Wells, P., Revington, A. & Omotoso, O. 2011. MFT drying – Technology update. Proceedings, Tailings and Mine Waste, Vancouver, November 7-9.

Wilson, G.W., Kabwe, L.K., Beier, N.A., and Scott, J.D. 2018. Effect of various treatments on consolidation of oil sands fluid fine tailings, Canadian Geotechnical Journal, **55**(8): 1059-1066.

Yao, Y., van Tol, A.F., and van Paassen, L. 2012. The effect of flocculant on the geotechnical properties of mature fine tailings: An experimental study. *In* International Oil Sands Tailings Conference, pp. 391-398.

Znidarčić, D., Van Zyl, D., Ramirez, M., Mittal, K., and Kaminsky, H. 2016. Consolidation characteristics of flocculated MFT – Experimental column and SICT data. *Fifth International Oil Sands Tailings Conference*, Lake Louise, University of Alberta, Edmonton, Alberta, pp. 408-415.

Appendices

Appendix A: Laboratory Test Data

A1. Large strain consolidation test results

Table A-1: Large strain consolidation with vane shear test of untreated FFT

Load	Effective stress (kPa)	Height (mm)	ΔH (mm)	Void ratio, e	Solids content (%)	Hydraulic gradient, i	Hydraulic conductivity (m/s)	Undrained shear strength (kPa)
1	-	127.0	-	5.17	30.5	-	1.48E-07	-
2	0.1	96.0	31.00	3.66	38.3	0.20	1.92E-08	0.01
3	0.32	89.42	6.58	3.32	40.6	0.44	7.52E-09	0.04
4	0.64	81.12	8.30	2.88	44.1	0.64	3.00E-09	0.12
5	1.25	65.21	15.91	1.93	54.0	1.98	2.48E-09	0.25
6	2.57	55.95	9.26	1.45	61.1	2.31	1.50E-09	0.55
7	5.26	50.69	5.26	1.19	65.6	3.33	7.94E-10	1.45
8	8.28	46.79	3.90	1.01	69.3	4.22	7.85E-10	2.74
9	19.5	42.79	4.00	0.82	73.4	4.37	5.04E-10	5.94
10	40.47	38.59	4.20	0.62	78.4	8.84	1.01E-10	41.26
11	79.96	37.39	1.20	0.57	80.0	9.15	8.70E-11	46.06

Table A-2: Large strain consolidation without vane shear test of neutral PT S2

Load	Effective stress (kPa)	Height (mm)	ΔH (mm)	Void ratio, e	Solids content (%)	Hydraulic gradient, i	Hydraulic conductivity (m/s)	Undrained shear strength (kPa)
1	-	151.00	-	14.25	13.7	-	1.72E-02	-
2	0.10	59.00	92.00	4.96	31.5	0.37	3.11E-06	-
3	0.32	49.69	9.31	3.84	37.2	0.70	1.02E-06	-
4	0.62	47.11	2.58	3.58	38.9	1.34	2.31E-08	-
5	1.18	43.01	4.10	3.14	42.1	1.67	9.82E-09	-
6	2.40	38.63	4.38	2.67	46.0	2.95	4.27E-09	-
7	4.87	34.99	3.64	2.29	49.9	5.49	2.17E-09	-
8	10.39	33.48	1.51	2.14	51.6	5.26	1.38E-09	-
9	20.12	30.64	2.84	1.85	55.2	5.74	7.49E-10	-
10	40.08	27.38	3.27	1.51	60.2	6.43	3.47E-10	-
11	80.07	25.29	2.08	1.30	63.6	6.96	1.89E-10	-
12	159.88	23.43	1.86	1.12	67.1	7.51	9.47E-11	-
13	318.28	21.35	2.08	0.91	71.4	8.24	5.32E-11	-
14	499.99	20.07	1.28	0.79	74.3	8.77	3.51E-11	-
15	900.00	18.42	1.65	0.63	78.4	31.27	1.84E-11	-

Table A-3: Large strain consolidation with vane shear test of neutral PT S1

Load	Effective stress (kPa)	Height (mm)	ΔH (mm)	Void ratio, e	Solids content (%)	Hydraulic gradient, i	Hydraulic conductivity (m/s)	Undrained shear strength (kPa)
1	-	202.00	-	14.25	13.7	-	1.72E-02	-
2	0.10	99.10	102.90	6.48	25.8	0.06	1.55E-05	0.36
3	0.30	92.92	6.18	5.98	27.4	0.06	7.53E-06	0.55
4	0.62	80.64	12.28	4.92	31.5	0.04	2.80E-06	1.08
5	1.74	73.01	7.63	4.30	34.4	0.45	2.42E-07	3.80
6	3.41	60.94	12.07	3.25	41.0	1.39	2.68E-08	9.06
7	6.77	55.95	4.98	2.87	44.0	2.69	8.06E-09	10.60
8	10.19	50.41	5.55	2.45	48.0	2.42	3.09E-09	22.58
9	20.35	44.76	5.64	2.01	52.9	4.83	6.53E-10	37.31
10	39.86	40.47	4.29	1.69	57.2	4.35	1.91E-10	73.87
11	79.74	36.96	3.51	1.44	61.1	4.76	1.24E-10	100.74
12	159.37	33.36	3.60	1.17	65.8	5.28	1.57E-10	162.55
13	319.11	29.68	3.69	0.90	71.4	10.38	7.42E-11	288.95
14	497.93	27.67	2.01	0.77	74.7	17.13	4.50E-11	393.92
15	873.84	25.29	2.38	0.60	79.0	18.75	2.91E-11	539.34

Table A-4: Large strain consolidation without vane shear test of cationic PT S1

Load	Effective stress (kPa)	Height (mm)	ΔH (mm)	Void ratio, e	Solids content (%)	Hydraulic gradient, i	Hydraulic conductivity (m/s)	Undrained shear strength (kPa)
1	-	169.00	-	7.44	23.6	-	9.17E-07	-
2	0.10	141.50	27.50	6.06	27.9	0.20	6.03E-07	-
3	0.32	129.47	12.03	5.41	31.7	0.29	6.42E-07	-
4	0.63	119.94	9.53	4.90	35.4	0.35	1.42E-07	-
5	1.22	110.40	9.54	4.39	39.1	0.49	9.10E-08	-
6	2.33	99.12	11.28	3.78	42.8	0.59	4.44E-08	-
7	4.55	88.40	10.73	3.20	46.6	0.96	1.86E-08	-
8	9.15	80.47	7.93	2.78	50.3	2.01	1.16E-08	-
9	20.38	68.91	11.55	2.15	54.0	2.34	4.33E-09	-
10	40.14	60.44	8.47	1.71	57.8	3.76	1.84E-09	-
11	79.88	54.00	6.44	1.38	61.5	4.20	7.78E-10	-
12	160.22	50.29	3.71	1.21	65.2	4.51	5.23E-10	-
13	319.01	50.13	0.16	1.20	65.4	4.53	4.40E-10	-
14	498.47	50.01	0.12	1.20	65.5	9.00	4.24E-10	-
15	820.63	49.85	0.02	1.19	65.6	9.03	4.14E-10	-

Table A-5: Large strain consolidation with vane shear test of cationic PT S2

Load	Effective stress (kPa)	Height (mm)	ΔH (mm)	Void ratio, e	Solids content (%)	Hydraulic gradient, i	Hydraulic conductivity (m/s)	Undrained shear strength (kPa)
1	-	170.00	-	7.44	23.6	-	9.17E-07	-
2	0.10	140.50	29.50	5.97	27.4	0.12	4.48E-07	0.11
3	0.33	125.12	15.38	5.12	30.6	0.30	4.96E-07	0.38
4	0.62	116.89	8.23	4.69	32.5	0.44	-	0.67
5	1.21	106.87	10.02	4.15	35.3	0.42	6.34E-08	1.29
6	2.34	101.45	5.43	3.88	36.8	1.50	4.49E-08	2.09
7	4.68	93.87	7.57	3.48	39.4	1.62	2.71E-08	4.84
8	7.51	83.75	10.13	2.94	43.5	2.60	1.23E-08	9.08
9	10.00	82.48	1.27	2.88	44.0	2.23	1.20E-08	9.20
10	21.31	73.32	9.16	2.40	48.6	2.50	5.47E-09	15.05
11	40.22	64.35	8.97	1.92	54.1	3.45	2.20E-09	39.02
12	79.38	58.69	5.66	1.64	58.0	3.78	1.14E-09	62.99
13	159.02	51.82	6.86	1.29	63.7	4.28	6.28E-10	102.40
14	319.24	45.71	6.11	0.98	69.7	4.86	1.44E-10	174.95
15	497.31	43.04	2.67	0.86	72.4	6.99	1.25E-10	261.11
16	854.90	39.53	3.51	0.70	76.5	11.38	1.06E-10	454.87

Table A-6: Large strain consolidation without vane shear test of anionic PT S1

Load	Effective stress (kPa)	Height (mm)	ΔH (mm)	Void ratio, e	Solids content (%)	Hydraulic gradient, i	Hydraulic conductivity (m/s)	Undrained shear strength (kPa)
1	-	139.00	-	5.63	28.8	-	2.11E-07	-
2	0.10	106.00	33.00	4.05	35.9	0.21	2.33E-07	-
3	0.30	96.00	10.00	3.53	39.2	0.48	3.51E-08	-
4	0.62	86.00	10.00	3.00	43.1	0.45	1.56E-08	-
5	1.21	76.33	9.67	2.49	47.7	1.32	3.06E-09	-
6	2.43	69.33	7.00	2.14	51.5	1.43	1.50E-09	-
7	4.88	63.06	6.27	1.83	55.4	1.57	7.84E-10	-
8	9.92	58.07	4.99	1.58	58.9	2.62	4.48E-10	-
9	19.84	54.88	3.19	1.43	61.3	6.98	2.75E-10	-
10	40.00	49.07	5.81	1.15	66.4	6.03	1.47E-10	-
11	80.00	45.75	3.32	0.99	69.6	8.71	8.71E-11	-
12	160.00	42.77	2.97	0.85	72.7	9.34	5.58E-11	-
13	404.47	38.06	4.71	0.62	78.5	10.56	2.69E-11	-
14	901.84	37.06	1.00	0.58	79.7	-	-	-

Table A-7: Large strain consolidation with vane shear test of anionic PT S2

Load	Effective stress (kPa)	Height (mm)	ΔH (mm)	Void ratio, e	Solids content (%)	Hydraulic gradient, i	Hydraulic conductivity (m/s)	Undrained shear strength (kPa)
1	-	145.0	-	5.63	28.8	-	2.11E-07	-
2	0.10	105.0	40.00	3.80	37.4	0.20	1.38E-07	0.27
3	0.30	95.0	10.00	3.29	40.8	0.60	3.15E-08	0.81
4	0.62	87.0	8.00	2.90	43.9	0.78	1.35E-08	1.45
5	1.22	78.8	8.17	2.49	47.7	0.97	4.17E-09	2.42
6	2.44	73.4	5.41	2.24	50.4	1.02	2.04E-09	3.50
7	4.88	66.4	7.00	1.90	54.5	1.12	9.22E-10	5.74
8	9.63	60.2	6.21	1.60	58.7	2.02	5.07E-10	11.54
9	19.87	54.3	5.89	1.32	63.3	5.69	2.93E-10	21.63
10	40.00	48.6	5.73	1.04	68.5	5.59	1.35E-10	43.73
11	80.00	45.6	3.20	0.91	71.4	7.01	1.16E-10	-
12	160.00	42.6	2.80	0.77	74.6	7.01	1.14E-10	115.37
13	402.06	38.6	4.00	0.59	79.4	8.59	2.31E-11	199.46
14	905.83	37.4	1.20	0.55	80.6	15.32	1.32E-11	443.96

Table A-8: Large strain consolidation without vane shear test of aged anionic PT S1

Load	Effective stress (kPa)	Height (mm)	ΔH (mm)	Void ratio, e	Solids content (%)	Hydraulic gradient, i	Hydraulic conductivity (m/s)	Undrained shear strength (kPa)
1	-	145.00	-	5.63	28.8	-	2.11E-07	-
2	0.10	109.00	36.00	3.44	39.8	0.23	1.36E-07	-
3	0.30	99.32	9.68	3.00	43.0	0.35	9.02E-09	-
4	0.62	94.92	4.41	2.82	44.6	0.72	9.22E-09	-
5	1.26	83.60	11.32	2.30	49.7	1.13	3.06E-09	-
6	2.52	74.18	9.42	1.88	54.7	1.82	1.59E-09	-
7	5.09	64.90	9.28	1.47	60.7	5.66	1.04E-09	-
8	10.14	57.11	7.79	1.13	66.7	6.42	5.31E-10	-
9	20.00	50.39	6.72	0.85	72.8	6.70	2.85E-10	-
10	40.00	46.16	4.23	0.68	77.0	7.31	1.64E-10	-
11	80.00	42.64	3.52	0.54	80.8	7.90	9.49E-11	-
12	200.00	37.98	4.66	0.35	86.6	13.32	2.85E-11	-

Table A-9: Large strain consolidation without vane shear test of aged anionic PT S2

Load	Effective stress (kPa)	Height (mm)	ΔH (mm)	Void ratio, e	Solids content (%)	Hydraulic gradient, i	Hydraulic conductivity (m/s)	Undrained shear strength (kPa)
1	-	146.00	-	5.63	28.8	-	2.11E-07	-
2	0.10	111.00	35.00	3.54	39.1	0.28	4.90E-08	0.70 (aged)
3	0.30	100.38	10.62	3.06	42.6	0.32	1.53E-08	1.08
4	0.62	90.40	9.99	2.61	46.5	0.56	5.55E-09	1.60
5	1.30	78.50	11.90	2.06	52.4	1.15	4.20E-09	3.05
6	2.57	70.65	7.85	1.72	56.9	1.90	2.05E-09	4.69
7	5.17	62.39	8.26	1.36	62.5	5.16	1.14E-09	6.21
8	10.83	54.82	7.57	1.03	68.7	5.89	6.29E-10	12.59
9	20.00	46.68	8.14	0.68	77.0	6.38	5.80E-10	27.34
10	40.00	43.91	2.77	0.57	79.8	6.79	1.69E-10	37.05
11	80.00	39.61	4.31	0.40	84.9	7.52	1.08E-10	66.55
12	200.00	34.69	4.92	0.20	91.8	15.57	2.97E-11	130.56

A2.Dean stark analysis by AGAT laboratories Ltd.

Table A-10: Dean stark results for untreated FFT

Hydrocarbons (%wt.)	2.415
Water (%wt.)	69.214
Solids (%wt.)	28.218

A3.Water chemistry analysis by AGAT laboratories Ltd.

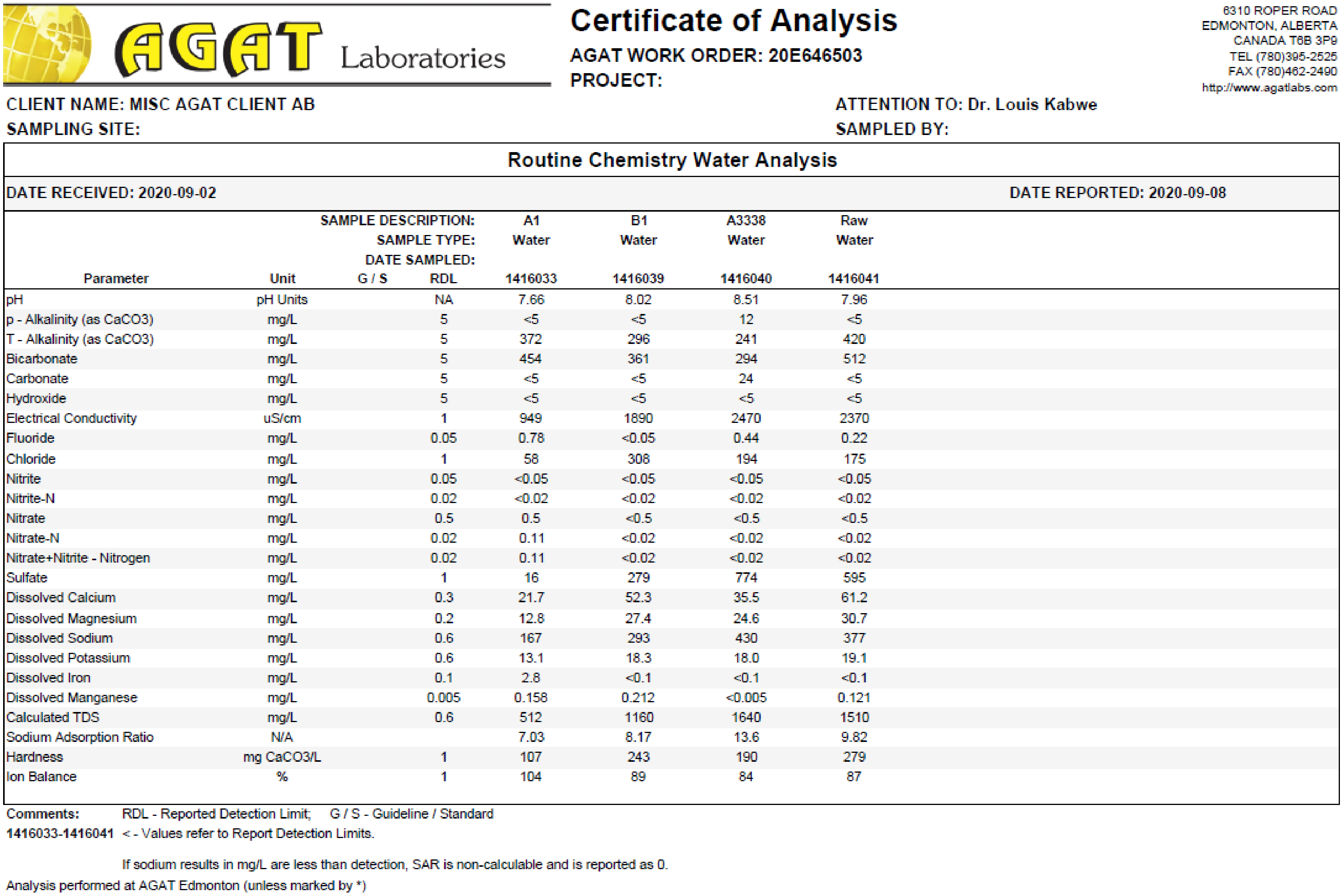

AGAT Laboratories

Certificate of Analysis

AGAT WORK ORDER: 20E646503

PROJECT:

6310 ROPER ROAD
EDMONTON, ALBERTA
CANADA T6B 3P9
TEL (780)395-2525
FAX (780)462-2490
http://www.agatlabs.com

CLIENT NAME: MISC AGAT CLIENT AB

SAMPLING SITE:

ATTENTION TO: Dr. Louis Kabwe

SAMPLED BY:

Routine Chemistry Water Analysis

DATE RECEIVED: 2020-09-02

DATE REPORTED: 2020-09-08

			SAMPLE DESCRIPTION:	A1	B1	A3338	Raw
			SAMPLE TYPE:	Water	Water	Water	Water
			DATE SAMPLED:				
Parameter	Unit	G / S	RDL	1416033	1416039	1416040	1416041
pH	pH Units		NA	7.66	8.02	8.51	7.96
p - Alkalinity (as CaCO3)	mg/L		5	<5	<5	12	<5
T - Alkalinity (as CaCO3)	mg/L		5	372	296	241	420
Bicarbonate	mg/L		5	454	361	294	512
Carbonate	mg/L		5	<5	<5	24	<5
Hydroxide	mg/L		5	<5	<5	<5	<5
Electrical Conductivity	uS/cm		1	949	1890	2470	2370
Fluoride	mg/L		0.05	0.78	<0.05	0.44	0.22
Chloride	mg/L		1	58	308	194	175
Nitrite	mg/L		0.05	<0.05	<0.05	<0.05	<0.05
Nitrite-N	mg/L		0.02	<0.02	<0.02	<0.02	<0.02
Nitrate	mg/L		0.5	0.5	<0.5	<0.5	<0.5
Nitrate-N	mg/L		0.02	0.11	<0.02	<0.02	<0.02
Nitrate+Nitrite - Nitrogen	mg/L		0.02	0.11	<0.02	<0.02	<0.02
Sulfate	mg/L		1	16	279	774	595
Dissolved Calcium	mg/L		0.3	21.7	52.3	35.5	61.2
Dissolved Magnesium	mg/L		0.2	12.8	27.4	24.6	30.7
Dissolved Sodium	mg/L		0.6	167	293	430	377
Dissolved Potassium	mg/L		0.6	13.1	18.3	18.0	19.1
Dissolved Iron	mg/L		0.1	2.8	<0.1	<0.1	<0.1
Dissolved Manganese	mg/L		0.005	0.158	0.212	<0.005	0.121
Calculated TDS	mg/L		0.6	512	1160	1640	1510
Sodium Adsorption Ratio	N/A			7.03	8.17	13.6	9.82
Hardness	mg CaCO3/L		1	107	243	190	279
Ion Balance	%		1	104	89	84	87

Comments: RDL - Reported Detection Limit; G / S - Guideline / Standard

1416033-1416041 < - Values refer to Report Detection Limits.

If sodium results in mg/L are less than detection, SAR is non-calculable and is reported as 0.

Analysis performed at AGAT Edmonton (unless marked by *)

Appendix B: Methods and Test Procedures

B1. Polymer preparation protocol (prepared by Khushbu Vandara)

Oil sands tailings/Fluid fine tailings details:

- » Location of collection: Tailings ponds, northern Alberta, Canada
- » The sands to the fine ratio (SFR): 0.25.
- » The total solids content: 31 wt% (Clay fractions: 68-72% kaolinite, 28-32% illite)
- » The total dissolved solids content in pore water: 1500-1700 micro-S/cm with the dominant cation of sodium with the concentration of 300-340 mg/L.

Polymers details:

Code	Polymer Name	Nature	Type & other details
A-1	Polyacrylamide-g-amylopectin	Neutral	Brush type structure with linear chains of acrylamide are attached to big backbone of amylopectin chain
B-1	Poly (vinyl benzyl) trimethylammonium chloride	Cationic	A linear polymer of Vb+

Details of polymer dosage:

Polymer	Dosage (ppm)	Polymer qty. for 500 ml sol. (gm)	% Solution	Mixing time (min.)
A-1	8000	1.0	0.2	2.5
B-1	4000	2.0	0.4	1.5

Polymer stock solution:

- Weigh the polymers with analytical balance and add them in respective beakers of 500 ml.
- Add distilled water in the beaker to complete the solution of 500 ml.
- Stir the mixture with jar tester at 200 rpm for 5 minutes and at 125 rpm for the following 55 minutes.
- Keep the polymer solutions aside for maturation for 15 minutes.

Polymer amended tailings:

- Mix pre-determined volumes based on dosing requirements of polymer stock solution with fluid fine tailings at 315 rpm for respective mixing time mentioned in above Table for each polymer.
- Immediately utilize the mixture for the analysis to minimize the errors in outputs and preserve the original characteristics of the mixture.

Procedure:

- Pour the freshly made mixture of polymer amended tailings into 100 ml cylinders (Φ 2.8 cm) and seal and leave them undisturbed.
- For each polymer, keep two identical cylinders for the settlement observation and record the results every day.
- Utilize the remaining mixture for CST test to measure the initial CST.
- After considerable short-term settling of the mixture (which was observed after 12 days), collect the supernatant from the cylinders with the help of a syringe and save them in different containers for further supernatant analysis.
- As there were two replicate cylinders for each flocculant, use one of them for optical microscopy and CST test, and other one for the measurement of total solids, gravimetric water content, and density.
- After removing the supernatant from one column, collect the sample for optical microscopy on glass slide immediately from the topmost layer with the needle, and do the CST test for the topmost layer and the bottom-most layer.

- Whereas for the other cylinder, after removal of water from the top, starting from top to bottom, collect approximately 10 ml of the sample with a spatula on small aluminum foil containers.
- Record the mass of empty containers, the mass of containers with the sample, the cylinder mass with the sample, and height of sample in the cylinder after removing each ~10 ml sample.
- Following that, keep the aluminum containers for drying in an oven at 105°C temperature for 24 hours to measure the total solid content.
- On the next day, record the mass of containers after drying and keep for further drying at 600°C for 30 minutes to measure the volatile solids as well as gravimetric water content.
- After that, weigh the containers again once they reach room temperature.
- Note down the mass of empty graduated cylinders, the mass of cylinders with and without supernatant, the initial level of the sample, etc.
- After recording all the data, calculate the volume of sample, the mass of the sample, the mass of solids and water in the sample, gravimetric water content, density, etc. using below formulas;

The volume of sample:

$V_{sample} = {}^{\pi}/_{4}\, D^2$; where D = Diameter of graduated cylinder

Mass of sample:

$$M_{sample} = M_{container+sample} - M_{container}$$

Mass of solids in sample:

$$M_{solids} = M_{container\ after\ drying\ at\ 105°C} - M_{container}$$

Mass of water in sample:

$$M_{water} = M_{container+sample} - M_{container\ after\ drying\ at\ 105°C}$$

Gravimetric water content:

$$GWC\ (W\%) = \frac{M_{water}}{M_{solids}} \times 100$$

Volatile solids:

$$VS\ (W\%) = \left(\frac{M_{container\ after\ drying\ at\ 105°C} - M_{container\ after\ drying\ at\ 600°C}}{M_{sample}}\right) \times 100$$

Fixed solids:

$$FS(W\%) = \left(\frac{M_{container\ after\ drying\ at\ 600°C}\ -\ M_{container}}{M_{sample}}\right) \times 100$$

Total Solids:

$$TS(W\%) = VS(W\%) + FS(W\%)$$

Density:

$$\rho = \frac{M_{sample}}{V_{sample}}$$

» Next, determine the basic parameters for separately collected supernatant samples i.e. pH with Thermo-scientific pH meter, turbidity with Thermo-scientific Orion AQ3010 turbidity meter, and total solids by a similar process of oven drying at 105°C for 24 hours with the sample size of 10 ml.

B2. Dean Stark extraction

The bitumen, water and mineral solids constituents of the FFT are determined by the Dean-Stark extraction method with the aid of the Soxhlet extractor shown in **Error! Reference source not found.**. The test samples are first oven-dried to remove all moisture, leaving only bitumen and tailings solids for the bitumen content test.

Figure B-1: Dean-Stark extraction of bitumen from FFT

The extractor consists of a boiler (at the bottom), a syphon (in the middle) and a reflux condenser containing distilled water (at the top). During the extraction process, toluene (the solvent) is boiled in the flask to generate toluene vapour, which rises to the siphon where the sample is held in a thimble (a filter container capable of retaining fine tailings solids). Toluene vapour separates bitumen from the sample, leaving only the tailings solids in the thimble. In the siphon, toluene is condensed while extracting bitumen from the sample, and condensed water is simultaneously separated in a water trap. The resulting toluene-bitumen solution is returned to the boiler by reflux and recirculated until dissolved bitumen is no more observed in the condensed toluene. At the end of the extraction process, both the remaining sample and thimble are re-weighed to determine the percentage of bitumen.

B3. Specific Gravity

The specific gravity is an essential soil parameter in determining other soil characteristics, such as the particle-size distribution of fine-grained soils, void ratio and dry density. Two subsamples of homogenized FFT were analyzed for specific gravity in accordance with the test procedure described in ASTM D854 – 14 "Standard Test Methods for Specific Gravity of Soil Solids by Water Pycnometer." After dispersing and blending the specimen, the slurry was transferred into a 500 mL pycnometer. Water was added to the slurry to about half of the pycnometer depth and the mixture was agitated. To de-air the slurry, relatively constant vacuum was applied to the slurry for a few hours, after which, the pycnometer was filled with de-aired water, as shown in Figure B-2.

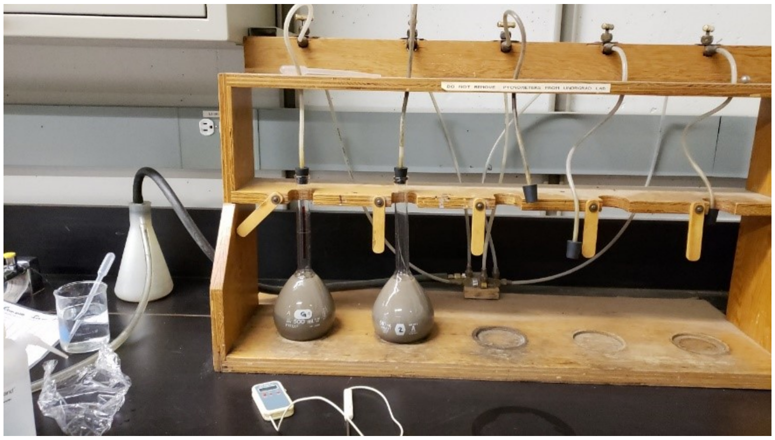

Figure B-2: Specific gravity test by water pycnometer method

The pycnometer was kept overnight with a thermometer in an insulated container to achieve thermal equilibrium. The mass of the pycnometer plus FFT-water mixture and the temperature of the mixture were measured and recorded. After transferring all the mixture into a pan of known mass and oven-drying overnight at a constant temperature of 105°C, the dry solids mass of the specimen was measured and recorded as well. The specific gravity was determined using equations 2, 3, 4 and 5 listed in ASTM D854 – 14.

B4. Particle Size Distribution

The particle or floc size distribution of candidate FFT samples was obtained by examining subsamples of each material type in a hydrometer test. The test was modified to include both dispersed and non-dispersed conditions for the untreated FFT, but the polymer amended FFT was analyzed without adding a dispersant. Based on the percent solids, approximately 162 grams of untreated FFT, representing 50 g of solids, was dispersed with 125 mL of 4% solution of sodium hexametaphosphate as the dispersing agent. The mixture was transferred into a graduated cylinder and topped up to 1 litre with distilled water. A second graduated cylinder, containing 125 mL of the deflocculating agent and distilled water up to the 1-litre mark, was prepared as a control reference for the sedimentation test. The solution was mixed by repeated shaking and allowed to equilibrate. With the hydrometer plunged in the control solution, the zero correction (F_z), the meniscus correction (F_m) and the temperature of the solution at equilibrium were recorded. In addition, a third graduated cylinder, containing a litre of 50 g of untreated FFT and water suspension without a dispersant, was prepared for sedimentation. With a rubber cap on each cylinder, the sedimentation test was conducted for both dispersed and non-dispersed FFT-water mixtures by first homogenizing the suspension. After homogenizing, a stopwatch for each test was immediately started and the hydrometer was inserted in the FFT-water suspension at set elapsed times of 15 sec, 30 sec, 1 min, 2 min, 4 min, 8 min, 15 min, 30 min, 1 hr, 2 hr, 4 hr, 8 hr and 24 hr for readings to be taken. Usually, the hydrometer was allowed to equilibrate in the suspension for about 30 seconds before taking the reading. After each reading, the hydrometer was removed and kept in the control solution until the next reading, as shown in Figure B-3, and the temperature of the suspension was measured using the thermometer. Similarly, the procedure for the non-dispersed hydrometer test was applied to the polymer amended FFT samples.

Since the coarse fraction of untreated FFT was very small, the wet sieve analysis was not performed on the suspension from the hydrometer test. For a measurable coarse fraction to be obtained, about 500 grams of untreated FFT were washed with tap water through a No 200 (75-µm) sieve until clear water was observed. The fraction retained on the sieve was oven-dried and weighed, and the measured mass was corrected to complete the particle size distribution curve. The datasheets for the wet sieve and hydrometer analysis are found in Appendix A.

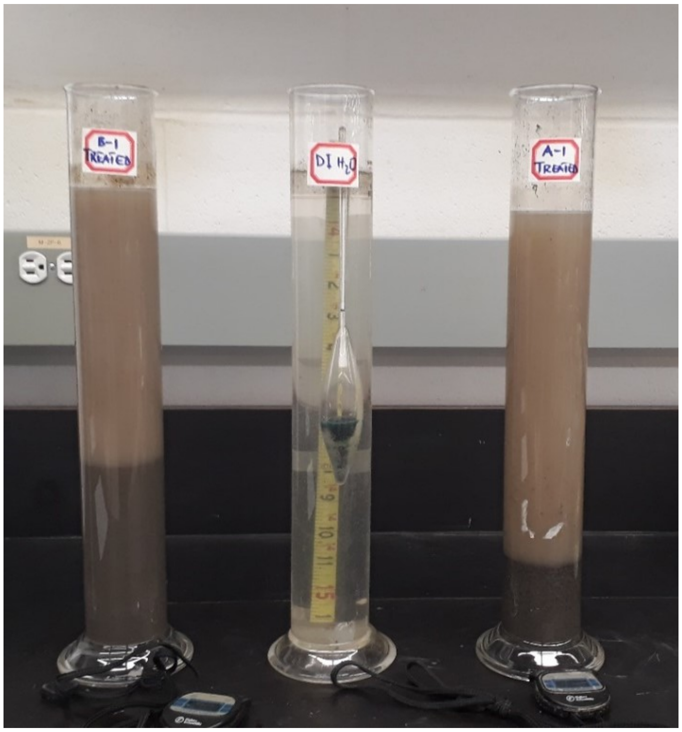

Figure B-3: Hydrometer test